CONFIDENTIAL

Copy 242

RM A58F02

NACA

RESEARCH MEMORANDUM

APPROXIMATE SOLUTIONS FOR THE FLOW ABOUT FLAT-TOP WING-BODY CONFIGURATIONS AT HIGH SUPERSONIC AIRSPEEDS

By Raymond C. Savin

Ames Aeronautical Laboratory
Moffett Field, Calif.

NATIONAL ADVISORY COMMITTEE
FOR AERONAUTICS

WASHINGTON

September 15, 1958

CONFIDENTIAL

NATIONAL ADVISORY COMMITTEE FOR AERONAUTICS

RESEARCH MEMORANDUM

APPROXIMATE SOLUTIONS FOR THE FLOW ABOUT FLAT-TOP WING-BODY CONFIGURATIONS AT HIGH SUPERSONIC AIRSPEEDS*

By Raymond C. Savin

SUMMARY

The flow about slender flat-top wing-body configurations traveling at high supersonic speeds and small angles of attack is investigated analytically. In the case of conical configurations, approximate algebraic solutions to the flow field are obtained. In the case of configurations which are conical at the vertex but curved in the stream direction, these solutions are combined with a slender-body approximation to the generalized shock-expansion method to obtain the flow downstream of the vertex.

Surface pressures were obtained experimentally at Mach numbers from 3.0 to 6.0 and angles of attack up to 6° for several flat-top wing-body configurations. These configurations consisted of half-bodies of revolution mounted beneath thin highly swept wings. Three different bodies were employed. The two conical bodies consisted of one-half of a fineness-ratio-5 cone and one-half of a fineness-ratio-2-1/2 cone. The body of the third configuration consisted of one-half of a fineness-ratio-5 ogive. For the ogive configuration, the leading edges of the wing were curved and designed to just maintain the theoretically determined bow shock along the leading edge at a Mach number of 5.0 and an angle of attack of 3°. The predictions of the conical flow theory of this paper for the surface pressures are found to be in good agreement with experiment at Mach numbers of 5.0 and 6.0 up to angles of attack of approximately 3°. Estimated lift, drag, and pitching-moment coefficients, as well as maximum lift-drag ratio, are also in good agreement with existing experimental data at a Mach number of 5.0 for a conical configuration having an arrow plan-form wing. It is also found that the generalized shock-expansion method yields reasonably good agreement with experiment for the surface pressures on the half-ogive configuration at a Mach number of 5.0 and an angle of attack of 3°.

*Title, Unclassified.

INTRODUCTION

A class of flat-top wing-body combinations was proposed in reference 1 as being capable of developing high lift-drag ratios at high supersonic speeds. The type of configuration suggested consists of a thin highly swept wing of essentially arrow plan form beneath which is mounted a half-body of revolution with its vertex common to the vertex of the wing. Theoretical and experimental results presented in references 1 and 2 indicated that these configurations have a high aerodynamic efficiency at high supersonic speeds. It is of interest, therefore, to consider more refined theoretical methods for treating the flow about flat-top wing-body combinations. Such methods are necessary if accurate estimates of pressure forces and moments as well as detailed local flow properties are to be obtained. Local flow conditions are required, of course, in order to determine skin-friction and heat-transfer characteristics which are so important at hypersonic speeds.

A method for estimating the aerodynamic forces on flat-top wing-body configurations has been presented in reference 3. This method was obtained with the aid of linear theory. In fact, in the past, virtually all treatments of the flow about wing-body combinations have employed linear theory (see, e.g., refs. 3 through 7). Although these methods have been shown to be adequate for low supersonic speeds, their application to hypersonic speeds is questionable due to the restrictions of linear theory. Thus, at the present time, there is no well-established theory applicable to the accurate prediction of the aerodynamic characteristics of wing-body combinations traveling at high supersonic speeds. The objective of the present paper, therefore, is to obtain an improved theoretical method for predicting the flow about flat-top wing-body configurations having supersonic leading edges. In this connection, a hypersonic theory applicable to conical configurations is obtained. This result is then combined with a slender-body approximation to the generalized shock-expansion method to obtain the flow about configurations which are curved in the stream direction.

NOTATION

a local speed of sound, ft/sec

C_A axial-force coefficient, $\frac{\text{axial force}}{q_\infty S}$

C_D drag coefficient, $\frac{\text{drag}}{q_\infty S}$

C_L lift coefficient, $\frac{\text{lift}}{q_\infty S}$

C_m pitching-moment coefficient, $\frac{\text{moment about vertex}}{q_\infty S l}$

C_N normal-force coefficient, $\frac{\text{normal force}}{q_\infty S}$

C_p pressure coefficient, $\frac{p - p_\infty}{q_\infty}$

c_p specific heat at constant pressure, ft-lb/slug $^\circ$R

c_v specific heat at constant volume, ft-lb/slug $^\circ$R

E entropy, ft-lb/slug $^\circ$R

l characteristic reference length, ft

M Mach number (ratio of local airspeed to local speed of sound)

p static pressure, lb/sq ft

p_t total pressure, lb/sq ft

q dynamic pressure, lb/sq ft

R gas constant, ft-lb/slug $^\circ$R

r distance along conical ray measured from vertex, ft

S total plan area, sq ft

u velocity component parallel to r, ft/sec

v velocity component normal to u in a meridian plane, ft/sec

V resultant velocity, $\sqrt{u^2 + v^2 + w^2}$, ft/sec

$\hat{V}$ maximum velocity obtainable by expanding to zero temperature, ft/sec

w velocity component normal to a meridian plane, ft/sec

α angle of attack, radians unless otherwise specified

γ ratio of specific heats, $\frac{c_p}{c_v}$

δ angle of flow inclination in meridian plane measured from configuration axis, radians unless otherwise specified

δ_w wedge angle of wing in streamwise direction

Δ angle of flow inclination in meridian plane measured from free-stream direction, radians unless otherwise specified

ϵ angular difference between free-stream direction and locus of points representing center of curvature of shock in plane of symmetry, radians unless otherwise specified

λ semivertex angle of wing (i.e., complement of leading-edge sweep angle; see fig. 1), radians unless otherwise specified

μ Mach angle, radians unless otherwise specified

ρ mass density, slugs/cu ft

φ angle of meridian plane with respect to plane of symmetry, radians unless otherwise specified (see fig. 1)

ψ dihedral angle at shock between streamwise plane normal to shock and plane containing axis of configuration, radians unless otherwise specified

Ψ dihedral angle at shock between streamwise plane normal to shock and plane containing free-stream velocity vector, radians unless otherwise specified

ω angle between axis of cone and ray passing through vertex of cone, radians unless otherwise specified

Ω angle of ray on conical shock measured with respect to free-stream direction, radians unless otherwise specified

Subscripts

B body

c evaluated at cone surface

e evaluated at external surface of vortical layer

S evaluated at shock wave

W wing

∞ free-stream conditions

o conditions at $\varphi = 0$

$\frac{\pi}{2}$ conditions at $\varphi = \frac{\pi}{2}$

THEORY

The purpose of this analysis is to obtain a simplified theory for predicting flow fields about a class of flat-top wing-body configurations traveling at hypersonic speeds and at small angles of attack. The configuration to be treated is assumed to consist of a half-body of revolution mounted beneath a thin wing, the vertex of which is common to the vertex of the body and whose leading edges are sharp and always supersonic. Furthermore, the configuration is assumed slender and the surface slopes are everywhere small compared to 1. In addition, the free-stream Mach number is assumed large compared to 1 and the angle of attack small compared to 1. Thus, the local Mach number will be large compared to 1 and the inclination of the nose shock wave will be small. Only flow fields which are either wholly conical or conical at the vertex are studied. Consider now the flow field as it would appear in cross-section view normal to the configuration axis. A conical flow field of the double shock type is shown in sketch (a), where region 1 is three-dimensional in type and is generated by the body, and region 2 is a two-dimensional flow field generated by the wing (the configuration is presumed to be at angle of attack). Another conical flow field is a single-shock type as represented in sketch (b). Experimental observations of the shock-wave patterns to

Sketch (a)

Sketch (b)

date indicate that the flow field is of the single-shock type, at least for configurations having highly swept wings. It was also found that the pressures on the wing were not only continuous across the entire wing but were also higher in region 2 than the pressures which would be expected if the flow were two-dimensional in this region. In the following analysis, approximate solutions to the flow field satisfying the boundary conditions corresponding to the single-shock type will be obtained.

Flow About Conical Flat-Top Wing-Body Configurations

For conical flow fields, all derivatives with respect to radial distance vanish and the equations of motion and continuity in spherical polar coordinates become (a schematic diagram of the polar coordinate system is shown in fig. 1)

$$v\frac{\partial u}{\partial \omega} + \frac{w}{\sin \omega}\frac{\partial u}{\partial \varphi} - v^2 - w^2 = 0 \qquad (1a)$$

$$v\frac{\partial v}{\partial \omega} + \frac{w}{\sin \omega}\frac{\partial v}{\partial \varphi} + \frac{1}{\rho}\frac{\partial p}{\partial \omega} + uv - w^2 \cot \omega = 0 \tag{1b}$$

$$v\frac{\partial w}{\partial \omega} + \frac{w}{\sin \omega}\frac{\partial w}{\partial \varphi} + \frac{1}{\rho \sin \omega}\frac{\partial p}{\partial \varphi} + uw + vw \cot \omega = 0 \tag{1c}$$

and

$$2\rho u \sin \omega + v \sin \omega \frac{\partial \rho}{\partial \omega} + \rho \sin \omega \frac{\partial v}{\partial \omega} + v\rho \cos \omega + w\frac{\partial \rho}{\partial \varphi} + \rho \frac{\partial w}{\partial \varphi} = 0 \tag{2}$$

respectively. Now the law of conservation of energy requires the following relations to be satisfied:

$$\left.\begin{aligned} \frac{\gamma}{\gamma - 1}\left(\frac{1}{\rho}\frac{\partial p}{\partial \varphi} - \frac{p}{\rho^2}\frac{\partial \rho}{\partial \varphi}\right) &= -\left(u\frac{\partial u}{\partial \varphi} + v\frac{\partial v}{\partial \varphi} + w\frac{\partial w}{\partial \varphi}\right) \\ \frac{\gamma}{\gamma - 1}\left(\frac{1}{\rho}\frac{\partial p}{\partial \omega} - \frac{p}{\rho^2}\frac{\partial \rho}{\partial \omega}\right) &= -\left(u\frac{\partial u}{\partial \omega} + v\frac{\partial v}{\partial \omega} + w\frac{\partial w}{\partial \omega}\right) \end{aligned}\right\} \tag{3}$$

The entropy at any point in the flow field may be expressed in the form

$$E - E_\infty = \frac{R}{\gamma - 1} \ln\left[\frac{p}{p_\infty}\left(\frac{\rho_\infty}{\rho}\right)^\gamma\right] \tag{4}$$

Equations (1), (2), and (3) together with the relation

$$a^2 = \frac{\gamma - 1}{2}\left(\hat{V}^2 - V^2\right)$$

may be combined (by eliminating the pressure and density terms) to obtain the equation of motion

$$\frac{\gamma - 1}{2}\left(\hat{V}^2 - V^2\right)\left(2u + v \cot \omega + \frac{\partial v}{\partial \omega} + \frac{1}{\sin \omega}\frac{\partial w}{\partial \varphi}\right) - uv^2 - uw^2 -$$

$$v^2\frac{\partial v}{\partial \omega} - \frac{w^2}{\sin \omega}\frac{\partial w}{\partial \varphi} - \frac{vw}{\sin \omega}\frac{\partial v}{\partial \varphi} - vw\frac{\partial w}{\partial \omega} = 0 \tag{5}$$

which is general for all steady-state conical flows.

It is convenient first to define the flow conditions on the leeward or expansion side of the wing.[1] For flows of the type under consideration, the expressions defining the Mach number and pressure are simply those applicable to a flat plate and may be written (see ref. 8)

[1]Since the shock wave is assumed to be always attached to the leading edge of the wing, the flow fields on the windward and leeward sides may be treated independently.

$$\frac{M_\infty}{M} = 1 - \frac{\gamma - 1}{2} M_\infty(\alpha - \delta_W) \tag{6}$$

and

$$\frac{p}{p_\infty} = \left[1 - \frac{\gamma - 1}{2} M_\infty(\alpha - \delta_W)\right]^{\frac{2\gamma}{\gamma - 1}} \tag{7}$$

respectively, where α is the angle of attack and δ_W is the streamwise wedge angle of the wing.

The remaining part of this analysis will be concerned with the study of the interference flow field on the high-pressure side of flat-top wing-body configurations. Before proceeding with the actual solution for the flow field, it is convenient first to consider the basic assumptions underlying the solution and to outline briefly the method of attack in obtaining this solution. As mentioned earlier, only hypersonic flows and slender configurations at small angles of attack are considered in this paper. Thus, the following simplifications are employed throughout this analysis:

$$M \gg 1 \qquad \omega \ll 1$$
$$\delta \ll 1 \qquad \alpha \ll 1$$

It is further assumed that the present flow fields represent only a small departure from flow fields generated by circular cones. The subsequent analysis, then, will be similar in many respects to that presented in reference 9 for the flow about circular cones at small angles of attack. In particular, the flow in the region of the plane of symmetry (i.e., at $\varphi = 0$) is assumed to be identical to that generated by a circular cone in this region. The general form of the expression for the w component of velocity employed in reference 9 is also assumed to be applicable for the present flow fields.

The following procedure is employed with the above assumptions to obtain a solution for the interference flow field. An expression defining the w component of velocity throughout the flow field (see fig. 1) is first obtained. The flow is then treated in four parts as shown in sketch (c), which represents the boundaries of the flow field in a plane normal to the configuration axis.

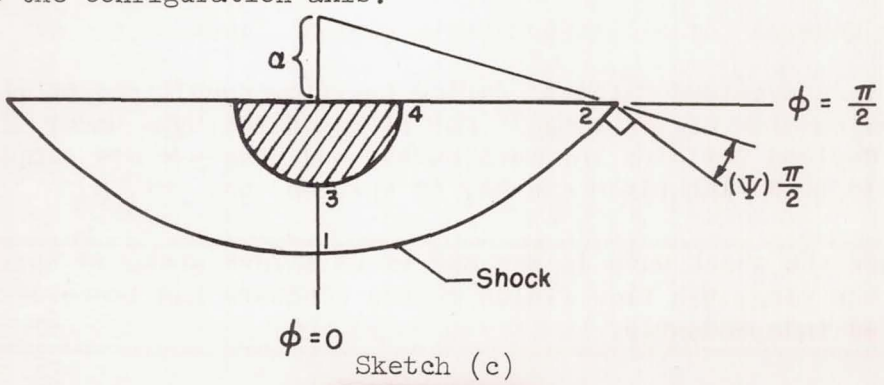

Sketch (c)

Expressions which define flow conditions along the shock (1-2), in the plane of symmetry (1-3), in the plane of the wing (2-4), and around the surface of the body (3-4) will be obtained in terms of flow conditions at $\varphi = 0$ and $\varphi = \pi/2$. Solution of the flow in the plane of symmetry determines all conditions at $\varphi = 0$. All the expressions obtained, then, may be written in terms of known quantities and/or $(\Psi)_{\pi/2}$. The parameter $(\Psi)_{\pi/2}$ is obtained by an iteration process which involves matching at point 4 the pressure calculated by proceeding along 1-3-4 to the pressure calculated by proceeding along 2-4. A discussion of the evaluation of $(\Psi)_{\pi/2}$ is presented. An analysis of the flow off the surface, that is, between the body surface and the shock, is discussed and expressions defining this part of the flow field will be obtained. Finally, analytic expressions in closed form are obtained for the lift, drag, and pitching-moment coefficients for conical flat-top wing-body combinations. With these points in mind, the analysis for the w component of velocity will now be considered.

Determination of w component of velocity.- It was found in reference 9 that the ω and φ dependence of w could be separated into a product for the case of circular cones. Since the present flow fields represent a small departure from that of the circular cone, the same dependence is assumed here; namely,

$$\frac{w}{V_\infty} = w_1(\omega)w_2(\varphi) \tag{8}$$

Furthermore, the variation of w with ω is assumed to be the same as in the case of the circular cone so that this variation between the surface and the shock may be written (see ref. 9)

$$w_1(\omega) = \frac{\omega_S}{\omega}$$

Now it is obvious that the variation of w with φ will differ from that for a circular cone since the presence of the wing will alter the boundary conditions. The term $w_2(\varphi)$, then, will be defined by the polynomial (noting that w must be an odd function)

$$w_2(\varphi) = c_1\varphi + c_2\varphi^3 + c_3\varphi^5$$

Since $w = 0$ at $\varphi = 0$ because of the symmetry of the flow and also at $\varphi = \pi/2$ because of the presence of the wing, the coefficients in the above expression are easily evaluated in terms of $\partial w_2/\partial\varphi$ at $\varphi = 0$ and $\varphi = \pi/2$ to yield (when combined with eq. (8))

$$\frac{w}{V_\infty} = \left(\frac{\omega_S}{\omega}\right)\varphi\left\{\left(\frac{\partial w_2}{\partial\varphi}\right)_0 - \frac{2}{\pi^2}\left[\left(\frac{\partial w_2}{\partial\varphi}\right)_{\pi/2} + 4\left(\frac{\partial w_2}{\partial\varphi}\right)_0\right]\varphi^2 + \frac{8}{\pi^4}\left[\left(\frac{\partial w_2}{\partial\varphi}\right)_{\pi/2} + 2\left(\frac{\partial w_2}{\partial\varphi}\right)_0\right]\varphi^4\right\} \tag{9}$$

Expression (9) defines the w component of the velocity throughout the flow field on the windward side of the configuration. There remains, however, the determination of the shock-wave angle, ω_S, and the quantities $(\partial w_2/\partial\varphi)_0$ and $(\partial w_2/\partial\varphi)_{\pi/2}$. An expression for ω_S will now be obtained by considering the flow conditions at the conical shock.

Flow conditions at the shock.- The shape of the shock wave will be influenced by the shape of the body, the angle of attack, and the leading-edge sweep of the wing. For example, at $\alpha = 0^\circ$ the conical shock will be circular between the planes $\varphi = 0$ and $\varphi = \pi/2$ provided the leading-edge angle of the wing, λ, is equal to the axially symmetric shock angle for the complete circular cone. If $\lambda > (\omega_S)_{\alpha=0}$, then the shock will impinge on the wing leading edge at an acute angle similar to that shown in sketch (d). The angle $(\psi)_{\pi/2}$ shown in this sketch (see also fig. 1)

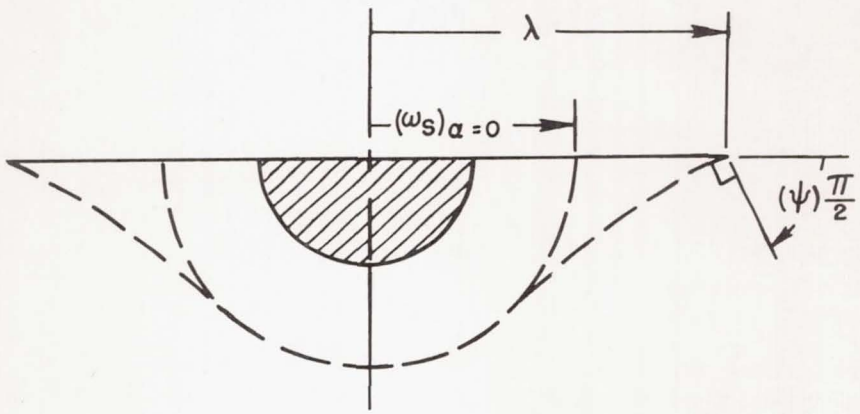

Sketch (d)

is the angle of the dihedral between a plane normal to the shock and the plane of the wing and

$$\tan\psi = \frac{1}{\omega_S}\frac{\partial\omega_S}{\partial\varphi} \tag{10}$$

which holds for any meridian plane. Consider now the case where $\alpha > 0$. As the angle of attack increases, the pressures on the body, and therefore throughout the flow field, increase causing the shock in the plane of the wing to "spread" beyond that for $\alpha = 0^\circ$. Now if the shock is to remain attached to the leading edge, the leading-edge sweep must be decreased. Thus, in the present analysis, there is a minimum λ (maximum sweep) which can be treated for each angle of attack. It is clear from the foregoing discussion that if a reasonably accurate prediction of the flow field is to be obtained, particular attention must be paid to the shape of the shock wave. The conical shock will then be defined by a power series in φ where the coefficients are determined from the following conditions:

at $\varphi = 0$,

$$\omega_S = (\omega_S)_o \qquad \frac{\partial \omega_S}{\partial \varphi} = 0$$

at $\varphi = \frac{\pi}{2}$,

$$\omega_S = \lambda \qquad \frac{\partial \omega_S}{\partial \varphi} = \lambda \tan(\psi)_{\pi/2}$$

Thus, the expression

$$\frac{\omega_S}{\delta_c} = \left(\frac{\omega_S}{\delta_c}\right)_o + \left(\frac{2}{\pi}\right)^2 \left(\frac{\lambda}{\delta_c}\right) \left\{ 2 \left[1 - \frac{(\omega_S)_o}{\lambda} \right] - \frac{\pi}{4} \tan(\psi)_{\pi/2} \right\} \varphi^2 - \left(\frac{2}{\pi}\right)^4 \left(\frac{\lambda}{\delta_c}\right) \left[1 - \frac{(\omega_S)_o}{\lambda} - \frac{\pi}{4} \tan(\psi)_{\pi/2} \right] \varphi^4 \tag{11}$$

defines the conical shock with respect to the configuration axis. The tangent operator on ψ is retained in the above expression since at $\varphi = \pi/2$ this angle represents the attenuation of the shock due to leading-edge sweep and there is no way of determining a priori its order of magnitude. Now for small angles of attack, the shock-wave angle, Ω, and flow-deflection angle, Δ, measured from the wind axis may be related to the shock angle, ω_S and flow-deflection angle, δ_S, measured from the configuration axis by

$$\Omega = \omega_S + \alpha \cos \varphi \tag{12}$$

and

$$\Delta = \delta_S + \alpha \cos \varphi \tag{13}$$

respectively. It can also be shown that, consistent with the above approximations,

$$\Psi = \psi - \frac{\alpha \sin \varphi}{\omega_S + \alpha \cos \varphi} \tag{14}$$

where Ψ is the angle of the dihedral at a point on the shock between a streamwise plane normal to the shock and the plane containing the wind axis. Thus, the oblique-shock-wave relations may be written

$$\left(\frac{M_S}{M_\infty}\right)^2 = \frac{(\gamma + 1)^2 M_\infty^2 \Omega^2 \cos^2 \Psi}{[2\gamma M_\infty^2 \Omega^2 \cos^2 \Psi - (\gamma - 1)][(\gamma - 1) M_\infty^2 \Omega^2 \cos^2 \Psi + 2]} \tag{15}$$

$$\frac{\Delta}{\delta_c} = \frac{M_\infty^2 \Omega^2 \cos^2 \Psi - 1}{\frac{\gamma + 1}{2} M_\infty \delta_c M_\infty \Omega \cos \Psi} \tag{16}$$

$$\frac{p_S}{p_\infty} = \frac{2\gamma M_\infty^2 \Omega^2 \cos^2\Psi - (\gamma - 1)}{\gamma + 1} \tag{17}$$

Equations (11) through (17) completely define conditions immediately downstream of the shock wave in terms of flow parameters referred to the configuration axis. It is clear, of course, that $(\omega_S)_0$ and $(\Psi)_{\pi/2}$ are yet to be determined.

Flow conditions in the plane $\varphi = 0$.- As a by-product of the solution of the flow in this plane, the two quantities $(\omega_S)_0$ and $(\partial w_2/\partial\varphi)_0$ will be determined. Because of the symmetry of the flow in this plane, $w = 0$ and the equation of motion (eq. (5)) reduces to

$$\frac{\gamma - 1}{2}(\hat{V}^2 - V^2)\left(2u + v\cot\omega + \frac{\partial v}{\partial\omega} + \frac{1}{\sin\omega}\frac{\partial w}{\partial\varphi}\right) - v^2\left(u + \frac{\partial v}{\partial\omega}\right) = 0 \tag{18}$$

Now from the flow pattern, the velocity components may be written

$$u = V\cos(\omega - \delta)$$

$$v = -V\sin(\omega - \delta)$$

and from equation (1a)

$$v = \frac{\partial u}{\partial\omega}$$

It can also be shown that

$$\frac{dV}{V} = -\tan(\omega - \delta)d\delta \tag{19}$$

Substitution of the above expressions into equation (18) results in

$$\frac{\gamma - 1}{2}\left[\left(\frac{\hat{V}}{V}\right)^2 - 1\right]\left[\cot(\omega - \delta)\left(1 + \frac{\partial\delta}{\partial\omega}\right) - \cot\omega + \tan(\omega - \delta)\frac{\partial\delta}{\partial\omega} + \frac{\csc(\omega - \delta)}{V\sin\omega}\frac{\partial w}{\partial\varphi}\right] - \tan(\omega - \delta)\frac{\partial\delta}{\partial\omega} = 0$$

Consistent now with the assumption of $\delta \ll 1$ and $\omega \ll 1$, the above expression may be written

$$\frac{\delta}{\omega} + \frac{\partial\delta}{\partial\omega}\left[1 - (M\omega)^2\left(1 - \frac{\delta}{\omega}\right)^2\right] + \frac{1}{V\omega}\frac{\partial w}{\partial\varphi} = 0$$

Furthermore, since $M\omega$ and δ/ω are both of the order of 1, there is finally obtained (by virtue of eq. (8))

$$\frac{\partial \delta}{\partial \omega} + \frac{\delta}{\omega} + \frac{V_\infty}{V} \frac{\omega_S}{\omega^2} \left(\frac{\partial w_2}{\partial \varphi} \right)_0 = 0 \tag{20}$$

Consider now the term $(\partial w_2/\partial \varphi)_0$. If the angle of attack is small and the leading-edge angle of the wing does not differ too greatly from the angle of the shock wave generated by the equivalent circular cone, then one might expect the flow in the plane of symmetry to differ but little from that of the circular cone.[2] It is assumed, therefore, that, as a first approximation, the flow in this plane will be the same as that for the circular cone. Then (see ref. 9)

$$\left(\frac{\partial w}{\partial \varphi} \right)_0 = V_\infty \epsilon \frac{\omega_S}{\omega}$$

where ϵ is the angle between the axis of the conical shock and the free-stream-velocity vector. It follows, then, from equation (8) that

$$\left(\frac{\partial w_2}{\partial \varphi} \right)_0 = \epsilon$$

and, therefore, equation (20) yields upon integration (noting that $V_\infty/V \cong 1$)

$$\frac{\delta}{\delta_c} = \frac{\delta_c}{\omega} - \left(\frac{\epsilon}{\delta_c} \right) \left(\frac{\omega_S}{\omega} \right) \ln \frac{\omega}{\delta_c} \tag{21}$$

which defines the flow-deflection angle. The expression for the flow velocity is obtained by integration of the resulting combination of equations (19) and (21) and may be written

$$\frac{V}{V_S} = \left(\frac{\omega}{\omega_S} \right)^{(\delta_c{}^2 + \epsilon \omega_S)} e^{\frac{1}{2}(\delta^2 - \delta_S{}^2)} - \frac{\epsilon \omega_S}{2} \left[\left(\ln \frac{\omega}{\delta_c} \right)^2 - \left(\ln \frac{\omega_S}{\delta_c} \right)^2 \right] \tag{22}$$

Now the Mach number may be expressed in terms of the above velocity ratio by

$$M^2 = \frac{\left(\frac{V}{V_S} \right)^2 M_S{}^2}{1 - \frac{\gamma - 1}{2} M_S{}^2 \left[\left(\frac{V}{V_S} \right)^2 - 1 \right]}$$

[2]Experimental results indicate (as will be shown later) that, at small angles of attack, the shock-wave angles and pressure coefficients in the plane $\varphi = 0$ are approximately the same as those for the circular cone.

which, after substitution of equation (22) and neglecting second-order terms, becomes

$$\left(\frac{M_S}{M}\right)^2 = 1 - \frac{\gamma - 1}{2}\left(M_S\delta_c\right)^2\left\{\left(\frac{\delta}{\delta_c}\right)^2 - \left(\frac{\delta_S}{\delta_c}\right)^2 - 2\left(1 + \frac{\epsilon\omega_S}{\delta_c{}^2}\right)\ln\frac{\omega_S}{\omega} - \frac{\epsilon\omega_S}{\delta_c{}^2}\left[\left(\ln\frac{\omega}{\delta_c}\right)^2 - \left(\ln\frac{\omega_S}{\delta_c}\right)^2\right]\right\} \tag{23}$$

Finally, flow conditions at the shock are obtained from the oblique-shock relations given by equations (15), (16), and (17) reduced to the form

$$\left(\frac{M_S}{M_\infty}\right)^2 = \frac{(\gamma + 1)^2 M_\infty{}^2(\omega_S + \alpha)^2}{[2\gamma M_\infty{}^2(\omega_S + \alpha)^2 - (\gamma - 1)][(\gamma - 1)M_\infty{}^2(\omega_S + \alpha)^2 + 2]} \tag{24}$$

$$M_\infty(\delta_S + \alpha) = \frac{M_\infty{}^2(\omega_S + \alpha)^2 - 1}{\frac{\gamma + 1}{2}M_\infty(\omega_S + \alpha)} \tag{25}$$

and

$$\frac{p_S}{p_\infty} = \frac{2\gamma M_\infty{}^2(\omega_S + \alpha)^2 - (\gamma - 1)}{\gamma + 1} \tag{26}$$

respectively.

There remains the determination of ϵ in order to obtain the shock-wave angle, ω_S, from equations (21) and (25). It can be shown by an analysis identical to that presented in reference 9 that[3]

$$\frac{\epsilon}{\alpha} = \frac{\gamma + 1}{4}\frac{1 + \frac{\gamma + 3}{2}(M_\infty\delta_c)^2}{\left[1 + \frac{\gamma + 1}{2}(M_\infty\delta_c)^2\right]\left\{1 - \frac{\gamma + 1}{8}\ln\left[\frac{(M_\infty\delta_c)^2}{1 + \frac{\gamma + 1}{2}(M_\infty\delta_c)^2}\right]\right\}} \tag{27}$$

The shock angle can now be evaluated by the simultaneous solution of equations (21), (25), and (27). This has been done with the aid of the

[3]An expression for $1 - \epsilon/\alpha$ was developed in reference 9 and differs from the present relation in the logarithm term since only the first term of a logarithm series was retained in that development.

IBM 650 electronic computing machine, and results in the form $(\omega_S/\delta_c)_o$ for values of $M_\infty\delta_c$ from 0.1 to 3.0 and α/δ_c from 0 to 1 are presented in table I. Once the shock-wave angle has been obtained from the table, it is a simple matter to determine all the other flow quantities in the plane $\varphi = 0$ from equations (21) through (27).

Flow conditions in the plane of the wing ($\varphi = \pi/2$).- Because of the presence of the wing in this plane, $w = 0$ and the conical-flow equations obtained for the plane $\varphi = 0$ hold identically in the plane of the wing. Thus, the flow-deflection angle is defined by (noting that $(\omega_S)_{\pi/2} = \lambda$)

$$\frac{\delta}{\delta_c} = \frac{\delta_c}{\omega} - \frac{1}{\delta_c}\left(\frac{\partial w_2}{\partial \varphi}\right)_{\pi/2}\left(\frac{\lambda}{\omega}\right) \ln \frac{\omega}{\delta_c} \tag{28}$$

Similarly, the expressions for the velocity and Mach number become

$$\frac{V}{V_S} = \left(\frac{\omega}{\lambda}\right)^{\delta_c^2+\lambda\left(\frac{\partial w_2}{\partial \varphi}\right)_{\pi/2}} e^{\frac{1}{2}(\delta^2-\delta_S^2) - \frac{\lambda}{2}\left(\frac{\partial w_2}{\partial \varphi}\right)_{\pi/2}\left[\left(\ln \frac{\omega}{\delta_c}\right)^2 - \left(\ln \frac{\lambda}{\delta_c}\right)^2\right]} \tag{29}$$

and

$$\left(\frac{M_S}{M}\right)^2 = 1 - \frac{\gamma - 1}{2}(M_S\delta_c)^2\left\{\left(\frac{\delta}{\delta_c}\right)^2 - \left(\frac{\delta_S}{\delta_c}\right)^2 - 2\left[1 + \frac{\lambda}{\delta_c^2}\left(\frac{\partial w_2}{\partial \varphi}\right)_{\pi/2}\right] \ln \frac{\lambda}{\omega} - \frac{\lambda}{\delta_c^2}\left(\frac{\partial w_2}{\partial \varphi}\right)_{\pi/2}\left[\left(\ln \frac{\omega}{\delta_c}\right)^2 - \left(\ln \frac{\lambda}{\delta_c}\right)^2\right]\right\} \tag{30}$$

respectively. The ratio of the local static pressure to the static pressure at the shock for hypersonic flow is given by

$$\frac{p}{p_S} = \left(\frac{M_S}{M}\right)^{\frac{2\gamma}{\gamma-1}} \tag{31}$$

The Mach number, flow deflection, and static pressure at the shock are, of course, obtained from the oblique-shock relations (15), (16), and (17) which now become

$$\left(\frac{M_S}{M_\infty}\right)^2 = \frac{(\gamma + 1)^2(M_\infty\lambda)^2\cos^2(\Psi)_{\pi/2}}{\left[2\gamma(M_\infty\lambda)^2\cos^2(\Psi)_{\pi/2} - (\gamma - 1)\right]\left[(\gamma - 1)(M_\infty\lambda)^2\cos^2(\Psi)_{\pi/2} + 2\right]} \tag{32}$$

$$\frac{\delta_S}{\delta_c} = \frac{(M_\infty\lambda)^2\cos^2(\Psi)_{\pi/2} - 1}{\frac{\gamma + 1}{2} M_\infty\delta_c M_\infty\lambda \cos(\Psi)_{\pi/2}} \tag{33}$$

and

$$\frac{p_S}{p_\infty} = \frac{2\gamma(M_\infty\lambda)^2\cos^2(\Psi)_{\pi/2} - (\gamma - 1)}{\gamma + 1} \tag{34}$$

respectively. Consider now equation (28) in combination with equation (33). Then,

$$\frac{1}{\delta_c}\left(\frac{\partial w_2}{\partial\varphi}\right)_{\pi/2} = \frac{1 + \frac{\gamma + 1}{2}(M_\infty\delta_c)^2\cos(\Psi)_{\pi/2} - (M_\infty\lambda)^2\cos^2(\Psi)_{\pi/2}}{\frac{\gamma + 1}{2} M_\infty\delta_c M_\infty\lambda \cos(\Psi)_{\pi/2} \ln\frac{\lambda}{\delta_c}} \tag{35}$$

The only remaining unknown in the foregoing expressions is $(\Psi)_{\pi/2}$. If this angle were known, flow conditions on the wing, as well as those around the shock and in the plane $\varphi = 0$, could be calculated by means of the expressions so far obtained. As mentioned earlier in the discussion of the flow pattern shown in sketch (c), $(\Psi)_{\pi/2}$ can be evaluated by matching at the wing-body juncture the pressure calculated in the plane of the wing to the pressure calculated on the surface of the body. Now the static pressure in the plane of the wing can be calculated by means of equations (31) and (34). However, in order to calculate the static pressure on the body surface, expressions defining the flow on this surface must be obtained. Attention is therefore turned to this matter.

Flow conditions on the body surface.- The concept of a vortical singularity in supersonic flow around a cone was introduced by Ferri in reference 10 where it was shown that all constant entropy surfaces must intersect along the generator lying in the meridian plane on the leeward side. It was also demonstrated that for small angles of attack the singularity lies on the surface itself. Holt, in reference 11, demonstrated that such a singularity can arise only at points where the resultant velocity is directed along the radial line (i.e., $w = v = 0$), and that at the singularity the velocity is many-valued and the vorticity is infinite, but the pressure is single-valued. For configurations of the type under

consideration, then, the lines of constant entropy in a plane normal to the configuration axis will appear something like those shown in sketch (e).

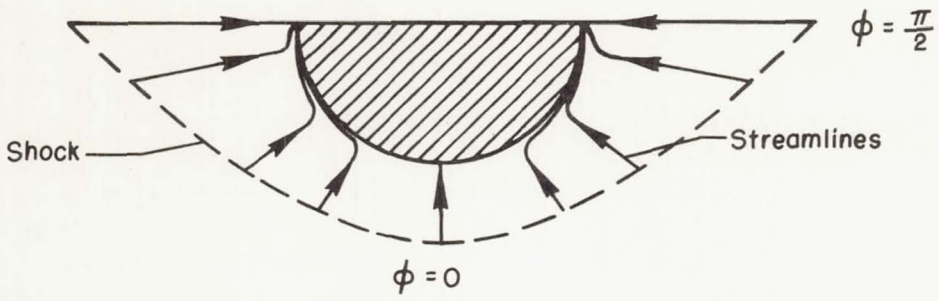

Sketch (e)

The singularities will occur at the wing-body junctures since $w = v = 0$ and $\partial w/\partial\varphi < 0$ at these points. Thus, the angle of attack is assumed sufficiently small that the singularity will remain on the surface of the cone. The thickness of the vortical layer around the cone surface can be neglected then, since it was shown in reference 10 to be the order of α^2. Since the entropy on the surface is constant it must have the value that exists in the plane $\varphi = 0$. Thus,

$$p_c = p_e$$

$$v_c = v_e = 0$$

and

$$E_c = (E)_o$$

where the subscripts c and e refer to conditions inside and outside the vortical layer, respectively. It follows then from equation (1a) that

$$\frac{\partial u}{\partial \varphi} = \delta_c w$$

or

$$\frac{u}{(V_c)_o} = 1 + \delta_c \int_o^{\varphi} \frac{w}{(V_c)_o}\, d\varphi \tag{36}$$

which holds on either side of the vortical layer, even though w is discontinuous across the layer. Consider now the w component of velocity on the surface externally adjacent to the vortical layer expressed in the form

$$\frac{w_e}{(V_c)_o} = F' \tag{37}$$

where the prime in the above expression refers to the derivative with respect to φ. Then, upon integration, equation (36) becomes

$$\frac{u_e}{(V_c)_o} = 1 + \delta_c F \tag{38}$$

and the resultant surface velocity may be written

$$\left[\frac{V_e}{(V_c)_o}\right]^2 = 1 + 2\delta_c F + (F')^2 \tag{39}$$

since, as will be shown subsequently, F and F' are first-order quantities. The corresponding Mach number ratio may be expressed as

$$\left[\frac{(M_c)_o}{M_e}\right]^2 = \frac{1 - \frac{\gamma - 1}{2}(M_c)_o^2\left\{\left[\frac{V_e}{(V_c)_o}\right]^2 - 1\right\}}{\left[\frac{V_e}{(V_c)_o}\right]^2} \tag{40}$$

which, by virtue of equation (39), reduces to

$$\left[\frac{(M_c)_o}{M_e}\right]^2 = 1 - \frac{\gamma - 1}{2}(M_c\delta_c)_o^2\left[2\frac{F}{\delta_c} + \left(\frac{F'}{\delta_c}\right)^2\right] \tag{41}$$

where (from eqs. (9), (11), and (37))

$$\frac{F'}{\delta_c} = \frac{\lambda}{\delta_c}\varphi\left\{\frac{(\omega_S)_o}{\lambda} + \left(\frac{2}{\pi}\right)^2\varphi^2\left[2\left(1 - \frac{(\omega_S)_o}{\lambda}\right) - \frac{\pi}{4}\tan(\psi)_{\pi/2}\right] - \left(\frac{2}{\pi}\right)^4\varphi^4\left[1 - \frac{\pi}{4}\tan(\psi)_{\pi/2} - \frac{(\omega_S)_o}{\lambda}\right]\right\}\left\{\frac{1}{\delta_c}\left(\frac{\partial w_2}{\partial \varphi}\right)_o - \frac{2}{\pi^2}\left[\frac{1}{\delta_c}\left(\frac{\partial w_2}{\partial \varphi}\right)_{\pi/2} + \frac{4}{\delta_c}\left(\frac{\partial w_2}{\partial \varphi}\right)_o\right]\varphi^2 + \frac{8}{\pi^4}\left[\frac{1}{\delta_c}\left(\frac{\partial w_2}{\partial \varphi}\right)_{\pi/2} + \frac{2}{\delta_c}\left(\frac{\partial w_2}{\partial \varphi}\right)_o\right]\varphi^4\right\} \tag{42}$$

and (upon integration of eq. (42))

$$\frac{F}{\delta_c} = \frac{(\omega_S)_o}{\delta_c}\varphi^2\left\{\frac{1}{2\delta_c}\left(\frac{\partial w_2}{\partial \varphi}\right)_o - \frac{1}{2\pi^2}\left[\frac{1}{\delta_c}\left(\frac{\partial w_2}{\partial \varphi}\right)_{\pi/2} + \frac{4}{\delta_c}\left(\frac{\partial w_2}{\partial \varphi}\right)_o\right]\varphi^2 + \frac{4}{3\pi^4}\left[\frac{1}{\delta_c}\left(\frac{\partial w_2}{\partial \varphi}\right)_{\pi/2} + \frac{2}{\delta_c}\left(\frac{\partial w_2}{\partial \varphi}\right)_o\right]\varphi^4\right\} +$$

$$\left(\frac{2}{\pi}\right)^2\left(\frac{\lambda}{\delta_c}\right)\varphi^4\left[2\left(1 - \frac{(\omega_S)_o}{\lambda}\right) - \frac{\pi}{4}\tan(\psi)_{\pi/2}\right]\left\{\frac{1}{4\delta_c}\left(\frac{\partial w_2}{\partial \varphi}\right)_o - \frac{1}{3\pi^2}\left[\frac{1}{\delta_c}\left(\frac{\partial w_2}{\partial \varphi}\right)_{\pi/2} + \frac{4}{\delta_c}\left(\frac{\partial w_2}{\partial \varphi}\right)_o\right]\varphi^2 + \frac{1}{\pi^4}\left[\frac{1}{\delta_c}\left(\frac{\partial w_2}{\partial \varphi}\right)_{\pi/2} + \frac{2}{\delta_c}\left(\frac{\partial w_2}{\partial \varphi}\right)_o\right]\varphi^4\right\} -$$

$$\left(\frac{2}{\pi}\right)^4\left(\frac{\lambda}{\delta_c}\right)\varphi^6\left[1 - \frac{\pi}{4}\tan(\psi)_{\pi/2} - \frac{(\omega_S)_o}{\lambda}\right]\left\{\frac{1}{6\delta_c}\left(\frac{\partial w_2}{\partial \varphi}\right)_o - \frac{1}{4\pi^2}\left[\frac{1}{\delta_c}\left(\frac{\partial w_2}{\partial \varphi}\right)_{\pi/2} + \frac{4}{\delta_c}\left(\frac{\partial w_2}{\partial \varphi}\right)_o\right]\varphi^2 + \frac{4}{5\pi^4}\left[\frac{1}{\delta_c}\left(\frac{\partial w_2}{\partial \varphi}\right)_{\pi/2} + \frac{2}{\delta_c}\left(\frac{\partial w_2}{\partial \varphi}\right)_o\right]\varphi^4\right\} \tag{43}$$

It can be seen from equations (42) and (43) that F' and F are of the order of δ_c. Thus, the two right-hand terms in equation (39) are second-order terms. The Mach number directly on the body surface, M_c, may be related to the Mach number at the vortical layer, M_e, by (see ref. 9)

$$\left(\frac{M_e}{M_c}\right)^2 = e^{\frac{E_c - E_e}{\gamma c_v}}$$

where (by virtue of eq. (4))

$$e^{\frac{E_c - E_e}{\gamma c_v}} = \left[\frac{2\gamma M_\infty^2(\omega_S + \alpha)_o^2 - (\gamma - 1)}{2\gamma(M_\infty\Omega)^2\cos^2\Psi - (\gamma - 1)}\right]^{\frac{1}{\gamma}}\left\{\frac{(M_\infty\Omega)^2\cos^2\Psi[(\gamma - 1)M_\infty^2(\omega_S + \alpha)_o^2 + 2]}{M_\infty^2(\omega_S + \alpha)_o^2[(\gamma - 1)(M_\infty\Omega)^2\cos^2\Psi + 2]}\right\} \tag{44}$$

and Ω and Ψ are defined by equations (12) and (14), respectively. Then,

$$\left[\frac{(M_S)_o}{M_c}\right]^2 = e^{\frac{E_c - E_e}{\gamma c_v}}\left[\frac{(M_c)_o}{M_e}\right]^2\left(\frac{M_S}{M_c}\right)_o^2 \tag{45}$$

and the ratio of the static pressure anywhere on the body surface to the static pressure at the shock at $\varphi = 0$ is given by

$$\frac{p_c}{(p_S)_o} = \left[\frac{(M_S)_o}{M_c}\right]^{\frac{2\gamma}{\gamma - 1}} \tag{46}$$

Finally, the ratio of the surface pressure to the free-stream static pressure may be obtained by the combination of equations (26) and (46) which yields

$$\frac{p_c}{p_\infty} = \left[\frac{2\gamma M_\infty^2(\omega_S + \alpha)_o^2 - (\gamma - 1)}{\gamma + 1}\right]\left[\frac{(M_S)_o}{M_c}\right]^{\frac{2\gamma}{\gamma-1}} \tag{47}$$

The pressure coefficient is, of course, given by the relation

$$C_p = \frac{2}{\gamma M_\infty^2}\left(\frac{p_c}{p_\infty} - 1\right) \tag{48}$$

It will be noted that the foregoing equations predict the ratios of local to free-stream Mach number and local to free-stream static pressures to be the same at corresponding points on related configurations, provided the flow fields about these configurations are defined by the same respective values of the hypersonic similarity parameters, $M_\infty\delta_c$, $M_\infty\alpha$ (or α/δ_c), and $M_\infty\lambda$ (or λ/δ_c). These predictions are in agreement with those of reference 12 for inviscid flow about slender three-dimensional shapes.

Evaluation of $(\Psi)_{\pi/2}$.- We are now in a position to calculate $(\Psi)_{\pi/2}$ and, therefore, all flow properties on the surface of the complete configuration. This may be accomplished in the following manner. If the Mach number, angle of attack, and the conical configuration are given, then $M_\infty\delta_c$, α/δ_c, and λ/δ_c are known and a value for $(\Psi)_{\pi/2}$ is assumed. Then $(\psi)_{\pi/2}$ is known from equation (14) and the pressure under the vortical layer at $\varphi = \pi/2$ can be calculated by means of equation (47). The pressure externally adjacent to the vortical layer in the plane of the wing can be calculated by means of equations (31) and (34). Since there is no pressure change across the vortical layer, an iteration on $(\Psi)_{\pi/2}$ can be performed until the pressures on both sides of the layer are equal. This iteration has been performed on the IBM 650 electronic computing machine and the resulting values of $(\Psi)_{\pi/2}$ for $M_\infty\delta_c$ from 0.1 to 3.0 and α/δ_c from 0 to 1 are given in table I for various values of λ/δ_c. The values of the ratio of the static pressure to the free-stream static pressure at the bottom of the body, $(p_c/p_\infty)_o$, at the wing-body juncture, $(p_c/p_\infty)_{\pi/2}$, and at the leading-edge of the wing, $(p/p_\infty)_\lambda$, are also given in table I.

It should be noted in table I that the range of α/δ_c is restricted for certain values of λ/δ_c. As was mentioned previously in the analysis for conditions at the shock, this results from the fact that there is a maximum angle of attack for a given configuration and Mach number at which the shock wave can no longer remain attached to the leading edge of the wing. This occurs at $(\Psi)_{\pi/2} = 0$, since it represents zero attenuation of the strength of the shock. Thus, the values of λ/δ_c given in table I for $(\Psi)_{\pi/2} = 0$ represent minimum values (maximum leading-edge sweeps) for which the present theory will apply for a particular α/δ_c and, of

course, $M_\infty\delta_c$. This is perhaps more clearly demonstrated in figure 2 where $(\lambda/\delta_c)_{min}$ is shown plotted as a function of $(\alpha/\delta_c)_{max}$ for various $M_\infty\delta_c$. Thus, for example, each line of constant $M_\infty\delta_c$ represents an upper limit of α/δ_c and a lower limit of λ/δ_c on the applicability of the theory for a given free-stream Mach number.

Flow conditions off the surface.- Since only flows at high Mach number are considered in this analysis, the variation of the magnitude of the resultant velocity in a meridian plane will be small. Hence, the variation of u and v will be small and may be represented by a power series in $(\omega - \delta_c)$ where the coefficients are evaluated in terms of the velocity component at the surface and at the shock and its derivative at the surface. Thus,

$$u = u_e + \left(\frac{\partial u}{\partial \omega}\right)_e (\omega - \delta_c)\left(\frac{\omega_S - \omega}{\omega_S - \delta_c}\right) + (u_S - u_e)\left(\frac{\omega - \delta_c}{\omega_S - \delta_c}\right)^2 \tag{49}$$

$$v = \left(\frac{\partial v}{\partial \omega}\right)_e (\omega - \delta_c)\left(\frac{\omega_S - \omega}{\omega_S - \delta_c}\right) + v_S\left(\frac{\omega - \delta_c}{\omega_S - \delta_c}\right)^2 \tag{50}$$

where it can be shown that (see ref. 9)

$$\left(\frac{\partial u}{\partial \omega}\right)_e = \left(\frac{w}{u}\right)_e \left[\left(\frac{\partial w}{\partial \omega}\right)_e + \frac{w_e}{\delta_c}\right]$$

and (setting $v = 0$ in eq. (5))

$$\left(\frac{\partial v}{\partial \omega}\right)_e = \left[u_e + \frac{1}{\delta_c}\left(\frac{\partial w}{\partial \varphi}\right)_e\right]\left[M_e^2\left(\frac{w}{v}\right)_e^2 - 1\right] - u_e$$

In the above expressions, ω_S, w_e, u_e, and M_e are given by equations (9), (11), (38), and (41), respectively, and $(\partial w/\partial \omega)_e$ and $(\partial w/\partial \varphi)_e$ may be obtained by the proper differentiation of equation (9). Finally, the radial component of velocity at the shock may be determined from the relation

$$u_S = V_\infty \cos(\omega_S + \alpha \cos \varphi)$$

and the normal component of velocity may be written

$$v_S = -\sqrt{V_S^2 - u_S^2 - w_S^2}$$

where

$$\left(\frac{V_S}{\hat{V}}\right)^2 = \frac{\frac{\gamma - 1}{2} M_S^2}{1 + \frac{\gamma - 1}{2} M_S^2}$$

The Mach number at the shock, M_S, is defined by equation (15). The components of the local velocity anywhere in the flow field external to the vortical layer and between the planes $\varphi = 0$ and $\varphi = \pi/2$ are now known from equations (9), (49), and (50). Hence, the magnitude and direction of the resultant velocity and, consequently, the Mach number may be easily determined. The local pressure coefficient, then, may be obtained from the relation

$$C_p = \frac{2}{\gamma M_\infty^2}\left(\frac{p_S}{p_\infty}\frac{p}{p_S} - 1\right)$$

where p_S/p_∞ is given by equation (17) and

$$\frac{p}{p_S} = \left(\frac{M_S}{M}\right)^{\frac{2\gamma}{\gamma-1}}$$

The flow field about slender, conical, flat-top wing-body configurations traveling at high supersonic speeds and at small angles of attack can be calculated by means of the foregoing expressions. Explicit expressions defining the lift, drag, and pitching-moment coefficients will now be obtained.

Lift, drag, and pitching-moment coefficients.- Because of the rather complicated nature of the expressions previously developed, resort must be made to graphical or numerical integration of the pressures acting on the surface in order to calculate the integrated aerodynamic forces. It is first undertaken, therefore, to obtain algebraic expressions, yielding the surface pressures, which are amenable to simple analytic integration. In this regard, the tabulated pressure ratios in table I may be used to good advantage. For example, it will be noted from equation (1c) that $\partial p/\partial\varphi = 0$ when $w = v = 0$. On the surface of the body, then, $\partial p/\partial\varphi = 0$ at $\varphi = 0$ and $\varphi = \pi/2$, since $w = v = 0$ at these two points. Therefore, to a good approximation, the variation of static pressure around the body surface may be expressed in the form

$$\frac{p_c}{p_\infty} = \left(\frac{p_c}{p_\infty}\right)_0 \cos^2\varphi + \left(\frac{p_c}{p_\infty}\right)_{\pi/2} \sin^2\varphi \qquad (51)$$

Similarly, the pressure at any axial station on the wing may be expressed in terms of the pressure at the wing-body juncture, the derivative at

this point, and the pressure at the leading edge. Thus[4]

$$\frac{p}{p_\infty} = \left(\frac{p_c}{p_\infty}\right)_{\pi/2} - \left[\left(\frac{p_c}{p_\infty}\right)_{\pi/2} - \left(\frac{p}{p_\infty}\right)_{\lambda}\right]\left(\frac{\tan \omega - \tan \delta_c}{\tan \lambda - \tan \delta_c}\right)^2 \tag{52}$$

since, from equation (1b), $\partial p/\partial \omega = 0$ when $w = v = 0$. The surface pressures can be easily calculated by means of equations (51) and (52) and with the aid of table I. These equations are also easily integrated to obtain the lift, drag, and pitching-moment coefficients. Thus, for example, the normal-force coefficient for the body may be written

$$C_{N_B} = \frac{2l_B{}^2 \tan \delta_c}{\gamma M_\infty{}^2 S} \int_0^{\pi/2} \left(\frac{p_c}{p_\infty} - 1\right) \cos \varphi \, d\varphi \tag{53}$$

whereas that due to the wing may be expressed in the form

$$C_{N_W} = \frac{2}{\gamma M_\infty{}^2 S} \int_{\delta_c}^{\lambda} \left(\frac{p}{p_\infty} - 1\right) r_{te}{}^2 d\omega - \frac{2}{\gamma M_\infty{}^2} \left\{\left[1 - \frac{\gamma - 1}{2} M_\infty(\alpha - \delta_W)\right]^{\frac{2\gamma}{\gamma - 1}} - 1\right\} \tag{54}$$

where S is the total plan area and r_{te} is the radial distance from the vertex of the wing to the trailing edge. The integral term in equation (54) represents the normal force due to the pressures acting on the exposed area of the windward side of the wing whereas the last term is the contribution due to the leeward side of the wing. The axial-force coefficient for the body and the wing may be written (neglecting base drag)

$$C_{A_B} = \frac{2l_B{}^2 \tan^2 \delta_c}{\gamma M_\infty{}^2 S} \int_0^{\pi/2} \left(\frac{p_c}{p_\infty} - 1\right) d\varphi \tag{55}$$

and

$$C_{A_W} = \frac{2 \tan \delta_W}{\gamma M_\infty{}^2} \left\{\left[1 - \frac{\gamma - 1}{2} M_\infty(\alpha - \delta_W)\right]^{\frac{2\gamma}{\gamma - 1}} - 1\right\} \tag{56}$$

[4]The tangents are retained rather than the angles in the following expression to facilitate a subsequent analytic integration to obtain the aerodynamic forces acting on the wing.

respectively. Consider now a configuration having an arrow plan-form wing as shown in sketch (f). Then

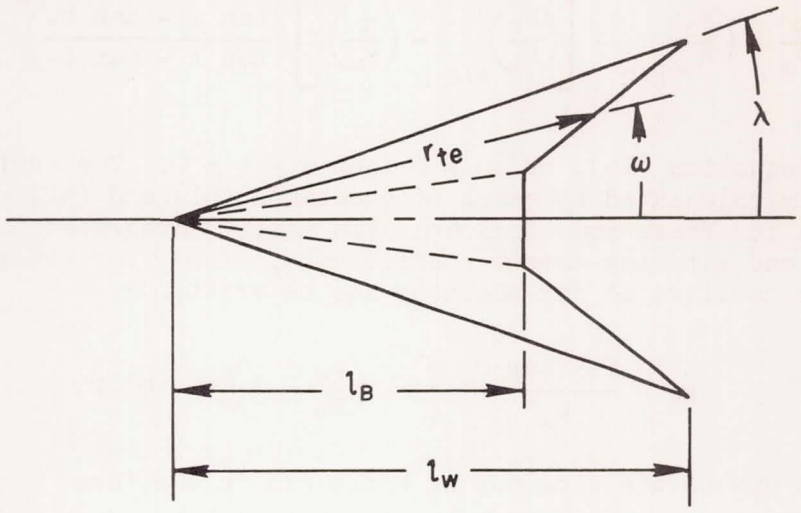

Sketch (f)

$$r_{te} = \frac{l_B l_W(\tan \lambda - \tan \delta_c)\sec \omega}{l_W \tan \lambda - l_B \tan \delta_c - (l_W - l_B)\tan \omega} \tag{57}$$

and

$$S = l_B l_W(\tan \lambda - \tan \delta_c) + l_B{}^2 \tan \delta_c \tag{58}$$

Thus, upon substitution of equations (51) and (58) into (53) and equations (52), (57), and (58) into (54) there is obtained, upon integration,

$$C_{N_B} = \frac{2\left[\frac{2}{3}\left(\frac{p_c}{p_\infty}\right)_0 + \frac{1}{3}\left(\frac{p_c}{p_\infty}\right)_{\pi/2} - 1\right]}{\gamma M_\infty{}^2\left[\left(\frac{l_W}{l_B}\right)\left(\frac{\tan \lambda}{\tan \delta_c} - 1\right) + 1\right]} \tag{59}$$

$$C_{N_W} = \frac{2\left(\frac{l_W}{l_B}\right)\left(\frac{\tan\lambda}{\tan\delta_c} - 1\right)}{\gamma M_\infty^2\left[\left(\frac{l_W}{l_B}\right)\left(\frac{\tan\lambda}{\tan\delta_c} - 1\right) + 1\right]}\left\{\left(\frac{p_c}{p_\infty}\right)_{\pi/2} - 1 - \frac{\left[\left(\frac{p_c}{p_\infty}\right)_{\pi/2} - \left(\frac{p}{p_\infty}\right)_\lambda\right]\left(\frac{l_W}{l_B}\right)\left[\left(\frac{l_W}{l_B}\right)^2 - 2\left(\frac{l_W}{l_B}\right)\ln\frac{l_W}{l_B} - 1\right]}{\left(\frac{l_W}{l_B} - 1\right)^3}\right\} -$$

$$\frac{2}{\gamma M_\infty^2}\left\{\left[1 - \frac{\gamma - 1}{2} M_\infty(\alpha - \delta_W)\right]^{\frac{2\gamma}{\gamma-1}} - 1\right\} \qquad (60)$$

In the case of a delta wing (i.e., $l_W = l_B$), equation (60) is indeterminate in its present form. However, it can be shown that when $l_W = l_B$

$$C_{N_W} = \frac{2\left(1 - \frac{\tan\delta_c}{\tan\lambda}\right)}{\gamma M_\infty^2}\left[\frac{2}{3}\left(\frac{p_c}{p_\infty}\right)_{\pi/2} + \frac{1}{3}\left(\frac{p}{p_\infty}\right)_\lambda - 1\right] -$$

$$\frac{2}{\gamma M_\infty^2}\left\{\left[1 - \frac{\gamma - 1}{2} M_\infty(\alpha - \delta_W)\right]^{\frac{2\gamma}{\gamma-1}} - 1\right\} \qquad (61)$$

The axial-force coefficient due to the body is obtained by the integration of equation (55) which yields

$$C_{A_B} = \frac{\pi \tan\delta_c\left[\frac{1}{2}\left(\frac{p_c}{p_\infty}\right)_0 + \frac{1}{2}\left(\frac{p_c}{p_\infty}\right)_{\pi/2} - 1\right]}{\gamma M_\infty^2\left[\left(\frac{l_W}{l_B}\right)\left(\frac{\tan\lambda}{\tan\delta_c} - 1\right) + 1\right]} \qquad (62)$$

The axial-force coefficient contributed by the wing is given by equation (56). Finally, the lift and pressure-drag coefficients may be calculated from the expressions

$$C_L = C_N \cos \alpha - C_A \sin \alpha \tag{63}$$

$$C_D = C_A \cos \alpha + C_N \sin \alpha \tag{64}$$

where, of course,

$$C_N = C_{N_B} + C_{N_W}$$

$$C_A = C_{A_B} + C_{A_W}$$

Now the expression for the pitching-moment coefficient due to the pressure forces acting on the fuselage side of an arrow plan-form wing may be written (see sketch (f))

$$(C_{m_W})_{lower} = -\frac{4}{3\gamma M_\infty^2 l_B S} \int_{\delta_c}^{\lambda} \left(\frac{p}{p_\infty} - 1\right) r_{te}^3 \cos \omega \, d\omega \tag{65}$$

which, upon substitution of equations (52), (57), and (58), may be integrated to yield

$$(C_{m_W})_{lower} = -\frac{2\left(\frac{l_W}{l_B}\right)\left(\frac{\tan \lambda}{\tan \delta_c} - 1\right)}{3\gamma M_\infty^2 \left[\left(\frac{l_W}{l_B}\right)\left(\frac{\tan \lambda}{\tan \delta_c} - 1\right) + 1\right]} \left\{ \left(\frac{l_W}{l_B} + 1\right)\left[\left(\frac{p_c}{p_\infty}\right)_{\pi/2} - 1\right] - \frac{\left(\frac{l_W}{l_B}\right)^2 \left[\left(\frac{p_c}{p_\infty}\right)_{\pi/2} - \left(\frac{p}{p_\infty}\right)_\lambda\right]\left[\left(\frac{l_W}{l_B} - 3\right)\left(\frac{l_W}{l_B} - 1\right) + 2 \ln \frac{l_W}{l_B}\right]}{\left(\frac{l_W}{l_B} - 1\right)^3} \right\} \tag{66}$$

Since the pressure on the leeward side of the wing is assumed constant, this contribution to the pitching-moment coefficient can be shown to be (by virtue of eq. (7))

$$\left(C_{m_W}\right)_{upper} = \frac{2}{\gamma M_\infty^2}\left\{\left[1 - \frac{\gamma - 1}{2} M_\infty(\alpha - \delta_W)\right]^{\frac{2\gamma}{\gamma-1}} - 1\right\}$$

$$\left\{\frac{2\left(\frac{l_W}{l_B}\right)^3 \frac{\tan\lambda}{\tan\delta_c} - \left(\frac{l_W}{l_B} - 1\right)\left[\left(\frac{l_W}{l_B}\right)\left(\frac{\tan\lambda}{\tan\delta_c} + 1\right) + 2\left(\frac{l_W}{l_B}\right)^2 \frac{\tan\lambda}{\tan\delta_c} + 2\right]}{3\left[\left(\frac{l_W}{l_B}\right)\left(\frac{\tan\lambda}{\tan\delta_c} - 1\right) + 1\right]}\right\} \tag{67}$$

The pitching-moment coefficient for slender conical bodies of revolution is defined by

$$C_{m_B} = -\frac{2}{3} C_{N_B}$$

Thus, the total pitching-moment coefficient may be written

$$C_m = -\frac{2}{3} C_{N_B} + \left(C_{m_W}\right)_{lower} + \left(C_{m_W}\right)_{upper} \tag{68}$$

In the case of a delta wing configuration (i.e., $l_W = l_B$), the total pitching-moment coefficient is, of course,

$$C_m = -\frac{2}{3} C_N$$

The lift and major portion of the pressure drag, as well as the pitching moment, may be calculated by means of the foregoing expressions[5] since the pressure ratios in these expressions are tabulated in table I. It is clear, of course, that the leading-edge drag, base-pressure drag, and skin-friction drag must also be considered in a complete evaluation of the lift and drag characteristics of the configuration.

[5]The retention of the trigonometric functions is optional in these expressions. They have been retained since they result from purely geometrical considerations.

Flow About Pointed Flat-Top Wing-Body Configurations Which are Curved in the Stream Direction

It was demonstrated in reference 13 that many three-dimensional hypersonic flows may be treated by a generalized shock-expansion method which is analogous to that employed in reference 8 for two-dimensional flows. Application of the method in meridian planes about curved bodies of revolution (see ref. 13) indicated that these flow fields could be calculated with good accuracy provided the hypersonic similarity parameter, $M_\infty \delta_c$, is about 1 or greater and the angle of attack is small. Since the present configurations are assumed to have half-bodies of revolution, the generalized shock-expansion method is also applicable to these configurations when $M_\infty \delta_c \geq 1$ and $\alpha \ll 1$. In fact, the general procedure of calculating the flow is identical to that employed in reference 9. It is clear, of course, that the initial conical flow conditions at the vertex are determined from the expressions previously developed in the present paper. In this connection, expressions defining the flow downstream of the vertex are obtained which are applicable to hypersonic flow about slender configurations and, thus, are compatible with those defining the flow at the vertex. The following expressions, then, can be deduced directly from those presented in reference 9 by applying the condition of hypersonic flow and slender bodies. With these points in mind, attention is first turned to the calculation of the flow on the surface of the body.

Flow conditions on the body surface.- The differential equation for Prandtl-Meyer flow relating the change in Mach number with flow inclination angle along a streamline[6] reduces to (see ref. 14)

$$d\mu = \frac{\gamma - 1}{2} d\delta$$

for hypersonic flows. This expression is easily integrated to yield

$$\frac{M_c}{M} = 1 - \frac{\gamma - 1}{2} (M_c \delta_c) \left(1 - \frac{\delta}{\delta_c}\right)$$

where M_c is the Mach number under the vortical layer at the vertex and is defined by equation (45). Now the pressure rise across the shock is given by equation (26) and the ratio of the pressure anywhere on the body surface to the pressure at the shock in the plane $\varphi = 0$ may be determined from the relation

[6]It should be noted that since $w = 0$ at $\varphi = 0$ and $\varphi = \pi/2$, the meridian lines in these two planes are exactly streamlines.

$$\frac{p}{(p_S)_o} = \left[\frac{(M_S)_o}{M}\right]^{\frac{2\gamma}{\gamma-1}}$$

Thus, the expression defining the pressure coefficient anywhere on the surface of the body may be written in the form

$$C_p = \frac{2}{\gamma M_\infty^2}\left\{\frac{2\gamma M_\infty^2(\omega_S+\alpha)_o^2 - (\gamma-1)}{\gamma+1}\left[\frac{(M_S)_o}{M_c} - \frac{\gamma-1}{2}(M_S\delta_c)_o\left(1-\frac{\delta}{\delta_c}\right)\right]^{\frac{2\gamma}{\gamma-1}} - 1\right\}$$

Flow conditions in the plane of the wing.- Flow properties on the wing surface are dictated by the flow field generated by the body in the plane $\varphi = \pi/2$, subject, of course, to the boundary conditions imposed by the wing. Thus, the calculation of the flow in this plane is similar to the calculation of the flow field between the body surface and the shock in a meridian plane for a body of revolution. Consistent, then, with the hypersonic approximations of the present paper, expressions presented in reference 9 for calculating the flow inclination, the static pressure, and the total pressure along a line normal to the body axis a short distance downstream of the vertex reduce to

$$\delta = \delta_B\left[1 - \zeta\left(\frac{y}{y_B} - 1\right)\right] + \left\{\delta_S - \delta_B\left[1 - \zeta\left(\frac{y_S}{y_B} - 1\right)\right]\right\}\left(\frac{y - y_B}{y_S - y_B}\right)^2$$

$$p = p_B\left[1 - \gamma K_B M_B^2(y - y_B)\right] + \left\{p_S - p_B\left[1 - \gamma K_B M_B^2(y_S - y_B)\right]\right\}\left(\frac{y - y_B}{y_S - y_B}\right)^2$$

and

$$p_t = (p_t)_B + \left[\frac{(dp_t/d\theta)(d\theta/dS)}{\theta - \delta}\right]_S (y - y_S) +$$

$$\left\{(p_t)_B - (p_t)_S - \left[\frac{(dp_t/d\theta)(d\theta/dS)}{\theta - \delta}\right]_S (y_B - y_S)\right\}\left(\frac{y - y_S}{y_B - y_S}\right)^2$$

respectively, where B and S are points on the line corresponding to the body surface (wing-body juncture) and the shock (wing leading edge), respectively. The derivatives in the above expressions reduce to

$$\frac{dp_t}{d\theta} = -\frac{4\gamma}{(\gamma+1)\theta}\left[\frac{(\gamma+1)^2(M_\infty\theta)^2}{2\gamma(M_\infty\theta)^2-(\gamma-1)}\right]^{\frac{\gamma}{\gamma-1}}\left\{\frac{[(M_\infty\theta)^2-1]^2}{[(\gamma-1)(M_\infty\theta)^2+2]^{\frac{2\gamma-1}{\gamma-1}}}\right\}$$

and

$$\left(\frac{d\theta}{dS}\right)_{vertex} = K_B\left[\frac{2\gamma(M_\infty\theta)^2-(\gamma-1)}{4M_\infty\theta}\right]\left(\frac{M_c}{M_\infty}\right)\left[1-M_c(\lambda-\delta_c)\right]^{\frac{1}{2\zeta}} \quad (69)$$

where K_B is the curvature of the body at the vertex;

$$\theta = \lambda\cos\Psi \quad (70)$$

$$\zeta = 1 + \frac{\lambda}{\delta_c{}^2}\left(\frac{\partial w_2}{\partial\varphi}\right)_{\pi/2}$$

and $(1/\delta_c)(\partial w_2/\partial\varphi)_{\pi/2}$ is given by equation (35). The derivative given by equation (69) is evaluated at the vertex and therefore can be determined from the previous solution of the flow about flat-top conical configurations. The shock-wave parameter, θ, in the above expressions is defined by equation (70) and represents the shock angle associated with the component of free-stream Mach number normal to the shock at the leading edge. Flow conditions on the surface of the wing in the region of the vertex can be completely determined by means of the foregoing expressions. The remainder of the flow field in the plane of the wing can be calculated by employing the procedure discussed in reference 9 pertaining to bodies of revolution. The pressure on the leeward side of the wing may be calculated from equation (7).

It is interesting to note that the flow about flat-top configurations having wings with straight leading edges, as well as those which are curved in the stream direction, can be calculated by means of the generalized shock-expansion method. To illustrate, consider the following three cases: (1) a wing with leading edges which are curved but with the shock always normal to the leading edge; (2) a wing with constant leading-edge sweep; and (3) a wing with curved leading edges but with local sweeps always less than case (1). All these wings, of course, have supersonic leading edges. Now if the shock is normal to the leading edge, then $\Psi = 0$ (see sketch (c)) and the variation of λ can be determined from equation (70). This is tantamount to replacing θ by λ in the Rankine-Hugoniot shock relations. Thus, case (1) corresponds to the calculation of the flow on a wing which is designed to just contain the flow field bounded by the body surface and the bow shock and the "design" plan form will vary with angle of attack. The flow on the wings corresponding to cases (2) and (3) can also be calculated since λ is known and, therefore, Ψ can be calculated from equation (70) once θ has been determined.

EXPERIMENT

In order to obtain a check on the predictions of the preceding theoretical analysis, the pressures acting on the surfaces of several wing-body configurations were determined experimentally at Mach numbers from 3.0 to 6.0 and at angles of attack up to 6°. A brief description of these tests follows.

Test Apparatus

Tests were conducted in the Ames 10- by 14-inch supersonic wind tunnel. A detailed description of the wind tunnel and auxiliary equipment may be found in reference 15. The pressures acting on the model surfaces were measured with a mercury U-tube manometer or by means of a dibutyl-phthalate U-tube manometer when the pressures were low enough to be recorded on the latter.

Pressure-distribution models were mounted on a 3° bent support which could be pitched through an angle-of-attack range of -3° to $+3^\circ$. The test models consisted of three basic configurations - two conical models and one ogive model. The conical models consisted of thin triangular wings beneath which were mounted fuselages composed of, in one case, one-half of a fineness-ratio-5 cone and, in the other, one-half of a fineness-ratio-2-1/2 cone. Two wings of different leading-edge sweep were tested on each body. In the case of the ogive model, the fuselage consisted of one-half of a fineness-ratio-5 ogive mounted beneath a thin wing, the leading edges of which were coincident with the theoretically determined shock wave for $(\Psi)_{\pi/2} = 0$ (case (1) in the analysis section) at a Mach number of 5.0 and an angle of attack of 3°. The dimensions of these models and the location of the pressure orifices are shown in figure 3.

Pressures on the model surfaces were measured at 0°, 3°, and 6° angles of attack at test Mach numbers of 3.0, 4.0, 5.0, and 6.0. The Reynolds number per foot varied from 8.6 million at Mach number 3.0 to 1.4 million at Mach number 6.0. The pressures around the body surface and on the high-pressure side of the wing were recorded simultaneously at each Mach number and angle of attack at stations symmetrically disposed with respect to the plane of symmetry (i.e., $\pm\varphi$; see fig. 3). These pressures were reduced to coefficient form and the average pressure coefficient was assumed to represent the pressure coefficient at each meridian angle, φ, and ray angle, ω.

Accuracy of Test Results

The variation in Mach number from the nominal value did not exceed ±0.05 in the region of the test section where the models were located. The precision of the computed pressure coefficients was affected by inaccuracies in the pressure measurements, as well as uncertainties in the stream angle and the free-stream dynamic pressure. The resulting errors in pressure coefficients were generally less than ±0.005 throughout the Mach number range for all angles of attack. The meridian angles and angular wing stations at which the pressure coefficients are plotted are considered accurate to within ±1°.

RESULTS AND DISCUSSION

It will be recalled in the development of the theory that the flow field in the plane of symmetry ($\varphi = 0$) was assumed to be the same as that for the circular cone. It is appropriate, therefore, to examine the validity of this assumption before proceeding with a comparison of the theoretical and experimental surface pressures. To this end, the shock-wave angle at $\varphi = 0$ was measured from shadowgraph pictures for each test Mach number at $\alpha = 3°$. The results of these measurements are compared in figure 4 with the shock angles for the complete cones which were also obtained from shadowgraph pictures. Only one set of data is shown for each fuselage since the effect of leading-edge sweep was not discernible from the shadowgraph pictures. Also shown for comparative purposes are the predictions of Stone's first-order theory for inclined circular cones (ref. 16), as presented in reference 17, along with the predictions of the theory of the present paper. It is evident that the wing has little effect on the shock-wave angle of the cone at $\varphi = 0$, at least for angles of attack up to 3°. It will be noted that the present theory yields shock-wave angles which are slightly too large. The variation of pressure coefficient at $\varphi = 0$ with angle of attack for the two test configurations is shown in figure 5 for the test Mach numbers 3.0 and 5.0. Experimental results taken from reference 9 are also shown for the fineness-ratio-2-1/2 cone ($\delta_c = 11.42°$). As in the case of the shock-wave angles, only one set of pressure data for each configuration is shown since the pressures were essentially unaffected by the small changes in leading-edge sweep of the test models. (Experimental data for a fineness-ratio-5 cone were not available.) Stone's second-order theory for inclined cones (ref. 18) applied in the manner described in reference 19 is also presented except for the case where $\delta_c = 11.42°$ and $M_\infty = 5.0$ which is beyond the range of the M.I.T. tables (ref. 20). For this case, the predictions of the theory for inclined cones presented in reference 9 are shown. It appears in figure 5 that the presence of the wing increases the pressures slightly in the plane $\varphi = 0$, particularly in the case of the more slender of the two configurations. However, this effect is sufficiently small

(approximately within the range of experimental scatter) so that it can, for all practical purposes, be neglected. It should be noted that agreement between the present theory and experiment improves with increasing slenderness and increasing Mach number. On the basis of the comparisons shown in figures 4 and 5 it is indicated that, at least for cases where the leading edges of the wing are subsonic ($M < 5$) or moderately supersonic, flow conditions in the plane $\varphi = 0$ can be considered to be the same as those associated with the corresponding circular cone with only a slight loss in accuracy.

The experimental pressure distributions obtained on the four conical flat-top wing-body combinations (see fig. 3) are shown in figures 6, 7, 8, and 9. The data are plotted in the form of surface pressure coefficients as a function of the meridian angle, φ, for the body and as a function of the difference between the ray angle, ω, and the body vertex angle, δ_c, for the wing. Also shown in these figures are the predictions of the present conical-flow theory, where applicable, as well as results obtained from reference 21 for noninclined cones. Although the latter results are strictly applicable only for the cases where the wing leading-edge angle is equal to the axially symmetric shock angle produced by the body (i.e., $M_\infty = 5.0$, $\lambda = 13^\circ$ and $\lambda = 16.9^\circ$; see figs. 6(c) and 8(c)), the theoretical pressure coefficients are nevertheless shown for all test Mach numbers at $\alpha = 0^\circ$. It is interesting to note that the results of reference 21 are in good agreement with experiment even for the subsonic leading-edge cases ($M_\infty < 5$). It also appears from the magnitude and continuous distribution of pressures on the wing at $M_\infty = 6.0$ that the bow shock remains attached to the leading edge and the cone pressure field is distributed over the entire surface of the wing. It should also be noted that the pressures on the body are negligibly affected by the wing at all test Mach numbers at $\alpha = 0^\circ$. Consider now the predictions of the conical flow theory of the present paper. Although the theory is not strictly applicable below a Mach number of 5.0 for the test configurations (see fig. 2), theoretical results obtained for $(\Psi)_{\pi/2} = 0$ are nevertheless shown for the lower test Mach numbers at $\alpha = 0^\circ$. As in the case of the predictions of reference 21, the present theory may, from a practical standpoint, also be considered applicable to wings whose leading edges lay inboard of the bow shock wave at $\alpha = 0^\circ$. It should be recalled, however, that the theory is applicable to hypersonic flow fields and, therefore, would be expected to yield good results only at relatively high Mach numbers. It can be seen from figure 2 that for $\lambda = 13^\circ$ ($\lambda/\delta_c = 2.28$) the theory is applicable only for $\alpha = 0^\circ$ at $M_\infty = 5.0$ and for angles of attack up to 3° ($\alpha/\delta_c = 0.525$) at $M_\infty = 6.0$ (fig. 6). Similarly, when $\lambda = 14.6^\circ$ ($\lambda/\delta_c = 2.55$), the theory is applicable for angles of attack up to 3° at $M_\infty = 5.0$ and for angles of attack up to 5.7° ($\alpha/\delta_c = 1$) at $M_\infty = 6.0$ (fig. 7). The same general remarks concerning the applicability of theory also apply to the less slender configurations. The predictions of theory where applicable are compared with experiment for these configurations in figures 8 and 9. It will be recalled that the development of the theory proceeded from the basic assumptions

that $\delta \ll 1$, $\omega \ll 1$, and $M \gg 1$. It would be expected, then, that theory should yield more reliable results for slender configurations at high Mach numbers. It is indicated by the results shown in figures 6 through 9 that agreement between theory and experiment improves with increasing Mach number and, in general, agreement is better for the more slender configurations. The pressure distributions calculated by means of equations (51) and (52) are also shown in figures 6, 7, 8, and 9 and, in general, are in reasonably good agreement with experiment, although equation (52) tends to overestimate the pressures slightly on the wing (compared to the more exact equation) at $\alpha = 0^\circ$. It should be noted in table I that $(\Psi)_{\pi/2}$ attains its maximum value at $\alpha = 0^\circ$ when $\lambda > (\omega_S)_{\alpha=0}$ and increases quite rapidly with increasing λ. Thus, for example, for the case where $\lambda = 14.6^\circ$ at $M_\infty = 6.0$ and $\alpha = 0^\circ$ (fig. 7(d)), $(\Psi)_{\pi/2}$ is 41°. From the definition of Ψ as shown in figure 1, it can readily be seen that the cross-sectional shape of the conical shock will deviate considerably from a circular arc when $(\Psi)_{\pi/2} = 41^\circ$.

Since the theory is based on the assumptions $\delta \ll 1$ and $\lambda \ll 1$, it is evident that when the wing semivertex angle is large compared to the axially symmetric shock angle produced by the body or, in effect, large values of λ/δ_c, the theory will tend to break down. More experimental data are needed to determine the practical range of applicability of the theory with respect to this parameter. It should be noted, however, that considerations of drag and aerodynamic heating will dictate high sweep and, hence, moderate values of λ/δ_c at hypersonic speeds.

It is of interest now to consider briefly the accuracy of the predictions of theory for the lift, drag, and pitching-moment coefficients. These coefficients have been calculated by means of equations (63), (64), and (68) (and, of course, table I) for a configuration having an arrow plan-form wing ($\lambda = 15^\circ$) beneath which is mounted one-half of a fineness-ratio-5 cone. The results of these calculations for a Mach number of 5.0 along with experimental results taken from reference 2 (model 6 in that reference) are shown in figure 10. The drag polar was obtained by calculating the variation of drag with angle of attack by means of equation (64). The drag coefficient was then matched with the experimentally measured drag coefficient at $\alpha = 0^\circ$. The difference in drag coefficient thus obtained was assumed constant over the angle-of-attack range. In effect, then, the skin-friction drag, leading-edge drag, and base-pressure drag were assumed to be independent of angle of attack. In general, agreement between theory and experiment is good.

As a final point, consideration is now given to the accuracy with which the solutions for flow about conical configurations in combination with the generalized shock-expansion method predict the flow about wing-body combinations which are curved in the stream direction. The pressure distributions on the surface of a configuration having a fuselage consisting of one-half of a fineness-ratio-5 ogive mounted beneath a thin wing whose leading edges were theoretically determined so that they coincided

with the shock wave for $(\Psi)_{\pi/2} = 0$ at $M_\infty = 5.0$ and $\alpha = 3^\circ$ were calculated using the methods of this paper. These distributions along with the results of pressure-distribution tests are presented in figure 11. The trend of the pressure distribution on the wing is in good agreement with experiment. Although the absolute magnitude of the pressure is low, it should be noted that the similarity parameter, $M_\infty \delta_c$, is 1 in this case and, thus, represents the minimum condition for applicability of the shock-expansion method.

CONCLUDING REMARKS

The flow about conical flat-top wing-body configurations at high supersonic speeds was investigated analytically. With the assumptions of high supersonic Mach numbers, slender configurations, supersonic leading edges, and small angles of attack, an approximate theory was developed yielding the Mach number and pressure distributions on the surface. Simple, explicit, algebraic expressions for calculating the lift, pressure-drag, and pitching-moment coefficients were also presented. A solution to the flow about pointed flat-top wing-body configurations which are curved in the stream direction was obtained by combining the conical flow solution with a slender-body approximation to the generalized shock-expansion method.

Surface pressures were obtained experimentally at Mach numbers from 3.0 to 6.0 and angles of attack up to 6° for several flat-top wing-body configurations. These configurations consisted of half-bodies of revolution mounted beneath thin highly swept triangular wings. The bodies of the conical configurations consisted of one-half of a fineness-ratio-5 cone in one case and one-half of a fineness-ratio-2-1/2 cone in the other. The body of the third configuration consisted of one-half of a fineness-ratio-5 ogive. For this configuration, the leading edges of the wing were curved and designed to just maintain the theoretically determined bow shock along the leading edge at a Mach number of 5.0 and an angle of attack of 3°. The predictions of the conical-flow theory of this paper for the surface pressures were in good agreement with experiment at Mach numbers of 5.0 and 6.0 up to angles of attack of approximately 3°. Estimated lift, drag due to lift, and pitching-moment coefficients were in good agreement with existing experiment for a conical configuration at a Mach number of 5.0. The generalized shock-expansion method yielded reasonably good agreement with experiment for the half-ogive configuration at a Mach number of 5.0 and angle of attack of 3°.

Ames Aeronautical Laboratory
National Advisory Committee for Aeronautics
Moffett Field, Calif., June 2, 1958

REFERENCES

1. Eggers, A. J., Jr., and Syvertson, Clarence A.: Aircraft Configurations Developing High Lift-Drag Ratios at High Supersonic Speeds. NACA RM A55L05, 1956.

2. Syvertson, Clarence A., Wong, Thomas J., and Gloria, Hermilo R.: Additional Experiments With Flat-Top Wing-Body Combinations at High Supersonic Speeds. NACA RM A56I11, 1957.

3. Migotsky, E., and Adams, Gaynor J.: Some Properties of Wing and Half-Body Arrangements at Supersonic Speeds. NACA RM A57E15, 1957.

4. Browne, S. H., Friedman, L., and Hodes, I.: A Wing-Body Problem in a Supersonic Conical Flow. Jour. Aero. Sci., vol. 15, no. 8, Aug. 1948, pp. 443-452.

5. Ferri, Antonio, Clarke, Joseph H., and Casaccio, Anthony: Drag Reduction in Lifting Systems by Advantageous Use of Interference. PIBAL Rep. 272, Polytechnic Institute of Brooklyn, Dept. of Aero. Engr. and Appl. Mech., May 1955.

6. Reyn, John W., and Clarke, Joseph H.: An Assessment of Body Lift Contributions and of Linearized Theory for Some Particular Wing-Body Configurations. PIBAL Rep. 305, Polytechnic Institute of Brooklyn, Dept. of Aero. Engr. and Appl. Mech., June 1956.

7. Rossow, Vernon J.: A Theoretical Study of the Lifting Efficiency at Supersonic Speeds of Wings Utilizing Indirect Lift Induced by Vertical Surfaces. NACA RM A55L08, 1956.

8. Eggers, A. J., Jr., Syvertson, Clarence A., and Kraus, Samuel: A Study of Inviscid Flow About Airfoils at High Supersonic Speeds. NACA Rep. 1123, 1953. (Supersedes NACA TN's 2646 and 2729)

9. Savin, Raymond C.: Application of the Generalized Shock-Expansion Method to Inclined Bodies of Revolution Traveling at High Supersonic Speeds. NACA TN 3349, 1955.

10. Ferri, Antonio: Supersonic Flow Around Circular Cones at Angles of Attack. NACA Rep. 1045, 1951. (Supersedes NACA TN 2236)

11. Holt, M.: A Vortical Singularity in Conical Flow. Quart. Jour. Mech. and Appl. Math., vol. VII, pt. 4, Dec. 1954, pp. 438-445.

12. Hamaker, Frank M., Neice, Stanford E., and Wong, Thomas J.: The Similarity Law for Hypersonic Flow and Requirements for Dynamic Similarity of Related Bodies in Free Flight. NACA Rep. 1147, 1953. (Supersedes NACA TN's 2443 and 2631)

13. Eggers, A. J., Jr., and Savin, Raymond C.: A Unified Two-Dimensional Approach to the Calculation of Three-Dimensional Hypersonic Flows, With Application to Bodies of Revolution. NACA Rep. 1249, 1955.

14. Eggers, A. J., Jr., and Savin, Raymond C.: Approximate Methods for Calculating the Flow About Nonlifting Bodies of Revolution. NACA TN 2579, 1951.

15. Eggers, A. J., Jr., and Nothwang, George J.: The Ames 10- by 14-Inch Supersonic Wind Tunnel. NACA TN 3095, 1954.

16. Stone, A. H.: On Supersonic Flow Past a Slightly Yawing Cone. Jour. Math. and Phys., vol. XXVII, no. 1, April 1948, pp. 67-81.

17. Staff of the Computing Section, under the Direction of Zdeněk Kopal: Tables of Supersonic Flow Around Yawing Cones. MIT, Dept. of Elec. Engr., Center of Analysis. Tech. Rep. No. 3, Cambridge, 1947.

18. Stone, A. H.: On Supersonic Flow Past a Slightly Yawing Cone. II. Jour. Math. and Phys., vol. XXX, no. 4, Jan. 1952, pp. 200-213.

19. Roberts, Richard C., and Riley, James D.: A Guide to the Use of the MIT Cone Tables. NAVORD Rep. 2606, 1953.

20. Staff of the Computing Section, under the Direction of Zdeněk Kopal: Tables of Supersonic Flow Around Cones of Large Yaw. MIT, Dept. of Elec. Engr., Center of Analysis. Tech. Rep. No. 5, Cambridge, 1947.

21. Staff of the Computing Section, under the Direction of Zdeněk Kopal: Tables of Supersonic Flow Around Cones. MIT, Dept. of Elec. Engr., Center of Analysis. Tech. Rep. No. 1, 1947.

TABLE I.- FUNCTIONS FOR CALCULATING THE FLOW ABOUT FLAT-TOP CONFIGURATIONS

$M_\infty \delta_c$	$\frac{\lambda}{\delta_c}$	$\frac{a}{\delta_c}$	$\left(\frac{\omega_s}{\delta_c}\right)_o$	$\left(\frac{p_c}{p_\infty}\right)_o$	$(\Psi)_{\pi/2}$	$\left(\frac{p_c}{p_\infty}\right)_{\pi/2}$	$\left(\frac{p}{p_\infty}\right)_\lambda$
0.10	10.1992	0.00	10.0598	01.0399	00.1660	01.0399	01.0138
0.10	10.1992	0.10	09.9854	01.0446	00.1595	01.0429	01.0163
0.10	10.1992	0.20	09.9112	01.0494	00.1522	01.0462	01.0191
0.10	10.1992	0.30	09.8374	01.0546	00.1440	01.0496	01.0220
0.10	10.1992	0.40	09.7638	01.0599	00.1348	01.0533	01.0250
0.10	10.1992	0.50	09.6906	01.0654	00.1243	01.0572	01.0283
0.10	10.1992	0.60	09.6177	01.0711	00.1123	01.0614	01.0317
0.10	10.1992	0.70	09.5451	01.0771	00.0982	01.0657	01.0353
0.10	10.1992	0.80	09.4728	01.0833	00.0809	01.0703	01.0390
0.10	10.1992	0.90	09.4008	01.0896	00.0575	01.0750	01.0429
0.10	10.1992	1.00	09.3292	01.0962	00.0000	01.0799	01.0469
0.10	10.1823	0.00	10.0598	01.0399	00.1557	01.0399	01.0138
0.10	10.1823	0.10	09.9854	01.0446	00.1487	01.0429	01.0164
0.10	10.1823	0.20	09.9112	01.0494	00.1409	01.0462	01.0191
0.10	10.1823	0.30	09.8374	01.0546	00.1320	01.0497	01.0220
0.10	10.1823	0.40	09.7638	01.0599	00.1218	01.0533	01.0251
0.10	10.1823	0.50	09.6906	01.0654	00.1101	01.0573	01.0283
0.10	10.1823	0.60	09.6177	01.0711	00.0964	01.0614	01.0317
0.10	10.1823	0.70	09.5451	01.0771	00.0794	01.0657	01.0353
0.10	10.1823	0.80	09.4728	01.0833	00.0565	01.0703	01.0391
0.10	10.1823	0.90	09.4008	01.0896	00.0000	01.0750	01.0429
0.10	10.1661	0.00	10.0598	01.0399	00.1452	01.0399	01.0139
0.10	10.1661	0.10	09.9854	01.0446	00.1376	01.0429	01.0164
0.10	10.1661	0.20	09.9112	01.0494	00.1290	01.0462	01.0191
0.10	10.1661	0.30	09.8374	01.0546	00.1192	01.0497	01.0220
0.10	10.1661	0.40	09.7638	01.0599	00.1078	01.0534	01.0251
0.10	10.1661	0.50	09.6906	01.0654	00.0944	01.0573	01.0284
0.10	10.1661	0.60	09.6177	01.0711	00.0779	01.0614	01.0318
0.10	10.1661	0.70	09.5451	01.0771	00.0555	01.0657	01.0354
0.10	10.1661	0.80	09.4728	01.0833	00.0000	01.0702	01.0391
0.10	10.1505	0.00	10.0598	01.0399	00.1342	01.0399	01.0139
0.10	10.1505	0.10	09.9854	01.0446	00.1259	01.0429	01.0164
0.10	10.1505	0.20	09.9112	01.0494	00.1164	01.0462	01.0192
0.10	10.1505	0.30	09.8374	01.0546	00.1055	01.0497	01.0221
0.10	10.1505	0.40	09.7638	01.0599	00.0924	01.0534	01.0252
0.10	10.1505	0.50	09.6906	01.0654	00.0763	01.0573	01.0284
0.10	10.1505	0.60	09.6177	01.0711	00.0544	01.0614	01.0318
0.10	10.1505	0.70	09.5451	01.0771	00.0000	01.0657	01.0354
0.10	10.1355	0.00	10.0598	01.0399	00.1227	01.0399	01.0139
0.10	10.1355	0.10	09.9854	01.0446	00.1136	01.0429	01.0165
0.10	10.1355	0.20	09.9112	01.0494	00.1029	01.0462	01.0192
0.10	10.1355	0.30	09.8374	01.0546	00.0903	01.0497	01.0221
0.10	10.1355	0.40	09.7638	01.0599	00.0746	01.0534	01.0252
0.10	10.1355	0.50	09.6906	01.0654	00.0532	01.0573	01.0284
0.10	10.1355	0.60	09.6177	01.0711	00.0000	01.0614	01.0318
0.10	10.1212	0.00	10.0598	01.0399	00.1105	01.0399	01.0139
0.10	10.1212	0.10	09.9854	01.0446	00.1003	01.0429	01.0165
0.10	10.1212	0.20	09.9112	01.0494	00.0881	01.0462	01.0192
0.10	10.1212	0.30	09.8374	01.0546	00.0728	01.0497	01.0221
0.10	10.1212	0.40	09.7638	01.0599	00.0521	01.0534	01.0252
0.10	10.1212	0.50	09.6906	01.0654	00.0000	01.0573	01.0285
0.10	10.1076	0.00	10.0598	01.0399	00.0975	01.0399	01.0139
0.10	10.1076	0.10	09.9854	01.0446	00.0857	01.0429	01.0165
0.10	10.1076	0.20	09.9112	01.0494	00.0710	01.0462	01.0192
0.10	10.1076	0.30	09.8374	01.0546	00.0508	01.0497	01.0222
0.10	10.1076	0.40	09.7638	01.0599	00.0000	01.0534	01.0252
0.10	10.0946	0.00	10.0598	01.0399	00.0833	01.0399	01.0140
0.10	10.0946	0.10	09.9854	01.0446	00.0690	01.0429	01.0165
0.10	10.0946	0.20	09.9112	01.0494	00.0495	01.0462	01.0193
0.10	10.0946	0.30	09.8374	01.0546	00.0000	01.0497	01.0222
0.10	10.0823	0.00	10.0598	01.0399	00.0670	01.0399	01.0140
0.10	10.0823	0.10	09.9854	01.0446	00.0481	01.0429	01.0165
0.10	10.0823	0.20	09.9112	01.0494	00.0000	01.0462	01.0193
0.10	10.0707	0.00	10.0598	01.0399	00.0466	01.0399	01.0140
0.10	10.0707	0.10	09.9854	01.0446	00.0000	01.0429	01.0166
0.10	10.0598	0.00	10.0598	01.0399	00.0000	01.0399	01.0140

TABLE I.- FUNCTIONS FOR CALCULATING THE FLOW ABOUT FLAT-TOP CONFIGURATIONS - Continued

$M_\infty\delta_c$	$\frac{\lambda}{\delta_c}$	$\frac{\alpha}{\delta_c}$	$\left(\frac{\omega_s}{\delta_c}\right)_o$	$\left(\frac{p_c}{p_\infty}\right)_o$	$(\Psi)_{\pi/2}$	$\left(\frac{p_c}{p_\infty}\right)_{\pi/2}$	$\left(\frac{p}{p_\infty}\right)_\lambda$
0.20	05.4437	0.00	05.1186	01.1246	00.3512	01.1246	01.0525
0.20	05.4437	0.10	05.0504	01.1422	00.3356	01.1372	01.0662
0.20	05.4437	0.20	04.9830	01.1606	00.3186	01.1505	01.0806
0.20	05.4437	0.30	04.9163	01.1797	00.2999	01.1645	01.0956
0.20	05.4437	0.40	04.8504	01.1996	00.2792	01.1793	01.1112
0.20	05.4437	0.50	04.7853	01.2202	00.2562	01.1948	01.1274
0.20	05.4437	0.60	04.7210	01.2415	00.2302	01.2110	01.1442
0.20	05.4437	0.70	04.6574	01.2637	00.2001	01.2280	01.1616
0.20	05.4437	0.80	04.5947	01.2866	00.1637	01.2456	01.1795
0.20	05.4437	0.90	04.5328	01.3102	00.1156	01.2639	01.1978
0.20	05.4437	1.00	04.4718	01.3347	00.0000	01.2824	01.2162
0.20	05.4080	0.00	05.1186	01.1246	00.3323	01.1246	01.0529
0.20	05.4080	0.10	05.0504	01.1422	00.3156	01.1372	01.0667
0.20	05.4080	0.20	04.9830	01.1606	00.2973	01.1505	01.0811
0.20	05.4080	0.30	04.9163	01.1797	00.2770	01.1646	01.0961
0.20	05.4080	0.40	04.8504	01.1996	00.2543	01.1793	01.1118
0.20	05.4080	0.50	04.7853	01.2202	00.2286	01.1948	01.1281
0.20	05.4080	0.60	04.7210	01.2415	00.1989	01.2111	01.1449
0.20	05.4080	0.70	04.6574	01.2637	00.1628	01.2280	01.1623
0.20	05.4080	0.80	04.5947	01.2866	00.1150	01.2456	01.1802
0.20	05.4080	0.90	04.5328	01.3102	00.0000	01.2635	01.1982
0.20	05.3730	0.00	05.1186	01.1246	00.3124	01.1246	01.0533
0.20	05.3730	0.10	05.0504	01.1422	00.2944	01.1372	01.0671
0.20	05.3730	0.20	04.9830	01.1606	00.2745	01.1505	01.0815
0.20	05.3730	0.30	04.9163	01.1797	00.2522	01.1646	01.0966
0.20	05.3730	0.40	04.8504	01.1996	00.2269	01.1794	01.1124
0.20	05.3730	0.50	04.7853	01.2202	00.1975	01.1949	01.1287
0.20	05.3730	0.60	04.7210	01.2415	00.1618	01.2111	01.1456
0.20	05.3730	0.70	04.6574	01.2637	00.1144	01.2280	01.1630
0.20	05.3730	0.80	04.5947	01.2866	00.0000	01.2453	01.1805
0.20	05.3385	0.00	05.1186	01.1246	00.2913	01.1246	01.0536
0.20	05.3385	0.10	05.0504	01.1422	00.2718	01.1372	01.0675
0.20	05.3385	0.20	04.9830	01.1606	00.2499	01.1506	01.0820
0.20	05.3385	0.30	04.9163	01.1797	00.2249	01.1646	01.0972
0.20	05.3385	0.40	04.8504	01.1996	00.1959	01.1794	01.1129
0.20	05.3385	0.50	04.7853	01.2202	00.1606	01.1950	01.1293
0.20	05.3385	0.60	04.7210	01.2415	00.1137	01.2111	01.1462
0.20	05.3385	0.70	04.6574	01.2637	00.0000	01.2277	01.1633
0.20	05.3047	0.00	05.1186	01.1246	00.2687	01.1246	01.0540
0.20	05.3047	0.10	05.0504	01.1422	00.2472	01.1372	01.0679
0.20	05.3047	0.20	04.9830	01.1606	00.2227	01.1506	01.0825
0.20	05.3047	0.30	04.9163	01.1797	00.1941	01.1647	01.0977
0.20	05.3047	0.40	04.8504	01.1996	00.1593	01.1795	01.1135
0.20	05.3047	0.50	04.7853	01.2202	00.1129	01.1950	01.1299
0.20	05.3047	0.60	04.7210	01.2415	00.0000	01.2109	01.1465
0.20	05.2716	0.00	05.1186	01.1246	00.2443	01.1246	01.0544
0.20	05.2716	0.10	05.0504	01.1422	00.2202	01.1373	01.0683
0.20	05.2716	0.20	04.9830	01.1606	00.1921	01.1506	01.0829
0.20	05.2716	0.30	04.9163	01.1797	00.1578	01.1647	01.0982
0.20	05.2716	0.40	04.8504	01.1996	00.1120	01.1795	01.1140
0.20	05.2716	0.50	04.7853	01.2202	00.0000	01.1948	01.1302
0.20	05.2393	0.00	05.1186	01.1246	00.2175	01.1246	01.0547
0.20	05.2393	0.10	05.0504	01.1422	00.1899	01.1373	01.0687
0.20	05.2393	0.20	04.9830	01.1606	00.1561	01.1507	01.0834
0.20	05.2393	0.30	04.9163	01.1797	00.1110	01.1647	01.0986
0.20	05.2393	0.40	04.8504	01.1996	00.0000	01.1794	01.1144
0.20	05.2078	0.00	05.1186	01.1246	00.1874	01.1246	01.0550
0.20	05.2078	0.10	05.0504	01.1422	00.1543	01.1373	01.0691
0.20	05.2078	0.20	04.9830	01.1606	00.1098	01.1507	01.0838
0.20	05.2078	0.30	04.9163	01.1797	00.0000	01.1646	01.0990
0.20	05.1771	0.00	05.1186	01.1246	00.1522	01.1246	01.0554
0.20	05.1771	0.10	05.0504	01.1422	00.1085	01.1373	01.0695
0.20	05.1771	0.20	04.9830	01.1606	00.0000	01.1506	01.0841
0.20	05.1474	0.00	05.1186	01.1246	00.1070	01.1246	01.0557
0.20	05.1474	0.10	05.0504	01.1422	00.0000	01.1373	01.0698
0.20	05.1186	0.00	05.1186	01.1246	00.0000	01.1246	01.0560

TABLE I.- FUNCTIONS FOR CALCULATING THE FLOW ABOUT FLAT-TOP CONFIGURATIONS - Continued

$M_\infty\delta_c$	$\frac{\lambda}{\delta_c}$	$\frac{\alpha}{\delta_c}$	$\left(\frac{\omega_B}{\delta_c}\right)_0$	$\left(\frac{p_c}{p_\infty}\right)_0$	$(\Psi)_{\pi/2}$	$\left(\frac{p_c}{p_\infty}\right)_{\pi/2}$	$\left(\frac{p}{p_\infty}\right)_\lambda$
0.30	03.9427	0.00	03.5087	01.2390	00.4847	01.2391	01.1112
0.30	03.9427	0.10	03.4464	01.2735	00.4617	01.2627	01.1417
0.30	03.9427	0.20	03.3853	01.3097	00.4368	01.2878	01.1735
0.30	03.9427	0.30	03.3255	01.3476	00.4098	01.3146	01.2065
0.30	03.9427	0.40	03.2670	01.3871	00.3802	01.3429	01.2407
0.30	03.9427	0.50	03.2099	01.4284	00.3477	01.3728	01.2761
0.30	03.9427	0.60	03.1541	01.4714	00.3112	01.4043	01.3125
0.30	03.9427	0.70	03.0997	01.5162	00.2694	01.4373	01.3499
0.30	03.9427	0.80	03.0466	01.5628	00.2194	01.4719	01.3882
0.30	03.9427	0.90	02.9950	01.6112	00.1539	01.5078	01.4272
0.30	03.9427	1.00	02.9447	01.6615	00.0000	01.5438	01.4655
0.30	03.8971	0.00	03.5087	01.2390	00.4608	01.2390	01.1127
0.30	03.8971	0.10	03.4464	01.2735	00.4362	01.2627	01.1433
0.30	03.8971	0.20	03.3853	01.3097	00.4095	01.2879	01.1752
0.30	03.8971	0.30	03.3255	01.3476	00.3802	01.3147	01.2084
0.30	03.8971	0.40	03.2670	01.3871	00.3478	01.3430	01.2428
0.30	03.8971	0.50	03.2099	01.4284	00.3115	01.3730	01.2782
0.30	03.8971	0.60	03.1541	01.4714	00.2699	01.4044	01.3147
0.30	03.8971	0.70	03.0997	01.5162	00.2199	01.4374	01.3521
0.30	03.8971	0.80	03.0466	01.5628	00.1544	01.4717	01.3903
0.30	03.8971	0.90	02.9950	01.6112	00.0000	01.5064	01.4280
0.30	03.8519	0.00	03.5087	01.2390	00.4353	01.2390	01.1142
0.30	03.8519	0.10	03.4464	01.2735	00.4089	01.2627	01.1450
0.30	03.8519	0.20	03.3853	01.3097	00.3799	01.2879	01.1770
0.30	03.8519	0.30	03.3255	01.3476	00.3478	01.3148	01.2103
0.30	03.8519	0.40	03.2670	01.3871	00.3117	01.3431	01.2448
0.30	03.8519	0.50	03.2099	01.4284	00.2701	01.3731	01.2803
0.30	03.8519	0.60	03.1541	01.4714	00.2203	01.4045	01.3168
0.30	03.8519	0.70	03.0997	01.5162	00.1549	01.4373	01.3542
0.30	03.8519	0.80	03.0466	01.5628	00.0000	01.4706	01.3913
0.30	03.8071	0.00	03.5087	01.2390	00.4079	01.2390	01.1157
0.30	03.8071	0.10	03.4464	01.2735	00.3793	01.2627	01.1466
0.30	03.8071	0.20	03.3853	01.3097	00.3474	01.2880	01.1788
0.30	03.8071	0.30	03.3255	01.3476	00.3116	01.3149	01.2122
0.30	03.8071	0.40	03.2670	01.3871	00.2702	01.3432	01.2467
0.30	03.8071	0.50	03.2099	01.4284	00.2206	01.3731	01.2823
0.30	03.8071	0.60	03.1541	01.4714	00.1552	01.4044	01.3188
0.30	03.8071	0.70	03.0997	01.5162	00.0000	01.4363	01.3552
0.30	03.7627	0.00	03.5087	01.2390	00.3782	01.2390	01.1172
0.30	03.7627	0.10	03.4464	01.2735	00.3467	01.2628	01.1482
0.30	03.7627	0.20	03.3853	01.3097	00.3112	01.2881	01.1805
0.30	03.7627	0.30	03.3255	01.3476	00.2701	01.3149	01.2141
0.30	03.7627	0.40	03.2670	01.3871	00.2207	01.3433	01.2487
0.30	03.7627	0.50	03.2099	01.4284	00.1555	01.3731	01.2842
0.30	03.7627	0.60	03.1541	01.4714	00.0000	01.4037	01.3199
0.30	03.7188	0.00	03.5087	01.2390	00.3457	01.2390	01.1187
0.30	03.7188	0.10	03.4464	01.2735	00.3105	01.2628	01.1499
0.30	03.7188	0.20	03.3853	01.3097	00.2698	01.2881	01.1823
0.30	03.7188	0.30	03.3255	01.3476	00.2206	01.3150	01.2159
0.30	03.7188	0.40	03.2670	01.3871	00.1557	01.3433	01.2505
0.30	03.7188	0.50	03.2099	01.4284	00.0000	01.3725	01.2854
0.30	03.6754	0.00	03.5087	01.2390	00.3094	01.2390	01.1202
0.30	03.6754	0.10	03.4464	01.2735	00.2691	01.2628	01.1515
0.30	03.6754	0.20	03.3853	01.3097	00.2203	01.2882	01.1840
0.30	03.6754	0.30	03.3255	01.3476	00.1557	01.3150	01.2176
0.30	03.6754	0.40	03.2670	01.3871	00.0000	01.3429	01.2517
0.30	03.6326	0.00	03.5087	01.2390	00.2681	01.2390	01.1217
0.30	03.6326	0.10	03.4464	01.2735	00.2198	01.2628	01.1531
0.30	03.6326	0.20	03.3853	01.3097	00.1556	01.2882	01.1856
0.30	03.6326	0.30	03.3255	01.3476	00.0000	01.3147	01.2189
0.30	03.5905	0.00	03.5087	01.2390	00.2189	01.2390	01.1231
0.30	03.5905	0.10	03.4464	01.2735	00.1552	01.2629	01.1546
0.30	03.5905	0.20	03.3853	01.3097	00.0000	01.2880	01.1870
0.30	03.5492	0.00	03.5087	01.2390	00.1547	01.2390	01.1246
0.30	03.5492	0.10	03.4464	01.2735	00.0000	01.2628	01.1560
0.30	03.5087	0.00	03.5087	01.2390	00.0000	01.2390	01.1260

TABLE I.- FUNCTIONS FOR CALCULATING THE FLOW ABOUT FLAT-TOP CONFIGURATIONS - Continued

$M_\infty\delta_c$	$\frac{\lambda}{\delta_c}$	$\frac{a}{\delta_c}$	$\left(\frac{\omega_s}{\delta_c}\right)_0$	$\left(\frac{p_c}{p_\infty}\right)_0$	$(\Psi)_{\pi/2}$	$\left(\frac{p_c}{p_\infty}\right)_{\pi/2}$	$\left(\frac{p}{p_\infty}\right)_\lambda$
0.40	03.2269	0.00	02.7295	01.3783	00.5840	01.3788	01.1862
0.40	03.2269	0.10	02.6729	01.4336	00.5546	01.4141	01.2381
0.40	03.2269	0.20	02.6181	01.4921	00.5231	01.4522	01.2920
0.40	03.2269	0.30	02.5652	01.5536	00.4893	01.4931	01.3477
0.40	03.2269	0.40	02.5141	01.6183	00.4527	01.5368	01.4052
0.40	03.2269	0.50	02.4649	01.6863	00.4128	01.5834	01.4643
0.40	03.2269	0.60	02.4176	01.7576	00.3684	01.6328	01.5250
0.40	03.2269	0.70	02.3721	01.8323	00.3180	01.6850	01.5871
0.40	03.2269	0.80	02.3285	01.9104	00.2580	01.7399	01.6506
0.40	03.2269	0.90	02.2867	01.9921	00.1799	01.7973	01.7149
0.40	03.2269	1.00	02.2467	02.0774	00.0000	01.8544	01.7771
0.40	03.1754	0.00	02.7295	01.3783	00.5567	01.3787	01.1901
0.40	03.1754	0.10	02.6729	01.4336	00.5254	01.4140	01.2421
0.40	03.1754	0.20	02.6181	01.4921	00.4916	01.4522	01.2961
0.40	03.1754	0.30	02.5652	01.5536	00.4551	01.4931	01.3519
0.40	03.1754	0.40	02.5141	01.6183	00.4151	01.5369	01.4094
0.40	03.1754	0.50	02.4649	01.6863	00.3706	01.5834	01.4686
0.40	03.1754	0.60	02.4176	01.7576	00.3200	01.6327	01.5293
0.40	03.1754	0.70	02.3721	01.8323	00.2598	01.6848	01.5913
0.40	03.1754	0.80	02.3285	01.9104	00.1814	01.7392	01.6543
0.40	03.1754	0.90	02.2867	01.9921	00.0000	01.7937	01.7155
0.40	03.1242	0.00	02.7295	01.3783	00.5273	01.3786	01.1939
0.40	03.1242	0.10	02.6729	01.4336	00.4938	01.4140	01.2460
0.40	03.1242	0.20	02.6181	01.4921	00.4573	01.4522	01.3001
0.40	03.1242	0.30	02.5652	01.5536	00.4173	01.4932	01.3560
0.40	03.1242	0.40	02.5141	01.6183	00.3728	01.5369	01.4136
0.40	03.1242	0.50	02.4649	01.6863	00.3220	01.5834	01.4728
0.40	03.1242	0.60	02.4176	01.7576	00.2617	01.6326	01.5334
0.40	03.1242	0.70	02.3721	01.8323	00.1829	01.6842	01.5950
0.40	03.1242	0.80	02.3285	01.9104	00.0000	01.7362	01.6553
0.40	03.0732	0.00	02.7295	01.3783	00.4956	01.3785	01.1977
0.40	03.0732	0.10	02.6729	01.4336	00.4592	01.4140	01.2499
0.40	03.0732	0.20	02.6181	01.4921	00.4193	01.4522	01.3041
0.40	03.0732	0.30	02.5652	01.5536	00.3748	01.4932	01.3601
0.40	03.0732	0.40	02.5141	01.6183	00.3239	01.5369	01.4177
0.40	03.0732	0.50	02.4649	01.6863	00.2634	01.5834	01.4768
0.40	03.0732	0.60	02.4176	01.7576	00.1844	01.6322	01.5371
0.40	03.0732	0.70	02.3721	01.8323	00.0000	01.6818	01.5964
0.40	03.0227	0.00	02.7295	01.3783	00.4609	01.3785	01.2015
0.40	03.0227	0.10	02.6729	01.4336	00.4211	01.4140	01.2539
0.40	03.0227	0.20	02.6181	01.4921	00.3766	01.4523	01.3081
0.40	03.0227	0.30	02.5652	01.5536	00.3258	01.4933	01.3642
0.40	03.0227	0.40	02.5141	01.6183	00.2651	01.5369	01.4217
0.40	03.0227	0.50	02.4649	01.6863	00.1858	01.5831	01.4806
0.40	03.0227	0.60	02.4176	01.7576	00.0000	01.6303	01.5388
0.40	02.9725	0.00	02.7295	01.3783	00.4225	01.3784	01.2053
0.40	02.9725	0.10	02.6729	01.4336	00.3782	01.4140	01.2578
0.40	02.9725	0.20	02.6181	01.4921	00.3274	01.4523	01.3121
0.40	02.9725	0.30	02.5652	01.5536	00.2667	01.4933	01.3681
0.40	02.9725	0.40	02.5141	01.6183	00.1872	01.5368	01.4255
0.40	02.9725	0.50	02.4649	01.6863	00.0000	01.5816	01.4827
0.40	02.9227	0.00	02.7295	01.3783	00.3795	01.3783	01.2091
0.40	02.9227	0.10	02.6729	01.4336	00.3288	01.4140	01.2616
0.40	02.9227	0.20	02.6181	01.4921	00.2681	01.4523	01.3160
0.40	02.9227	0.30	02.5652	01.5536	00.1886	01.4932	01.3719
0.40	02.9227	0.40	02.5141	01.6183	00.0000	01.5357	01.4279
0.40	02.8734	0.00	18.3036	11.8904	00.3299	01.3783	01.2129
0.40	02.8734	0.10	02.6729	01.4336	00.2693	01.4140	01.2655
0.40	02.8734	0.20	02.6181	01.4921	00.1898	01.4523	01.3197
0.40	02.8734	0.30	02.5652	01.5536	00.0000	01.4925	01.3746
0.40	02.8247	0.00	02.7295	01.3783	00.2702	01.3783	01.2166
0.40	02.8247	0.10	02.6729	01.4336	00.1908	01.4140	01.2692
0.40	02.8247	0.20	02.6181	01.4921	00.0000	01.4518	01.3228
0.40	02.7767	0.00	02.7295	01.3783	00.1916	01.3783	01.2203
0.40	02.7767	0.10	02.6729	01.4336	00.0000	01.4138	01.2725
0.40	02.7295	0.00	02.7295	01.3783	00.0000	01.3783	01.2240

TABLE I.- FUNCTIONS FOR CALCULATING THE FLOW ABOUT FLAT-TOP CONFIGURATIONS - Continued

$M_\infty \delta_c$	$\frac{\lambda}{\delta_c}$	$\frac{a}{\delta_c}$	$\left(\frac{\omega_s}{\delta_c}\right)_0$	$\left(\frac{p_c}{p_\infty}\right)_0$	$(\Psi)_{\pi/2}$	$\left(\frac{p_c}{p_\infty}\right)_{\pi/2}$	$\left(\frac{p}{p_\infty}\right)_\lambda$
0.50	02.8166	0.00	02.2804	01.5412	00.6607	01.5432	01.2758
0.50	02.8166	0.10	02.2294	01.6217	00.6257	01.5905	01.3536
0.50	02.8166	0.20	02.1808	01.7073	00.5886	01.6424	01.4339
0.50	02.8166	0.30	02.1345	01.7981	00.5493	01.6988	01.5165
0.50	02.8166	0.40	02.0906	01.8942	00.5071	01.7598	01.6014
0.50	02.8166	0.50	02.0489	01.9958	00.4614	01.8254	01.6886
0.50	02.8166	0.60	02.0095	02.1029	00.4109	01.8956	01.7780
0.50	02.8166	0.70	01.9722	02.2158	00.3538	01.9706	01.8694
0.50	02.8166	0.80	01.9371	02.3346	00.2863	02.0500	01.9626
0.50	02.8166	0.90	01.9040	02.4592	00.1987	02.1335	02.0570
0.50	02.8166	1.00	01.8728	02.5900	00.0000	02.2161	02.1472
0.50	02.7605	0.00	02.2804	01.5412	00.6305	01.5428	01.2835
0.50	02.7605	0.10	02.2294	01.6217	00.5933	01.5902	01.3611
0.50	02.7605	0.20	02.1808	01.7073	00.5538	01.6421	01.4412
0.50	02.7605	0.30	02.1345	01.7981	00.5114	01.6985	01.5237
0.50	02.7605	0.40	02.0906	01.8942	00.4654	01.7594	01.6084
0.50	02.7605	0.50	02.0489	01.9958	00.4146	01.8249	01.6953
0.50	02.7605	0.60	02.0095	02.1029	00.3571	01.8949	01.7844
0.50	02.7605	0.70	01.9722	02.2158	00.2892	01.9694	01.8753
0.50	02.7605	0.80	01.9371	02.3346	00.2010	02.0480	01.9675
0.50	02.7605	0.90	01.9040	02.4592	00.0000	02.1262	02.0560
0.50	02.7049	0.00	02.2804	01.5412	00.5979	01.5425	01.2912
0.50	02.7049	0.10	02.2294	01.6217	00.5582	01.5899	01.3686
0.50	02.7049	0.20	02.1808	01.7073	00.5156	01.6418	01.4485
0.50	02.7049	0.30	02.1345	01.7981	00.4693	01.6982	01.5308
0.50	02.7049	0.40	02.0906	01.8942	00.4183	01.7591	01.6153
0.50	02.7049	0.50	02.0489	01.9958	00.3604	01.8244	01.7019
0.50	02.7049	0.60	02.0095	02.1029	00.2920	01.8942	01.7904
0.50	02.7049	0.70	01.9722	02.2158	00.2032	01.9679	01.8804
0.50	02.7049	0.80	01.9371	02.3346	00.0000	02.0419	01.9673
0.50	02.6497	0.00	02.2804	01.5412	00.5625	01.5422	01.2988
0.50	02.6497	0.10	02.2294	01.6217	00.5197	01.5897	01.3760
0.50	02.6497	0.20	02.1808	01.7073	00.4733	01.6416	01.4557
0.50	02.6497	0.30	02.1345	01.7981	00.4219	01.6980	01.5377
0.50	02.6497	0.40	02.0906	01.8942	00.3638	01.7588	01.6219
0.50	02.6497	0.50	02.0489	01.9958	00.2949	01.8239	01.7081
0.50	02.6497	0.60	02.0095	02.1029	00.2056	01.8930	01.7958
0.50	02.6497	0.70	01.9722	02.2158	00.0000	01.9630	01.8811
0.50	02.5950	0.00	02.2804	01.5412	00.5237	01.5419	01.3063
0.50	02.5950	0.10	02.2294	01.6217	00.4771	01.5895	01.3833
0.50	02.5950	0.20	02.1808	01.7073	00.4255	01.6415	01.4628
0.50	02.5950	0.30	02.1345	01.7981	00.3670	01.6978	01.5445
0.50	02.5950	0.40	02.0906	01.8942	00.2978	01.7584	01.6283
0.50	02.5950	0.50	02.0489	01.9958	00.2079	01.8231	01.7138
0.50	02.5950	0.60	02.0095	02.1029	00.0000	01.8891	01.7975
0.50	02.5408	0.00	02.2804	01.5412	00.4806	01.5417	01.3138
0.50	02.5408	0.10	02.2294	01.6217	00.4289	01.5893	01.3906
0.50	02.5408	0.20	02.1808	01.7073	00.3702	01.6413	01.4698
0.50	02.5408	0.30	02.1345	01.7981	00.3007	01.6976	01.5511
0.50	02.5408	0.40	02.0906	01.8942	00.2102	01.7579	01.6343
0.50	02.5408	0.50	02.0489	01.9958	00.0000	01.8201	01.7163
0.50	02.4872	0.00	02.2804	01.5412	00.4321	01.5415	01.3213
0.50	02.4872	0.10	02.2294	01.6217	00.3732	01.5892	01.3977
0.50	02.4872	0.20	02.1808	01.7073	00.3034	01.6412	01.4766
0.50	02.4872	0.30	02.1345	01.7981	00.2126	01.6973	01.5573
0.50	02.4872	0.40	02.0906	01.8942	00.0000	01.7557	01.6376
0.50	02.4342	0.00	02.2804	01.5412	00.3760	01.5413	01.3286
0.50	02.4342	0.10	02.2294	01.6217	00.3060	01.5891	01.4048
0.50	02.4342	0.20	02.1808	01.7073	00.2148	01.6410	01.4831
0.50	02.4342	0.30	02.1345	01.7981	00.0000	01.6957	01.5616
0.50	02.3820	0.00	02.2804	01.5412	00.3083	01.5412	01.3359
0.50	02.3820	0.10	02.2294	01.6217	00.2169	01.5890	01.4116
0.50	02.3820	0.20	02.1808	01.7073	00.0000	01.6401	01.4882
0.50	02.3306	0.00	02.2804	01.5412	00.2188	01.5412	01.3430
0.50	02.3306	0.10	02.2294	01.6217	00.0000	01.5886	01.4176
0.50	02.2804	0.00	02.2804	01.5412	00.0000	01.5412	01.3500

TABLE I.- FUNCTIONS FOR CALCULATING THE FLOW ABOUT FLAT-TOP CONFIGURATIONS - Continued

$M_\infty\delta_c$	$\frac{\lambda}{\delta_c}$	$\frac{\alpha}{\delta_c}$	$\left(\frac{\omega_s}{\delta_c}\right)_o$	$\left(\frac{p_c}{p_\infty}\right)_o$	$(\Psi)_{\pi/2}$	$\left(\frac{p_c}{p_\infty}\right)_{\pi/2}$	$\left(\frac{p}{p_\infty}\right)_\lambda$
0.60	02.5563	0.00	01.9944	01.7278	00.7218	01.7336	01.3797
0.60	02.5563	0.10	01.9489	01.8384	00.6817	01.7931	01.4882
0.60	02.5563	0.20	01.9062	01.9567	00.6400	01.8595	01.5992
0.60	02.5563	0.30	01.8661	02.0830	00.5960	01.9329	01.7129
0.60	02.5563	0.40	01.8287	02.2175	00.5493	02.0132	01.8297
0.60	02.5563	0.50	01.7938	02.3603	00.4990	02.1006	01.9494
0.60	02.5563	0.60	01.7613	02.5118	00.4437	02.1952	02.0721
0.60	02.5563	0.70	01.7311	02.6719	00.3814	02.2970	02.1977
0.60	02.5563	0.80	01.7030	02.8410	00.3079	02.4058	02.3258
0.60	02.5563	0.90	01.6770	03.0191	00.2128	02.5209	02.4555
0.60	02.5563	1.00	01.6529	03.2063	00.0000	02.6341	02.5779
0.60	02.4964	0.00	01.9944	01.7278	00.6889	01.7325	01.3932
0.60	02.4964	0.10	01.9489	01.8384	00.6467	01.7921	01.5006
0.60	02.4964	0.20	01.9062	01.9567	00.6023	01.8585	01.6107
0.60	02.4964	0.30	01.8661	02.0830	00.5551	01.9317	01.7237
0.60	02.4964	0.40	01.8287	02.2175	00.5043	02.0119	01.8397
0.60	02.4964	0.50	01.7938	02.3603	00.4485	02.0991	01.9586
0.60	02.4964	0.60	01.7613	02.5118	00.3857	02.1932	02.0804
0.60	02.4964	0.70	01.7311	02.6719	00.3116	02.2942	02.2048
0.60	02.4964	0.80	01.7030	02.8410	00.2157	02.4015	02.3310
0.60	02.4964	0.90	01.6770	03.0191	00.0000	02.5079	02.4509
0.60	02.4372	0.00	01.9944	01.7278	00.6533	01.7315	01.4065
0.60	02.4372	0.10	01.9489	01.8384	00.6085	01.7911	01.5129
0.60	02.4372	0.20	01.9062	01.9567	00.5609	01.8575	01.6221
0.60	02.4372	0.30	01.8661	02.0830	00.5096	01.9307	01.7343
0.60	02.4372	0.40	01.8287	02.2175	00.4534	02.0108	01.8494
0.60	02.4372	0.50	01.7938	02.3603	00.3900	02.0976	01.9674
0.60	02.4372	0.60	01.7613	02.5118	00.3153	02.1912	02.0881
0.60	02.4372	0.70	01.7311	02.6719	00.2186	02.2909	02.2107
0.60	02.4372	0.80	01.7030	02.8410	00.0000	02.3907	02.3280
0.60	02.3785	0.00	01.9944	01.7278	00.6145	01.7306	01.4196
0.60	02.3785	0.10	01.9489	01.8384	00.5666	01.7903	01.5249
0.60	02.3785	0.20	01.9062	01.9567	00.5149	01.8567	01.6332
0.60	02.3785	0.30	01.8661	02.0830	00.4582	01.9299	01.7445
0.60	02.3785	0.40	01.8287	02.2175	00.3943	02.0097	01.8587
0.60	02.3785	0.50	01.7938	02.3603	00.3190	02.0961	01.9757
0.60	02.3785	0.60	01.7613	02.5118	00.2216	02.1886	02.0947
0.60	02.3785	0.70	01.7311	02.6719	00.0000	02.2822	02.2094
0.60	02.3206	0.00	01.9944	01.7278	00.5719	01.7298	01.4325
0.60	02.3206	0.10	01.9489	01.8384	00.5200	01.7896	01.5367
0.60	02.3206	0.20	01.9062	01.9567	00.4629	01.8561	01.6441
0.60	02.3206	0.30	01.8661	02.0830	00.3986	01.9291	01.7544
0.60	02.3206	0.40	01.8287	02.2175	00.3227	02.0086	01.8676
0.60	02.3206	0.50	01.7938	02.3603	00.2246	02.0942	01.9829
0.60	02.3206	0.60	01.7613	02.5118	00.0000	02.1817	02.0951
0.60	02.2634	0.00	01.9944	01.7278	00.5247	01.7291	01.4451
0.60	02.2634	0.10	01.9489	01.8384	00.4674	01.7891	01.5483
0.60	02.2634	0.20	01.9062	01.9567	00.4027	01.8555	01.6547
0.60	02.2634	0.30	01.8661	02.0830	00.3263	01.9284	01.7639
0.60	02.2634	0.40	01.8287	02.2175	00.2275	02.0073	01.8756
0.60	02.2634	0.50	01.7938	02.3603	00.0000	02.0889	01.9851
0.60	02.2072	0.00	01.9944	01.7278	00.4714	01.7286	01.4575
0.60	02.2072	0.10	01.9489	01.8384	00.4065	01.7886	01.5596
0.60	02.2072	0.20	01.9062	01.9567	00.3298	01.8550	01.6649
0.60	02.2072	0.30	01.8661	02.0830	00.2304	01.9275	01.7728
0.60	02.2072	0.40	01.8287	02.2175	00.0000	02.0033	01.8794
0.60	02.1520	0.00	01.9944	01.7278	00.4098	01.7282	01.4696
0.60	02.1520	0.10	01.9489	01.8384	00.3329	01.7882	01.5706
0.60	02.1520	0.20	01.9062	01.9567	00.2331	01.8545	01.6745
0.60	02.1520	0.30	01.8661	02.0830	00.0000	01.9247	01.7784
0.60	02.0980	0.00	01.9944	01.7278	00.3356	01.7279	01.4814
0.60	02.0980	0.10	01.9489	01.8384	00.2357	01.7880	01.5812
0.60	02.0980	0.20	01.9062	01.9567	00.0000	01.8528	01.6819
0.60	02.0454	0.00	01.9944	01.7278	00.2378	01.7277	01.4929
0.60	02.0454	0.10	01.9489	01.8384	00.0000	01.7872	01.5904
0.60	01.9944	0.00	01.9944	01.7278	00.0000	01.7278	01.5040

TABLE I.- FUNCTIONS FOR CALCULATING THE FLOW ABOUT FLAT-TOP CONFIGURATIONS - Continued

$M_\infty\delta_c$	$\frac{\lambda}{\delta_c}$	$\frac{\alpha}{\delta_c}$	$\left(\frac{\omega_s}{\delta_c}\right)_0$	$\left(\frac{p_c}{p_\infty}\right)_0$	$(\Psi)_{\pi/2}$	$\left(\frac{p_c}{p_\infty}\right)_{\pi/2}$	$\left(\frac{p}{p_\infty}\right)_\lambda$
0.70	023802	0.00	01.8002	01.9388	00.7711	01.9522	01.4990
0.70	023802	0.10	01.7598	02.0849	00.7265	02.0239	01.6431
0.70	023802	0.20	01.7225	02.2420	00.6807	02.1057	01.7894
0.70	023802	0.30	01.6880	02.4106	00.6330	02.1975	01.9388
0.70	023802	0.40	01.6563	02.5909	00.5825	02.2994	02.0918
0.70	023802	0.50	01.6273	02.7832	00.5284	02.4117	02.2488
0.70	023802	0.60	01.6006	02.9876	00.4692	02.5344	02.4098
0.70	023802	0.70	01.5761	03.2045	00.4027	02.6677	02.5747
0.70	023802	0.80	01.5538	03.4339	00.3244	02.8113	02.7429
0.70	023802	0.90	01.5333	03.6760	00.2234	02.9640	02.9130
0.70	023802	1.00	01.5147	03.9309	00.0000	03.1133	03.0720
0.70	023171	0.00	01.8002	01.9388	00.7357	01.9496	01.5204
0.70	023171	0.10	01.7598	02.0849	00.6891	02.0214	01.6618
0.70	023171	0.20	01.7225	02.2420	00.6407	02.1032	01.8059
0.70	023171	0.30	01.6880	02.4106	00.5897	02.1949	01.9535
0.70	023171	0.40	01.6563	02.5909	00.5350	02.2966	02.1049
0.70	023171	0.50	01.6273	02.7832	00.4752	02.4084	02.2603
0.70	023171	0.60	01.6006	02.9876	00.4080	02.5304	02.4196
0.70	023171	0.70	01.5761	03.2045	00.3290	02.6625	02.5823
0.70	023171	0.80	01.5538	03.4339	00.2269	02.8036	02.7473
0.70	023171	0.90	01.5333	03.6760	00.0000	02.9431	02.9027
0.70	022548	0.00	01.8002	01.9388	00.6973	01.9473	01.5412
0.70	022548	0.10	01.7598	02.0849	00.6483	02.0192	01.6800
0.70	022548	0.20	01.7225	02.2420	00.5967	02.1010	01.8220
0.70	022548	0.30	01.6880	02.4106	00.5414	02.1925	01.9677
0.70	022548	0.40	01.6563	02.5909	00.4810	02.2940	02.1174
0.70	022548	0.50	01.6273	02.7832	00.4132	02.4053	02.2710
0.70	022548	0.60	01.6006	02.9876	00.3335	02.5264	02.4283
0.70	022548	0.70	01.5761	03.2045	00.2305	02.6565	02.5880
0.70	022548	0.80	01.5538	03.4339	00.0000	02.7864	02.7397
0.70	021932	0.00	01.8002	01.9388	00.6555	01.9452	01.5614
0.70	021932	0.10	01.7598	02.0849	00.6034	02.0173	01.6977
0.70	021932	0.20	01.7225	02.2420	00.5476	02.0991	01.8376
0.70	021932	0.30	01.6880	02.4106	00.4867	02.1905	01.9815
0.70	021932	0.40	01.6563	02.5909	00.4183	02.2916	02.1293
0.70	021932	0.50	01.6273	02.7832	00.3379	02.4022	02.2809
0.70	021932	0.60	01.6006	02.9876	00.2340	02.5218	02.4352
0.70	021932	0.70	01.5761	03.2045	00.0000	02.6425	02.5831
0.70	021325	0.00	01.8002	01.9388	00.6095	01.9434	01.5811
0.70	021325	0.10	01.7598	02.0849	00.5534	02.0156	01.7149
0.70	021325	0.20	01.7225	02.2420	00.4921	02.0974	01.8527
0.70	021325	0.30	01.6880	02.4106	00.4232	02.1887	01.9946
0.70	021325	0.40	01.6563	02.5909	00.3422	02.2893	02.1404
0.70	021325	0.50	01.6273	02.7832	00.2375	02.3987	02.2892
0.70	021325	0.60	01.6006	02.9876	00.0000	02.5107	02.4331
0.70	02.0730	0.00	01.8002	01.9388	00.5585	01.9418	01.6002
0.70	02.0730	0.10	01.7598	02.0849	00.4969	02.0142	01.7316
0.70	02.0730	0.20	01.7225	02.2420	00.4277	02.0960	01.8673
0.70	02.0730	0.30	01.6880	02.4106	00.3462	02.1870	02.0071
0.70	02.0730	0.40	01.6563	02.5909	00.2408	02.2867	02.1502
0.70	02.0730	0.50	01.6273	02.7832	00.0000	02.3902	02.2899
0.70	02.0147	0.00	01.8002	01.9388	00.5009	01.9406	01.6187
0.70	02.0147	0.10	01.7598	02.0849	00.4316	02.0131	01.7478
0.70	02.0147	0.20	01.7225	02.2420	00.3498	02.0948	01.8812
0.70	02.0147	0.30	01.6880	02.4106	00.2439	02.1852	02.0185
0.70	02.0147	0.40	01.6563	02.5909	00.0000	02.2804	02.1538
0.70	01.9580	0.00	01.8002	01.9388	00.4346	01.9396	01.6366
0.70	01.9580	0.10	01.7598	02.0849	00.3529	02.0123	01.7633
0.70	01.9580	0.20	01.7225	02.2420	00.2468	02.0937	01.8943
0.70	01.9580	0.30	01.6880	02.4106	00.0000	02.1808	02.0250
0.70	01.9031	0.00	01.8002	01.9388	00.3550	01.9390	01.6538
0.70	01.9031	0.10	01.7598	02.0849	00.2491	02.0116	01.7781
0.70	01.9031	0.20	01.7225	02.2420	00.0000	02.0910	01.9039
0.70	01.8504	0.00	01.8002	01.9388	00.2507	01.9387	01.6703
0.70	01.8504	0.10	01.7598	02.0849	00.0000	02.0104	01.7907
0.70	01.8002	0.00	01.8002	01.9388	00.0000	01.9388	01.6860

TABLE I.- FUNCTIONS FOR CALCULATING THE FLOW ABOUT FLAT-TOP CONFIGURATIONS - Continued

$M_\infty\delta_c$	$\frac{\lambda}{\delta_c}$	$\frac{\alpha}{\delta_c}$	$\left(\frac{\omega_s}{\delta_c}\right)_0$	$\left(\frac{p_c}{p_\infty}\right)_0$	$(\Psi)_{\pi/2}$	$\left(\frac{p_c}{p_\infty}\right)_{\pi/2}$	$\left(\frac{p}{p_\infty}\right)_\lambda$
0.80	02.2554	0.00	01.6621	02.1751	00.8110	02.2017	01.6354
0.80	02.2554	0.10	01.6264	02.3623	00.7622	02.2852	01.8204
0.80	02.2554	0.20	01.5939	02.5647	00.7130	02.3829	02.0066
0.80	02.2554	0.30	01.5643	02.7827	00.6621	02.4947	02.1961
0.80	02.2554	0.40	01.5376	03.0165	00.6086	02.6207	02.3901
0.80	02.2554	0.50	01.5133	03.2666	00.5514	02.7610	02.5891
0.80	02.2554	0.60	01.4914	03.5330	00.4891	02.9159	02.7933
0.80	02.2554	0.70	01.4716	03.8161	00.4191	03.0855	03.0026
0.80	02.2554	0.80	01.4538	04.1159	00.3371	03.2694	03.2162
0.80	02.2554	0.90	01.4376	04.4326	00.2313	03.4658	03.4320
0.80	02.2554	1.00	01.4230	04.7662	00.0000	03.6570	03.6316
0.80	02.1897	0.00	01.6621	02.1751	00.7733	02.1965	01.6667
0.80	02.1897	0.10	01.6264	02.3623	00.7230	02.2803	01.8463
0.80	02.1897	0.20	01.5939	02.5647	00.6713	02.3782	02.0285
0.80	02.1897	0.30	01.5643	02.7827	00.6170	02.4898	02.2148
0.80	02.1897	0.40	01.5376	03.0165	00.5592	02.6154	02.4060
0.80	02.1897	0.50	01.5133	03.2666	00.4961	02.7551	02.6024
0.80	02.1897	0.60	01.4914	03.5330	00.4254	02.9091	02.8039
0.80	02.1897	0.70	01.4716	03.8161	00.3424	03.0770	03.0099
0.80	02.1897	0.80	01.4538	04.1159	00.2355	03.2573	03.2186
0.80	02.1897	0.90	01.4376	04.4326	00.0000	03.4349	03.4135
0.80	02.1247	0.00	01.6621	02.1751	00.7325	02.1917	01.6967
0.80	02.1247	0.10	01.6264	02.3623	00.6800	02.2760	01.8714
0.80	02.1247	0.20	01.5939	02.5647	00.6251	02.3739	02.0497
0.80	02.1247	0.30	01.5643	02.7827	00.5666	02.4854	02.2328
0.80	02.1247	0.40	01.5376	03.0165	00.5029	02.6107	02.4211
0.80	02.1247	0.50	01.5133	03.2666	00.4315	02.7497	02.6146
0.80	02.1247	0.60	01.4914	03.5330	00.3477	02.9023	02.8129
0.80	02.1247	0.70	01.4716	03.8161	00.2396	03.0674	03.0143
0.80	02.1247	0.80	01.4538	04.1159	00.0000	03.2319	03.2042
0.80	02.0607	0.00	01.6621	02.1751	00.6880	02.1875	01.7256
0.80	02.0607	0.10	01.6264	02.3623	00.6326	02.2721	01.8955
0.80	02.0607	0.20	01.5939	02.5647	00.5736	02.3702	02.0702
0.80	02.0607	0.30	01.5643	02.7827	00.5094	02.4816	02.2501
0.80	02.0607	0.40	01.5376	03.0165	00.4373	02.6064	02.4353
0.80	02.0607	0.50	01.5133	03.2666	00.3527	02.7444	02.6255
0.80	02.0607	0.60	01.4914	03.5330	00.2437	02.8949	02.8194
0.80	02.0607	0.70	01.4716	03.8161	00.0000	03.0468	03.0040
0.80	01.9977	0.00	01.6621	02.1751	00.6390	02.1839	01.7534
0.80	01.9977	0.10	01.6264	02.3623	00.5798	02.2688	01.9189
0.80	01.9977	0.20	01.5939	02.5647	00.5152	02.3669	02.0898
0.80	01.9977	0.30	01.5643	02.7827	00.4427	02.4781	02.2664
0.80	01.9977	0.40	01.5376	03.0165	00.3575	02.6023	02.4483
0.80	01.9977	0.50	01.5133	03.2666	00.2476	02.7387	02.6343
0.80	01.9977	0.60	01.4914	03.5330	00.0000	02.8785	02.8132
0.80	01.9362	0.00	01.6621	02.1751	00.5846	02.1808	01.7800
0.80	01.9362	0.10	01.6264	02.3623	00.5200	02.2661	01.9413
0.80	01.9362	0.20	01.5939	02.5647	00.4473	02.3642	02.1086
0.80	01.9362	0.30	01.5643	02.7827	00.3618	02.4751	02.2817
0.80	01.9362	0.40	01.5376	03.0165	00.2512	02.5981	02.4594
0.80	01.9362	0.50	01.5133	03.2666	00.0000	02.7260	02.6324
0.80	01.8763	0.00	01.6621	02.1751	00.5233	02.1783	01.8056
0.80	01.8763	0.10	01.6264	02.3623	00.4509	02.2639	01.9628
0.80	01.8763	0.20	01.5939	02.5647	00.3654	02.3620	02.1264
0.80	01.8763	0.30	01.5643	02.7827	00.2544	02.4720	02.2954
0.80	01.8763	0.40	01.5376	03.0165	00.0000	02.5887	02.4620
0.80	01.8185	0.00	01.6621	02.1751	00.4528	02.1765	01.8300
0.80	01.8185	0.10	01.6264	02.3623	00.3678	02.2623	01.9833
0.80	01.8185	0.20	01.5939	02.5647	00.2571	02.3600	02.1429
0.80	01.8185	0.30	01.5643	02.7827	00.0000	02.4655	02.3025
0.80	01.7632	0.00	01.6621	02.1751	00.3686	02.1754	01.8533
0.80	01.7632	0.10	01.6264	02.3623	00.2588	02.2611	02.0026
0.80	01.7632	0.20	01.5939	02.5647	00.0000	02.3560	02.1546
0.80	01.7109	0.00	01.6621	02.1751	00.2593	02.1749	01.8753
0.80	01.7109	0.10	01.6264	02.3623	00.0000	02.2594	02.0189
0.80	01.6621	0.00	01.6621	02.1751	00.0000	02.1751	01.8960

TABLE I.- FUNCTIONS FOR CALCULATING THE FLOW ABOUT FLAT-TOP CONFIGURATIONS - Continued

$M_\infty \delta_c$	$\frac{\lambda}{\delta_c}$	$\frac{\alpha}{\delta_c}$	$\left(\frac{\omega_s}{\delta_c}\right)_0$	$\left(\frac{p_c}{p_\infty}\right)_0$	$(\Psi)_{\pi/2}$	$\left(\frac{p_c}{p_\infty}\right)_{\pi/2}$	$\left(\frac{p}{p_\infty}\right)_\lambda$
0.90	02.1638	0.00	01.5603	02.4374	00.8430	02.4847	01.7914
0.90	02.1638	0.10	01.5288	02.6719	00.7907	02.5790	02.0222
0.90	02.1638	0.20	01.5006	02.9261	00.7385	02.6931	02.2527
0.90	02.1638	0.30	01.4753	03.2007	00.6850	02.8263	02.4867
0.90	02.1638	0.40	01.4527	03.4959	00.6291	02.9786	02.7261
0.90	02.1638	0.50	01.4325	03.8121	00.5694	03.1502	02.9720
0.90	02.1638	0.60	01.4144	04.1495	00.5044	03.3414	03.2244
0.90	02.1638	0.70	01.3983	04.5082	00.4318	03.5522	03.4831
0.90	02.1638	0.80	01.3840	04.8883	00.3467	03.7821	03.7472
0.90	02.1638	0.90	01.3711	05.2900	00.2373	04.0286	04.0135
0.90	02.1638	1.00	01.3596	05.7133	00.0000	04.2673	04.2579
0.90	02.0959	0.00	01.5603	02.4374	00.8034	02.4751	01.8342
0.90	02.0959	0.10	01.5288	02.6719	00.7500	02.5705	02.0560
0.90	02.0959	0.20	01.5006	02.9261	00.6955	02.6850	02.2802
0.90	02.0959	0.30	01.4753	03.2007	00.6387	02.8182	02.5094
0.90	02.0959	0.40	01.4527	03.4959	00.5782	02.9701	02.7446
0.90	02.0959	0.50	01.4325	03.8121	00.5125	03.1410	02.9866
0.90	02.0959	0.60	01.4144	04.1495	00.4389	03.3309	03.2350
0.90	02.0959	0.70	01.3983	04.5082	00.3528	03.5395	03.4891
0.90	02.0959	0.80	01.3840	04.8883	00.2420	03.7647	03.7463
0.90	02.0959	0.90	01.3711	05.2900	00.0000	03.9856	03.9847
0.90	02.0288	0.00	01.5603	02.4374	00.7606	02.4665	01.8747
0.90	02.0288	0.10	01.5288	02.6719	00.7053	02.5629	02.0885
0.90	02.0288	0.20	01.5006	02.9261	00.6478	02.6777	02.3067
0.90	02.0288	0.30	01.4753	03.2007	00.5867	02.8109	02.5310
0.90	02.0288	0.40	01.4527	03.4959	00.5202	02.9625	02.7620
0.90	02.0288	0.50	01.4325	03.8121	00.4459	03.1325	02.9997
0.90	02.0288	0.60	01.4144	04.1495	00.3588	03.3208	03.2435
0.90	02.0288	0.70	01.3983	04.5082	00.2467	03.5256	03.4911
0.90	02.0288	0.80	01.3840	04.8883	00.0000	03.7293	03.7230
0.90	01.9627	0.00	01.5603	02.4374	00.7138	02.4589	01.9133
0.90	01.9627	0.10	01.5288	02.6719	00.6559	02.5562	02.1196
0.90	01.9627	0.20	01.5006	02.9261	00.5943	02.6714	02.3321
0.90	01.9627	0.30	01.4753	03.2007	00.5274	02.8045	02.5515
0.90	01.9627	0.40	01.4527	03.4959	00.4524	02.9556	02.7780
0.90	01.9627	0.50	01.4325	03.8121	00.3645	03.1245	03.0110
0.90	01.9627	0.60	01.4144	04.1495	00.2512	03.3097	03.2486
0.90	01.9627	0.70	01.3983	04.5082	00.0000	03.4968	03.4735
0.90	01.8978	0.00	01.5603	02.4374	00.6622	02.4524	01.9500
0.90	01.8978	0.10	01.5288	02.6719	00.6007	02.5504	02.1495
0.90	01.8978	0.20	01.5006	02.9261	00.5336	02.6659	02.3564
0.90	01.8978	0.30	01.4753	03.2007	00.4582	02.7989	02.5709
0.90	01.8978	0.40	01.4527	03.4959	00.3697	02.9493	02.7925
0.90	01.8978	0.50	01.4325	03.8121	00.2555	03.1159	03.0194
0.90	01.8978	0.60	01.4144	04.1495	00.0000	03.2869	03.2368
0.90	01.8345	0.00	01.5603	02.4374	00.6049	02.4470	01.9851
0.90	01.8345	0.10	01.5288	02.6719	00.5382	02.5456	02.1781
0.90	01.8345	0.20	01.5006	02.9261	00.4629	02.6613	02.3795
0.90	01.8345	0.30	01.4753	03.2007	00.3742	02.7940	02.5888
0.90	01.8345	0.40	01.4527	03.4959	00.2594	02.9428	02.8044
0.90	01.8345	0.50	01.4325	03.8121	00.0000	03.0982	03.0137
0.90	01.7733	0.00	01.5603	02.4374	00.5404	02.4427	02.0184
0.90	01.7733	0.10	01.5288	02.6719	00.4659	02.5419	02.2053
0.90	01.7733	0.20	01.5006	02.9261	00.3775	02.6576	02.4012
0.90	01.7733	0.30	01.4753	03.2007	00.2627	02.7893	02.6046
0.90	01.7733	0.40	01.4527	03.4959	00.0000	02.9297	02.8050
0.90	01.7147	0.00	01.5603	02.4374	00.4664	02.4397	02.0500
0.90	01.7147	0.10	01.5288	02.6719	00.3791	02.5392	02.2311
0.90	01.7147	0.20	01.5006	02.9261	00.2650	02.6545	02.4212
0.90	01.7147	0.30	01.4753	03.2007	00.0000	02.7802	02.6117
0.90	01.6592	0.00	01.5603	02.4374	00.3784	02.4378	02.0799
0.90	01.6592	0.10	01.5288	02.6719	00.2659	02.5373	02.2552
0.90	01.6592	0.20	01.5006	02.9261	00.0000	02.6490	02.4349
0.90	01.6075	0.00	01.5603	02.4374	00.2649	02.4371	02.1079
0.90	01.6075	0.10	01.5288	02.6719	00.0000	02.5350	02.2754
0.90	01.5603	0.00	01.5603	02.4374	00.0000	02.4374	02.1340

TABLE I.- FUNCTIONS FOR CALCULATING THE FLOW ABOUT FLAT-TOP CONFIGURATIONS - Continued

$M_\infty \delta_c$	$\frac{\lambda}{\delta_c}$	$\frac{\alpha}{\delta_c}$	$\left(\frac{\omega_s}{\delta_c}\right)_0$	$\left(\frac{p_c}{p_\infty}\right)_0$	$(\Psi)_{\pi/2}$	$\left(\frac{p_c}{p_\infty}\right)_{\pi/2}$	$\left(\frac{p}{p_\infty}\right)_\lambda$
1.00	02.0945	0.00	01.4832	02.7266	00.8685	02.8033	01.9691
1.00	02.0945	0.10	01.4555	03.0143	00.8132	02.9071	02.2502
1.00	02.0945	0.20	01.4310	03.3271	00.7587	03.0376	02.5290
1.00	02.0945	0.30	01.4093	03.6656	00.7031	03.1934	02.8118
1.00	02.0945	0.40	01.3902	04.0300	00.6451	03.3742	03.1013
1.00	02.0945	0.50	01.3733	04.4207	00.5834	03.5804	03.3986
1.00	02.0945	0.60	01.3584	04.8379	00.5164	03.8120	03.7040
1.00	02.0945	0.70	01.3452	05.2816	00.4415	04.0691	04.0172
1.00	02.0945	0.80	01.3335	05.7520	00.3540	04.3508	04.3367
1.00	02.0945	0.90	01.3232	06.2491	00.2417	04.6538	04.6585
1.00	02.0945	1.00	01.3140	06.7728	00.0000	04.9458	04.9517
1.00	02.0249	0.00	01.4832	02.7266	00.8274	02.7872	02.0244
1.00	02.0249	0.10	01.4555	03.0143	00.7714	02.8934	02.2922
1.00	02.0249	0.20	01.4310	03.3271	00.7147	03.0249	02.5622
1.00	02.0249	0.30	01.4093	03.6656	00.6558	03.1810	02.8382
1.00	02.0249	0.40	01.3902	04.0300	00.5932	03.3617	03.1219
1.00	02.0249	0.50	01.3733	04.4207	00.5253	03.5671	03.4139
1.00	02.0249	0.60	01.3584	04.8379	00.4495	03.7972	03.7140
1.00	02.0249	0.70	01.3452	05.2816	00.3608	04.0515	04.0210
1.00	02.0249	0.80	01.3335	05.7520	00.2469	04.3270	04.3314
1.00	02.0249	0.90	01.3232	06.2491	00.0000	04.5964	04.6171
1.00	01.9561	0.00	01.4832	02.7266	00.7829	02.7730	02.0763
1.00	01.9561	0.10	01.4555	03.0143	00.7254	02.8811	02.3324
1.00	01.9561	0.20	01.4310	03.3271	00.6658	03.0136	02.5940
1.00	01.9561	0.30	01.4093	03.6656	00.6026	03.1701	02.8633
1.00	01.9561	0.40	01.3902	04.0300	00.5339	03.3505	03.1411
1.00	01.9561	0.50	01.3733	04.4207	00.4572	03.5549	03.4274
1.00	01.9561	0.60	01.3584	04.8379	00.3674	03.7830	03.7212
1.00	01.9561	0.70	01.3452	05.2816	00.2521	04.0323	04.0195
1.00	01.9561	0.80	01.3335	05.7520	00.0000	04.2798	04.2972
1.00	01.8882	0.00	01.4832	02.7266	00.7343	02.7605	02.1253
1.00	01.8882	0.10	01.4555	03.0143	00.6744	02.8704	02.3708
1.00	01.8882	0.20	01.4310	03.3271	00.6109	03.0037	02.6243
1.00	01.8882	0.30	01.4093	03.6656	00.5417	03.1604	02.8869
1.00	01.8882	0.40	01.3902	04.0300	00.4644	03.3404	03.1585
1.00	01.8882	0.50	01.3733	04.4207	00.3737	03.5435	03.4384
1.00	01.8882	0.60	01.3584	04.8379	00.2571	03.7677	03.7239
1.00	01.8882	0.70	01.3452	05.2816	00.0000	03.9941	03.9928
1.00	01.8217	0.00	01.4832	02.7266	00.6807	02.7499	02.1716
1.00	01.8217	0.10	01.4555	03.0143	00.6174	02.8613	02.4074
1.00	01.8217	0.20	01.4310	03.3271	00.5483	02.9953	02.6532
1.00	01.8217	0.30	01.4093	03.6656	00.4706	03.1521	02.9090
1.00	01.8217	0.40	01.3902	04.0300	00.3794	03.3312	03.1739
1.00	01.8217	0.50	01.3733	04.4207	00.2618	03.5315	03.4456
1.00	01.8217	0.60	01.3584	04.8379	00.0000	03.7373	03.7049
1.00	01.7570	0.00	01.4832	02.7266	00.6210	02.7412	02.2156
1.00	01.7570	0.10	01.4555	03.0143	00.5526	02.8538	02.4424
1.00	01.7570	0.20	01.4310	03.3271	00.4753	02.9883	02.6806
1.00	01.7570	0.30	01.4093	03.6656	00.3841	03.1448	02.9292
1.00	01.7570	0.40	01.3902	04.0300	00.2659	03.3221	03.1861
1.00	01.7570	0.50	01.3733	04.4207	00.0000	03.5080	03.4348
1.00	01.6947	0.00	01.4832	02.7266	00.5538	02.7344	02.2572
1.00	01.6947	0.10	01.4555	03.0143	00.4777	02.8479	02.4756
1.00	01.6947	0.20	01.4310	03.3271	00.3872	02.9827	02.7062
1.00	01.6947	0.30	01.4093	03.6656	00.2692	03.1380	02.9468
1.00	01.6947	0.40	01.3902	04.0300	00.0000	03.3046	03.1838
1.00	01.6354	0.00	01.4832	02.7266	00.4767	02.7296	02.2966
1.00	01.6354	0.10	01.4555	03.0143	00.3879	02.8438	02.5070
1.00	01.6354	0.20	01.4310	03.3271	00.2711	02.9781	02.7296
1.00	01.6354	0.30	01.4093	03.6656	00.0000	03.1260	02.9534
1.00	01.5798	0.00	01.4832	02.7266	00.3854	02.7268	02.3336
1.00	01.5798	0.10	01.4555	03.0143	00.2712	02.8411	02.5362
1.00	01.5798	0.20	01.4310	03.3271	00.0000	02.9709	02.7452
1.00	01.5289	0.00	01.4832	02.7266	00.2687	02.7258	02.3682
1.00	01.5289	0.10	01.4555	03.0143	00.0000	02.8382	02.5604
1.00	01.4832	0.00	01.4832	02.7266	00.0000	02.7266	02.4000

TABLE I.- FUNCTIONS FOR CALCULATING THE FLOW ABOUT FLAT-TOP CONFIGURATIONS - Continued

$M_\infty\delta_c$	$\frac{\lambda}{\delta_c}$	$\frac{\alpha}{\delta_c}$	$\left(\frac{\omega_s}{\delta_c}\right)_0$	$\left(\frac{p_c}{p_\infty}\right)_0$	$(\Psi)_{\pi/2}$	$\left(\frac{p_c}{p_\infty}\right)_{\pi/2}$	$\left(\frac{p}{p_\infty}\right)_\lambda$
1.20	0.19985	0.00	0.13764	0.33873	0.00.9046	0.35537	0.23959
1.20	0.19985	0.10	0.13549	0.38001	0.00.8451	0.36700	0.27884
1.20	0.19985	0.20	0.13364	0.42503	0.00.7873	0.38324	0.31757
1.20	0.19985	0.30	0.13204	0.47384	0.00.7286	0.40366	0.35686
1.20	0.19985	0.40	0.13066	0.52647	0.00.6676	0.42812	0.39712
1.20	0.19985	0.50	0.12947	0.58293	0.00.6030	0.45660	0.43853
1.20	0.19985	0.60	0.12843	0.64324	0.00.5330	0.48911	0.48111
1.20	0.19985	0.70	0.12753	0.70740	0.00.4549	0.52560	0.52478
1.20	0.19985	0.80	0.12675	0.77541	0.00.3639	0.56591	0.56931
1.20	0.19985	0.90	0.12607	0.84726	0.00.2474	0.60945	0.61408
1.20	0.19985	1.00	0.12548	0.92296	0.00.0000	0.65107	0.65432
1.20	0.19264	0.00	0.13764	0.33873	0.00.8616	0.35171	0.24775
1.20	0.19264	0.10	0.13549	0.38001	0.00.8020	0.36408	0.28471
1.20	0.19264	0.20	0.13364	0.42503	0.00.7421	0.38069	0.32198
1.20	0.19264	0.30	0.13204	0.47384	0.00.6802	0.40129	0.36016
1.20	0.19264	0.40	0.13066	0.52647	0.00.6145	0.42581	0.39950
1.20	0.19264	0.50	0.12947	0.58293	0.00.5435	0.45425	0.44005
1.20	0.19264	0.60	0.12843	0.64324	0.00.4642	0.48657	0.48177
1.20	0.19264	0.70	0.12753	0.70740	0.00.3718	0.52264	0.52446
1.20	0.19264	0.80	0.12675	0.77541	0.00.2535	0.56199	0.56755
1.20	0.19264	0.90	0.12607	0.84726	0.00.0000	0.60023	0.60675
1.20	0.18549	0.00	0.13764	0.33873	0.00.8149	0.34853	0.25531
1.20	0.18549	0.10	0.13549	0.38001	0.00.7543	0.36150	0.29029
1.20	0.18549	0.20	0.13364	0.42503	0.00.6917	0.37843	0.32618
1.20	0.18549	0.30	0.13204	0.47384	0.00.6254	0.39920	0.36327
1.20	0.18549	0.40	0.13066	0.52647	0.00.5535	0.42377	0.40164
1.20	0.18549	0.50	0.12947	0.58293	0.00.4732	0.45212	0.44128
1.20	0.18549	0.60	0.12843	0.64324	0.00.3796	0.48415	0.48199
1.20	0.18549	0.70	0.12753	0.70740	0.00.2595	0.51948	0.52330
1.20	0.18549	0.80	0.12675	0.77541	0.00.0000	0.55443	0.56135
1.20	0.17844	0.00	0.13764	0.33873	0.00.7638	0.34579	0.26237
1.20	0.17844	0.10	0.13549	0.38001	0.00.7013	0.35925	0.29560
1.20	0.17844	0.20	0.13364	0.42503	0.00.6348	0.37647	0.33016
1.20	0.17844	0.30	0.13204	0.47384	0.00.5625	0.39737	0.36615
1.20	0.17844	0.40	0.13066	0.52647	0.00.4815	0.42195	0.40353
1.20	0.17844	0.50	0.12947	0.58293	0.00.3869	0.45014	0.44212
1.20	0.17844	0.60	0.12843	0.64324	0.00.2653	0.48162	0.48150
1.20	0.17844	0.70	0.12753	0.70740	0.00.0000	0.51336	0.51828
1.20	0.17154	0.00	0.13764	0.33873	0.00.7072	0.34348	0.26901
1.20	0.17154	0.10	0.13549	0.38001	0.00.6416	0.35736	0.30065
1.20	0.17154	0.20	0.13364	0.42503	0.00.5696	0.37481	0.33394
1.20	0.17154	0.30	0.13204	0.47384	0.00.4885	0.39581	0.36881
1.20	0.17154	0.40	0.13066	0.52647	0.00.3933	0.42032	0.40509
1.20	0.17154	0.50	0.12947	0.58293	0.00.2707	0.44812	0.44237
1.20	0.17154	0.60	0.12843	0.64324	0.00.0000	0.47674	0.47771
1.20	0.16485	0.00	0.13764	0.33873	0.00.6441	0.34161	0.27529
1.20	0.16485	0.10	0.13549	0.38001	0.00.5736	0.35582	0.30546
1.20	0.16485	0.20	0.13364	0.42503	0.00.4933	0.37345	0.33750
1.20	0.16485	0.30	0.13204	0.47384	0.00.3983	0.39448	0.37120
1.20	0.16485	0.40	0.13066	0.52647	0.00.2752	0.41874	0.40617
1.20	0.16485	0.50	0.12947	0.58293	0.00.0000	0.44434	0.43990
1.20	0.15845	0.00	0.13764	0.33873	0.00.5727	0.34018	0.28124
1.20	0.15845	0.10	0.13549	0.38001	0.00.4947	0.35465	0.31004
1.20	0.15845	0.20	0.13364	0.42503	0.00.4010	0.37238	0.34083
1.20	0.15845	0.30	0.13204	0.47384	0.00.2785	0.39328	0.37322
1.20	0.15845	0.40	0.13066	0.52647	0.00.0000	0.41593	0.40510
1.20	0.15242	0.00	0.13764	0.33873	0.00.4909	0.33920	0.28688
1.20	0.15242	0.10	0.13549	0.38001	0.00.4002	0.35384	0.31436
1.20	0.15242	0.20	0.13364	0.42503	0.00.2798	0.37155	0.34385
1.20	0.15242	0.30	0.13204	0.47384	0.00.0000	0.39135	0.37361
1.20	0.14687	0.00	0.13764	0.33873	0.00.3946	0.33865	0.29218
1.20	0.14687	0.10	0.13549	0.38001	0.00.2783	0.35336	0.31839
1.20	0.14687	0.20	0.13364	0.42503	0.00.0000	0.37042	0.34574
1.20	0.14192	0.00	0.13764	0.33873	0.00.2731	0.33852	0.29710
1.20	0.14192	0.10	0.13549	0.38001	0.00.0000	0.35295	0.32171
1.20	0.13764	0.00	0.13764	0.33873	0.00.0000	0.33873	0.30160

TABLE I.- FUNCTIONS FOR CALCULATING THE FLOW ABOUT FLAT-TOP CONFIGURATIONS - Continued

$M_\infty \delta_c$	$\frac{\lambda}{\delta_c}$	$\frac{\alpha}{\delta_c}$	$\left(\frac{\omega_s}{\delta_c}\right)_0$	$\left(\frac{p_c}{p_\infty}\right)_0$	$(\Psi)_{\pi/2}$	$\left(\frac{p_c}{p_\infty}\right)_{\pi/2}$	$\left(\frac{p}{p_\infty}\right)_\lambda$
1.40	01.9366	0.00	01.3077	04.1604	00.9271	04.4615	02.9220
1.40	01.9366	0.10	01.2911	04.7230	00.8653	04.5793	03.4386
1.40	01.9366	0.20	01.2770	05.3374	00.8054	04.7710	03.9494
1.40	01.9366	0.30	01.2651	06.0041	00.7448	05.0271	04.4687
1.40	01.9366	0.40	01.2551	06.7231	00.6820	05.3440	05.0021
1.40	01.9366	0.50	01.2465	07.4945	00.6154	05.7206	05.5514
1.40	01.9366	0.60	01.2392	08.3184	00.5434	06.1561	06.1168
1.40	01.9366	0.70	01.2330	09.1946	00.4632	06.6497	06.6968
1.40	01.9366	0.80	01.2277	10.1231	00.3700	07.1982	07.2880
1.40	01.9366	0.90	01.2232	11.1038	00.2508	07.7923	07.8811
1.40	01.9366	1.00	01.2193	12.1366	00.0000	08.3566	08.4091
1.40	01.8628	0.00	01.3077	04.1604	00.8832	04.3932	03.0296
1.40	01.8628	0.10	01.2911	04.7230	00.8216	04.5274	03.5137
1.40	01.8628	0.20	01.2770	05.3374	00.7598	04.7275	04.0038
1.40	01.8628	0.30	01.2651	06.0041	00.6958	04.9882	04.5075
1.40	01.8628	0.40	01.2551	06.7231	00.6282	05.3075	05.0276
1.40	01.8628	0.50	01.2465	07.4945	00.5550	05.6843	05.5647
1.40	01.8628	0.60	01.2392	08.3184	00.4736	06.1179	06.1176
1.40	01.8628	0.70	01.2330	09.1946	00.3787	06.6058	06.6833
1.40	01.8628	0.80	01.2277	10.1231	00.2574	07.1405	07.2537
1.40	01.8628	0.90	01.2232	11.1038	00.0000	07.6576	07.7679
1.40	01.7896	0.00	01.3077	04.1604	00.8355	04.3345	03.1289
1.40	01.7896	0.10	01.2911	04.7230	00.7731	04.4818	03.5850
1.40	01.7896	0.20	01.2770	05.3374	00.7086	04.6893	04.0554
1.40	01.7896	0.30	01.2651	06.0041	00.6402	04.9542	04.5435
1.40	01.7896	0.40	01.2551	06.7231	00.5661	05.2753	05.0498
1.40	01.7896	0.50	01.2465	07.4945	00.4835	05.6518	05.5736
1.40	01.7896	0.60	01.2392	08.3184	00.3873	06.0819	06.1120
1.40	01.7896	0.70	01.2330	09.1946	00.2640	06.5594	06.6577
1.40	01.7896	0.80	01.2277	10.1231	00.0000	07.0303	07.1565
1.40	01.7173	0.00	01.3077	04.1604	00.7830	04.2844	03.2215
1.40	01.7173	0.10	01.2911	04.7230	00.7189	04.4425	03.6526
1.40	01.7173	0.20	01.2770	05.3374	00.6505	04.6564	04.1042
1.40	01.7173	0.30	01.2651	06.0041	00.5760	04.9248	04.5765
1.40	01.7173	0.40	01.2551	06.7231	00.4927	05.2471	05.0682
1.40	01.7173	0.50	01.2465	07.4945	00.3954	05.6220	05.5769
1.40	01.7173	0.60	01.2392	08.3184	00.2704	06.0445	06.0959
1.40	01.7173	0.70	01.2330	09.1946	00.0000	06.4702	06.5772
1.40	01.6466	0.00	01.3077	04.1604	00.7247	04.2426	03.3087
1.40	01.6466	0.10	01.2911	04.7230	00.6576	04.4095	03.7172
1.40	01.6466	0.20	01.2770	05.3374	00.5837	04.6287	04.1504
1.40	01.6466	0.30	01.2651	06.0041	00.5003	04.8998	04.6063
1.40	01.6466	0.40	01.2551	06.7231	00.4024	05.2221	05.0821
1.40	01.6466	0.50	01.2465	07.4945	00.2763	05.5919	05.5717
1.40	01.6466	0.60	01.2392	08.3184	00.0000	05.9735	06.0331
1.40	01.5781	0.00	01.3077	04.1604	00.6593	04.2090	03.3914
1.40	01.5781	0.10	01.2911	04.7230	00.5874	04.3830	03.7788
1.40	01.5781	0.20	01.2770	05.3374	00.5053	04.6062	04.1938
1.40	01.5781	0.30	01.2651	06.0041	00.4077	04.8787	04.6326
1.40	01.5781	0.40	01.2551	06.7231	00.2813	05.1982	05.0892
1.40	01.5781	0.50	01.2465	07.4945	00.0000	05.5367	05.5280
1.40	01.5128	0.00	01.3077	04.1604	00.5851	04.1836	03.4703
1.40	01.5128	0.10	01.2911	04.7230	00.5058	04.3629	03.8378
1.40	01.5128	0.20	01.2770	05.3374	00.4101	04.5888	04.2344
1.40	01.5128	0.30	01.2651	06.0041	00.2846	04.8603	04.6538
1.40	01.5128	0.40	01.2551	06.7231	00.0000	05.1570	05.0663
1.40	01.4518	0.00	01.3077	04.1604	00.4999	04.1665	03.5455
1.40	01.4518	0.10	01.2911	04.7230	00.4081	04.3494	03.8939
1.40	01.4518	0.20	01.2770	05.3374	00.2853	04.5758	04.2712
1.40	01.4518	0.30	01.2651	06.0041	00.0000	04.8320	04.6530
1.40	01.3966	0.00	01.3077	04.1604	00.4000	04.1575	03.6168
1.40	01.3966	0.10	01.2911	04.7230	00.2825	04.3420	03.9466
1.40	01.3966	0.20	01.2770	05.3374	00.0000	04.5595	04.2931
1.40	01.3483	0.00	01.3077	04.1604	00.2751	04.1559	03.6834
1.40	01.3483	0.10	01.2911	04.7230	00.0000	04.3369	03.9900
1.40	01.3077	0.00	01.3077	04.1604	00.0000	04.1604	03.7440

TABLE I.- FUNCTIONS FOR CALCULATING THE FLOW ABOUT FLAT-TOP CONFIGURATIONS - Continued

$M_\infty\delta_c$	$\frac{\lambda}{\delta_c}$	$\frac{a}{\delta_c}$	$\left(\frac{\omega_s}{\delta_c}\right)_0$	$\left(\frac{p_c}{p_\infty}\right)_0$	$(\Psi)_{\pi/2}$	$\left(\frac{p_c}{p_\infty}\right)_{\pi/2}$	$\left(\frac{p}{p_\infty}\right)_\lambda$
1.60	01.8944	0.00	01.2612	05.0478	00.9414	05.5312	03.5468
1.60	01.8944	0.10	01.2482	05.7847	00.8785	05.6374	04.2003
1.60	01.8944	0.20	01.2375	06.5900	00.8174	05.8547	04.8497
1.60	01.8944	0.30	01.2286	07.4638	00.7555	06.1657	05.5123
1.60	01.8944	0.40	01.2212	08.4061	00.6914	06.5634	06.1941
1.60	01.8944	0.50	01.2151	09.4169	00.6235	07.0450	06.8974
1.60	01.8944	0.60	01.2099	10.4961	00.5502	07.6085	07.6218
1.60	01.8944	0.70	01.2056	11.6435	00.4686	08.2518	08.3651
1.60	01.8944	0.80	01.2020	12.8590	00.3738	08.9701	09.1224
1.60	01.8944	0.90	01.1989	14.1424	00.2528	09.7498	09.8812
1.60	01.8944	1.00	01.1964	15.4937	00.0000	10.4862	10.5515
1.60	01.8194	0.00	01.2612	05.0478	00.8973	05.4196	03.6799
1.60	01.8194	0.10	01.2482	05.7847	00.8345	05.5555	04.2917
1.60	01.8194	0.20	01.2375	06.5900	00.7715	05.7883	04.9142
1.60	01.8194	0.30	01.2286	07.4638	00.7062	06.1081	05.5561
1.60	01.8194	0.40	01.2212	08.4061	00.6372	06.5107	06.2204
1.60	01.8194	0.50	01.2151	09.4169	00.5626	06.9938	06.9071
1.60	01.8194	0.60	01.2099	10.4961	00.4797	07.5555	07.6147
1.60	01.8194	0.70	01.2056	11.6435	00.3831	08.1917	08.3385
1.60	01.8194	0.80	01.2020	12.8590	00.2598	08.8913	09.0675
1.60	01.8194	0.90	01.1989	14.1424	00.0000	09.5650	09.7202
1.60	01.7450	0.00	01.2612	05.0478	00.8491	05.3242	03.8028
1.60	01.7450	0.10	01.2482	05.7847	00.7857	05.4839	04.3783
1.60	01.7450	0.20	01.2375	06.5900	00.7199	05.7302	04.9751
1.60	01.7450	0.30	01.2286	07.4638	00.6501	06.0580	05.5962
1.60	01.7450	0.40	01.2212	08.4061	00.5745	06.4648	06.2420
1.60	01.7450	0.50	01.2151	09.4169	00.4904	06.9485	06.9108
1.60	01.7450	0.60	01.2099	10.4961	00.3923	07.5061	07.5985
1.60	01.7450	0.70	01.2056	11.6435	00.2669	08.1283	08.2952
1.60	01.7450	0.80	01.2020	12.8590	00.0000	08.7405	08.9279
1.60	01.6715	0.00	01.2612	05.0478	00.7959	05.2433	03.9177
1.60	01.6715	0.10	01.2482	05.7847	00.7308	05.4224	04.4607
1.60	01.6715	0.20	01.2375	06.5900	00.6611	05.6804	05.0325
1.60	01.6715	0.30	01.2286	07.4638	00.5851	06.0151	05.6324
1.60	01.6715	0.40	01.2212	08.4061	00.5002	06.4249	06.2585
1.60	01.6715	0.50	01.2151	09.4169	00.4010	06.9072	06.9067
1.60	01.6715	0.60	01.2099	10.4961	00.2738	07.4550	07.5681
1.60	01.6715	0.70	01.2056	11.6435	00.0000	08.0066	08.1780
1.60	01.5995	0.00	01.2612	05.0478	00.7366	05.1760	04.0263
1.60	01.5995	0.10	01.2482	05.7847	00.6685	05.3710	04.5394
1.60	01.5995	0.20	01.2375	06.5900	00.5932	05.6388	05.0866
1.60	01.5995	0.30	01.2286	07.4638	00.5083	05.9789	05.6645
1.60	01.5995	0.40	01.2212	08.4061	00.4085	06.3897	06.2688
1.60	01.5995	0.50	01.2151	09.4169	00.2801	06.8659	06.8909
1.60	01.5995	0.60	01.2099	10.4961	00.0000	07.3581	07.4747
1.60	01.5299	0.00	01.2612	05.0478	00.6697	05.1222	04.1301
1.60	01.5299	0.10	01.2482	05.7847	00.5969	05.3298	04.6150
1.60	01.5299	0.20	01.2375	06.5900	00.5134	05.6053	05.1375
1.60	01.5299	0.30	01.2286	07.4638	00.4141	05.9486	05.6919
1.60	01.5299	0.40	01.2212	08.4061	00.2853	06.3564	06.2699
1.60	01.5299	0.50	01.2151	09.4169	00.0000	06.7905	06.8235
1.60	01.4636	0.00	01.2612	05.0478	00.5935	05.0818	04.2299
1.60	01.4636	0.10	01.2482	05.7847	00.5134	05.2990	04.6879
1.60	01.4636	0.20	01.2375	06.5900	00.4162	05.5796	05.1852
1.60	01.4636	0.30	01.2286	07.4638	00.2886	05.9225	05.7129
1.60	01.4636	0.40	01.2212	08.4061	00.0000	06.3000	06.2310
1.60	01.4021	0.00	01.2612	05.0478	00.5059	05.0550	04.3261
1.60	01.4021	0.10	01.2482	05.7847	00.4133	05.2786	04.7580
1.60	01.4021	0.20	01.2375	06.5900	00.2889	05.5609	05.2285
1.60	01.4021	0.30	01.2286	07.4638	00.0000	05.8837	05.7051
1.60	01.3471	0.00	01.2612	05.0478	00.4033	05.0414	04.4183
1.60	01.3471	0.10	01.2482	05.7847	00.2851	05.2681	04.8244
1.60	01.3471	0.20	01.2375	06.5900	00.0000	05.5390	05.2530
1.60	01.2998	0.00	01.2612	05.0478	00.2759	05.0398	04.5049
1.60	01.2998	0.10	01.2482	05.7847	00.0000	05.2622	04.8795
1.60	01.2612	0.00	01.2612	05.0478	00.0000	05.0478	04.5840

TABLE I.- FUNCTIONS FOR CALCULATING THE FLOW ABOUT FLAT-TOP CONFIGURATIONS - Continued

$M_\infty\delta_c$	$\frac{\lambda}{\delta_c}$	$\frac{a}{\delta_c}$	$\left(\frac{\omega_B}{\delta_c}\right)_0$	$\left(\frac{p_c}{p_\infty}\right)_0$	$(\Psi)_{\pi/2}$	$\left(\frac{p_c}{p_\infty}\right)_{\pi/2}$	$\left(\frac{p}{p_\infty}\right)_\lambda$
1.80	01.8643	0.00	012283	06.0504	00.9509	06.7661	04.2679
1.80	01.8643	0.10	012182	06.9862	00.8874	06.8456	05.0718
1.80	01.8643	0.20	012100	08.0087	00.8255	07.0838	05.8758
1.80	01.8643	0.30	012033	09.1181	00.7629	07.4525	06.6986
1.80	01.8643	0.40	011979	10.3141	00.6978	07.9397	07.5471
1.80	01.8643	0.50	011935	11.5967	00.6291	08.5397	08.4232
1.80	01.8643	0.60	011898	12.9656	00.5548	09.2488	09.3263
1.80	01.8643	0.70	011869	14.4206	00.4722	10.0634	10.2532
1.80	01.8643	0.80	011844	15.9615	00.3763	10.9761	11.1973
1.80	01.8643	0.90	011824	17.5881	00.2540	11.9683	12.1421
1.80	01.8643	1.00	011808	19.3002	00.0000	12.9010	12.9718
1.80	01.7886	0.00	012283	06.0504	00.9068	06.5989	04.4264
1.80	01.7886	0.10	012182	06.9862	00.8434	06.7261	05.1798
1.80	01.7886	0.20	012100	08.0087	00.7796	06.9895	05.9503
1.80	01.7886	0.30	012033	09.1181	00.7134	07.3728	06.7471
1.80	01.7886	0.40	011979	10.3141	00.6435	07.8683	07.5732
1.80	01.7886	0.50	011935	11.5967	00.5678	08.4718	08.4281
1.80	01.7886	0.60	011898	12.9656	00.4838	09.1794	09.3094
1.80	01.7886	0.70	011869	14.4206	00.3861	09.9852	10.2109
1.80	01.7886	0.80	011844	15.9615	00.2614	10.8736	11.1181
1.80	01.7886	0.90	011824	17.5881	00.0000	11.7262	11.9259
1.80	01.7133	0.00	012283	06.0504	00.8585	06.4566	04.5732
1.80	01.7133	0.10	012182	06.9862	00.7943	06.6221	05.2820
1.80	01.7133	0.20	012100	08.0087	00.7277	06.9075	06.0203
1.80	01.7133	0.30	012033	09.1181	00.6570	07.3039	06.7908
1.80	01.7133	0.40	011979	10.3141	00.5804	07.8067	07.5931
1.80	01.7133	0.50	011935	11.5967	00.4951	08.4121	08.4249
1.80	01.7133	0.60	011898	12.9656	00.3957	09.1152	09.2804
1.80	01.7133	0.70	011869	14.4206	00.2688	09.9031	10.1466
1.80	01.7133	0.80	011844	15.9615	00.0000	10.6765	10.9293
1.80	01.6389	0.00	012283	06.0504	00.8050	06.3364	04.7111
1.80	01.6389	0.10	012182	06.9862	00.7391	06.5332	05.3795
1.80	01.6389	0.20	012100	08.0087	00.6685	06.8375	06.0861
1.80	01.6389	0.30	012033	09.1181	00.5915	07.2453	06.8295
1.80	01.6389	0.40	011979	10.3141	00.5054	07.7536	07.6063
1.80	01.6389	0.50	011935	11.5967	00.4048	08.3582	08.4113
1.80	01.6389	0.60	011898	12.9656	00.2760	09.0490	09.2324
1.80	01.6389	0.70	011869	14.4206	00.0000	09.7443	09.9865
1.80	01.5660	0.00	012283	06.0504	00.7450	06.2369	04.8422
1.80	01.5660	0.10	012182	06.9862	00.6761	06.4591	05.4729
1.80	01.5660	0.20	012100	08.0087	00.6000	06.7793	06.1480
1.80	01.5660	0.30	012033	09.1181	00.5139	07.1962	06.8629
1.80	01.5660	0.40	011979	10.3141	00.4128	07.7072	07.6114
1.80	01.5660	0.50	011935	11.5967	00.2826	08.3045	08.3822
1.80	01.5660	0.60	011898	12.9656	00.0000	08.9227	09.1030
1.80	01.4954	0.00	012283	06.0504	00.6771	06.1574	04.9683
1.80	01.4954	0.10	012182	06.9862	00.6036	06.4000	05.5631
1.80	01.4954	0.20	012100	08.0087	00.5191	06.7327	06.2063
1.80	01.4954	0.30	012033	09.1181	00.4185	07.1555	06.8905
1.80	01.4954	0.40	011979	10.3141	00.2880	07.6633	07.6045
1.80	01.4954	0.50	011935	11.5967	00.0000	08.2060	08.2865
1.80	01.4284	0.00	012283	06.0504	00.5995	06.0979	05.0908
1.80	01.4284	0.10	012182	06.9862	00.5187	06.3560	05.6507
1.80	01.4284	0.20	012100	08.0087	00.4205	06.6973	06.2609
1.80	01.4284	0.30	012033	09.1181	00.2913	07.1206	06.9099
1.80	01.4284	0.40	011979	10.3141	00.0000	07.5895	07.5461
1.80	01.3666	0.00	012283	06.0504	00.5100	06.0587	05.2103
1.80	01.3666	0.10	012182	06.9862	00.4168	06.3273	05.7359
1.80	01.3666	0.20	012100	08.0087	00.2913	06.6719	06.3106
1.80	01.3666	0.30	012033	09.1181	00.0000	07.0697	06.8930
1.80	01.3117	0.00	012283	06.0504	00.4054	06.0395	05.3260
1.80	01.3117	0.10	012182	06.9862	00.2866	06.3131	05.8175
1.80	01.3117	0.20	012100	08.0087	00.0000	06.6436	06.3374
1.80	01.2654	0.00	012283	06.0504	00.2762	06.0380	05.4357
1.80	01.2654	0.10	012182	06.9862	00.0000	06.3066	05.8857
1.80	01.2283	0.00	012283	06.0504	00.0000	06.0504	05.5360

TABLE I.- FUNCTIONS FOR CALCULATING THE FLOW ABOUT FLAT-TOP CONFIGURATIONS - Continued

$M_\infty \delta_c$	$\frac{\lambda}{\delta_c}$	$\frac{\alpha}{\delta_c}$	$\left(\frac{\omega_s}{\delta_c}\right)_0$	$\left(\frac{p_c}{p_\infty}\right)_0$	$(\Psi)_{\pi/2}$	$\left(\frac{p_c}{p_\infty}\right)_{\pi/2}$	$\left(\frac{p}{p_\infty}\right)_\lambda$
2.00	01.8422	0.00	01.2042	07.1690	00.9573	08.1681	05.0824
2.00	01.8422	0.10	01.1963	08.3278	00.8936	08.2043	06.0517
2.00	01.8422	0.20	01.1901	09.5939	00.8313	08.4584	07.0266
2.00	01.8422	0.30	01.1851	10.9671	00.7680	08.8875	08.0272
2.00	01.8422	0.40	01.1812	12.4471	00.7024	09.4730	09.0606
2.00	01.8422	0.50	01.1780	14.0337	00.6330	10.2051	10.1289
2.00	01.8422	0.60	01.1755	15.7266	00.5580	11.0778	11.2306
2.00	01.8422	0.70	01.1735	17.5256	00.4748	12.0851	12.3616
2.00	01.8422	0.80	01.1719	19.4302	00.3781	13.2169	13.5132
2.00	01.8422	0.90	01.1706	21.4404	00.2548	14.4484	14.6648
2.00	01.8422	1.00	01.1697	23.5559	00.0000	15.6018	15.6713
2.00	01.7659	0.00	01.2042	07.1690	00.9134	07.9329	05.2671
2.00	01.7659	0.10	01.1963	08.3278	00.8497	08.0398	06.1768
2.00	01.7659	0.20	01.1901	09.5939	00.7853	08.3314	07.1114
2.00	01.7659	0.30	01.1851	10.9671	00.7185	08.7825	08.0801
2.00	01.7659	0.40	01.1812	12.4471	00.6479	09.3806	09.0858
2.00	01.7659	0.50	01.1780	14.0337	00.5716	10.1185	10.1277
2.00	01.7659	0.60	01.1755	15.7266	00.4867	10.9903	11.2020
2.00	01.7659	0.70	01.1735	17.5256	00.3882	11.9872	12.3011
2.00	01.7659	0.80	01.1719	19.4302	00.2625	13.0883	13.4062
2.00	01.7659	0.90	01.1706	21.4404	00.0000	14.1421	14.3860
2.00	01.6900	0.00	01.2042	07.1690	00.8652	07.7334	05.4389
2.00	01.6900	0.10	01.1963	08.3278	00.8006	07.8972	06.2954
2.00	01.6900	0.20	01.1901	09.5939	00.7333	08.2215	07.1907
2.00	01.6900	0.30	01.1851	10.9671	00.6619	08.6922	08.1270
2.00	01.6900	0.40	01.1812	12.4471	00.5845	09.3014	09.1033
2.00	01.6900	0.50	01.1780	14.0337	00.4984	10.0432	10.1160
2.00	01.6900	0.60	01.1755	15.7266	00.3982	10.9100	11.1580
2.00	01.6900	0.70	01.1735	17.5256	00.2701	11.8845	12.2124
2.00	01.6900	0.80	01.1719	19.4302	00.0000	12.8395	13.1616
2.00	01.6149	0.00	01.2042	07.1690	00.8115	07.5653	05.6009
2.00	01.6149	0.10	01.1963	08.3278	00.7451	07.7756	06.4085
2.00	01.6149	0.20	01.1901	09.5939	00.6738	08.1280	07.2650
2.00	01.6149	0.30	01.1851	10.9671	00.5961	08.6158	08.1676
2.00	01.6149	0.40	01.1812	12.4471	00.5091	09.2338	09.1120
2.00	01.6149	0.50	01.1780	14.0337	00.4076	09.9757	10.0911
2.00	01.6149	0.60	01.1755	15.7266	00.2776	10.8275	11.0897
2.00	01.6149	0.70	01.1735	17.5256	00.0000	11.6844	12.0035
2.00	01.5413	0.00	01.2042	07.1690	00.7511	07.4263	05.7557
2.00	01.5413	0.10	01.1963	08.3278	00.6817	07.6746	06.5172
2.00	01.5413	0.20	01.1901	09.5939	00.6048	08.0507	07.3347
2.00	01.5413	0.30	01.1851	10.9671	00.5179	08.5523	08.2017
2.00	01.5413	0.40	01.1812	12.4471	00.4158	09.1751	09.1103
2.00	01.5413	0.50	01.1780	14.0337	00.2844	09.9085	10.0462
2.00	01.5413	0.60	01.1755	15.7266	00.0000	10.6685	10.9189
2.00	01.4700	0.00	01.2042	07.1690	00.6825	07.3155	05.9057
2.00	01.4700	0.10	01.1963	08.3278	00.6085	07.5941	06.6227
2.00	01.4700	0.20	01.1901	09.5939	00.5232	07.9891	07.4002
2.00	01.4700	0.30	01.1851	10.9671	00.4217	08.4999	08.2284
2.00	01.4700	0.40	01.1812	12.4471	00.2899	09.1198	09.0933
2.00	01.4700	0.50	01.1780	14.0337	00.0000	09.7843	09.9176
2.00	01.4025	0.00	01.2042	07.1690	00.6038	07.2328	06.0527
2.00	01.4025	0.10	01.1963	08.3278	00.5225	07.5345	06.7261
2.00	01.4025	0.20	01.1901	09.5939	00.4235	07.9426	07.4617
2.00	01.4025	0.30	01.1851	10.9671	00.2933	08.4553	08.2451
2.00	01.4025	0.40	01.1812	12.4471	00.0000	09.0265	09.0121
2.00	01.3403	0.00	01.2042	07.1690	00.5130	07.1786	06.1978
2.00	01.3403	0.10	01.1963	08.3278	00.4193	07.4960	06.8276
2.00	01.3403	0.20	01.1901	09.5939	00.2930	07.9097	07.5177
2.00	01.3403	0.30	01.1851	10.9671	00.0000	08.3909	08.2169
2.00	01.2856	0.00	01.2042	07.1690	00.4066	07.1524	06.3399
2.00	01.2856	0.10	01.1963	08.3278	00.2876	07.4776	06.9259
2.00	01.2856	0.20	01.1901	09.5939	00.0000	07.8742	07.5465
2.00	01.2400	0.00	01.2042	07.1690	00.2761	07.1513	06.4757
2.00	01.2400	0.10	01.1963	08.3278	00.0000	07.4706	07.0088
2.00	01.2042	0.00	01.2042	07.1690	00.0000	07.1690	06.6000

TABLE I.- FUNCTIONS FOR CALCULATING THE FLOW ABOUT FLAT-TOP CONFIGURATIONS - Continued

$M_\infty \delta_c$	$\frac{\lambda}{\delta_c}$	$\frac{\alpha}{\delta_c}$	$\left(\frac{\omega_s}{\delta_c}\right)_o$	$\left(\frac{p_c}{p_\infty}\right)_o$	$(\Psi)_{\pi/2}$	$\left(\frac{p_c}{p_\infty}\right)_{\pi/2}$	$\left(\frac{p}{p_\infty}\right)_\lambda$
2.50	01.8072	0.00	01.1662	10.4755	00.9667	12.4136	07.5173
2.50	01.8072	0.10	01.1621	12.2973	00.9028	12.2613	08.9691
2.50	01.8072	0.20	01.1592	14.2863	00.8399	12.5308	10.4449
2.50	01.8072	0.30	01.1570	16.4420	00.7758	13.1238	11.9677
2.50	01.8072	0.40	01.1554	18.7639	00.7093	13.9943	13.5453
2.50	01.8072	0.50	01.1543	21.2515	00.6389	15.1175	15.1790
2.50	01.8072	0.60	01.1535	23.9042	00.5629	16.4778	16.8655
2.50	01.8072	0.70	01.1530	26.7217	00.4785	18.0614	18.5974
2.50	01.8072	0.80	01.1528	29.7036	00.3806	19.8487	20.3603
2.50	01.8072	0.90	01.1527	32.8495	00.2559	21.7957	22.1205
2.50	01.8072	1.00	01.1527	36.1591	00.0000	23.6068	23.6466
2.50	01.7299	0.00	01.1662	10.4755	00.9232	11.9517	07.7739
2.50	01.7299	0.10	01.1621	12.2973	00.8591	11.9516	09.1415
2.50	01.7299	0.20	01.1592	14.2863	00.7939	12.3018	10.5575
2.50	01.7299	0.30	01.1570	16.4420	00.7262	12.9417	12.0318
2.50	01.7299	0.40	01.1554	18.7639	00.6546	13.8397	13.5661
2.50	01.7299	0.50	01.1543	21.2515	00.5771	14.9768	15.1581
2.50	01.7299	0.60	01.1535	23.9042	00.4911	16.3384	16.8008
2.50	01.7299	0.70	01.1530	26.7217	00.3912	17.9068	18.4813
2.50	01.7299	0.80	01.1528	29.7036	00.2640	19.6443	20.1691
2.50	01.7299	0.90	01.1527	32.8495	00.0000	21.2984	21.6545
2.50	01.6530	0.00	01.1662	10.4755	00.8753	11.5622	08.0145
2.50	01.6530	0.10	01.1621	12.2973	00.8100	11.6851	09.3049
2.50	01.6530	0.20	01.1592	14.2863	00.7418	12.1053	10.6619
2.50	01.6530	0.30	01.1570	16.4420	00.6694	12.7871	12.0859
2.50	01.6530	0.40	01.1554	18.7639	00.5909	13.7093	13.5740
2.50	01.6530	0.50	01.1543	21.2515	00.5034	14.8566	15.1195
2.50	01.6530	0.60	01.1535	23.9042	00.4018	16.2126	16.7102
2.50	01.6530	0.70	01.1530	26.7217	00.2720	17.7455	18.3186
2.50	01.6530	0.80	01.1528	29.7036	00.0000	19.2424	19.7568
2.50	01.5768	0.00	01.1662	10.4755	00.8215	11.2357	08.2433
2.50	01.5768	0.10	01.1621	12.2973	00.7543	11.4593	09.4610
2.50	01.5768	0.20	01.1592	14.2863	00.6820	11.9398	10.7586
2.50	01.5768	0.30	01.1570	16.4420	00.6031	12.6581	12.1299
2.50	01.5768	0.40	01.1554	18.7639	00.5148	13.5999	13.5673
2.50	01.5768	0.50	01.1543	21.2515	00.4117	14.7507	15.0586
2.50	01.5768	0.60	01.1535	23.9042	00.2799	16.0838	16.5790
2.50	01.5768	0.70	01.1530	26.7217	00.0000	17.4237	17.9623
2.50	01.5020	0.00	01.1662	10.4755	00.7607	10.9667	08.4642
2.50	01.5020	0.10	01.1621	12.2973	00.6904	11.2726	09.6119
2.50	01.5020	0.20	01.1592	14.2863	00.6123	11.8040	10.8485
2.50	01.5020	0.30	01.1570	16.4420	00.5241	12.5522	12.1631
2.50	01.5020	0.40	01.1554	18.7639	00.4204	13.5064	13.5428
2.50	01.5020	0.50	01.1543	21.2515	00.2871	14.6455	14.9642
2.50	01.5020	0.60	01.1535	23.9042	00.0000	15.8286	16.2827
2.50	01.4295	0.00	01.1662	10.4755	00.6910	10.7525	08.6815
2.50	01.4295	0.10	01.1621	12.2973	00.6160	11.1244	09.7597
2.50	01.4295	0.20	01.1592	14.2863	00.5295	11.6967	10.9325
2.50	01.4295	0.30	01.1570	16.4420	00.4265	12.4660	12.1843
2.50	01.4295	0.40	01.1554	18.7639	00.2928	13.4185	13.4927
2.50	01.4295	0.50	01.1543	21.2515	00.0000	14.4460	14.7345
2.50	01.3610	0.00	01.1662	10.4755	00.6106	10.5930	08.8989
2.50	01.3610	0.10	01.1621	12.2973	00.5284	11.0154	09.9070
2.50	01.3610	0.20	01.1592	14.2863	00.4281	11.6167	11.0114
2.50	01.3610	0.30	01.1570	16.4420	00.2961	12.3930	12.1894
2.50	01.3610	0.40	01.1554	18.7639	00.0000	13.2675	13.3394
2.50	01.2983	0.00	01.1662	10.4755	00.5173	10.4891	09.1186
2.50	01.2983	0.10	01.1621	12.2973	00.4228	10.9460	10.0550
2.50	01.2983	0.20	01.1592	14.2863	00.2953	11.5612	11.0836
2.50	01.2983	0.30	01.1570	16.4420	00.0000	12.2883	12.1243
2.50	01.2439	0.00	01.1662	10.4755	00.4080	10.4403	09.3392
2.50	01.2439	0.10	01.1621	12.2973	00.2886	10.9149	10.2018
2.50	01.2439	0.20	01.1592	14.2863	00.0000	11.5046	11.1158
2.50	01.1997	0.00	01.1662	10.4755	00.2751	10.4404	09.5535
2.50	01.1997	0.10	01.1621	12.2973	00.0000	10.9074	10.3281
2.50	01.1662	0.00	01.1662	10.4755	00.0000	10.4755	09.7500

TABLE I.- FUNCTIONS FOR CALCULATING THE FLOW ABOUT FLAT-TOP CONFIGURATIONS - Concluded

$M_\infty \delta_c$	$\frac{\lambda}{\delta_c}$	$\frac{\alpha}{\delta_c}$	$\left(\frac{\omega_s}{\delta_c}\right)_o$	$\left(\frac{p_c}{p_\infty}\right)_o$	$(\Psi)_{\pi/2}$	$\left(\frac{p_c}{p_\infty}\right)_{\pi/2}$	$\left(\frac{p}{p_\infty}\right)_\lambda$
3.00	01.7874	0.00	011450	14.5128	00.9714	17.7219	10.5103
3.00	01.7874	0.10	011433	17.1469	00.9076	17.2605	12.5474
3.00	01.7874	0.20	011422	20.0211	00.8444	17.5115	14.6318
3.00	01.7874	0.30	011416	23.1345	00.7799	18.2881	16.7897
3.00	01.7874	0.40	011414	26.4863	00.7129	19.5014	19.0295
3.00	01.7874	0.50	011414	30.0756	00.6420	21.1033	21.3515
3.00	01.7874	0.60	011416	33.9019	00.5654	23.0639	23.7501
3.00	01.7874	0.70	011420	37.9646	00.4805	25.3582	26.2139
3.00	01.7874	0.80	011425	42.2632	00.3819	27.9537	28.7211
3.00	01.7874	0.90	011430	46.7972	00.2564	30.7823	31.2222
3.00	01.7874	1.00	011436	51.5663	00.0000	33.4018	33.3801
3.00	01.7097	0.00	011450	14.5128	00.9284	16.9512	10.8510
3.00	01.7097	0.10	011433	17.1469	00.8641	16.7597	12.7750
3.00	01.7097	0.20	011422	20.0211	00.7985	17.1520	14.7765
3.00	01.7097	0.30	011416	23.1345	00.7303	18.0099	16.8657
3.00	01.7097	0.40	011414	26.4863	00.6581	19.2708	19.0435
3.00	01.7097	0.50	011414	30.0756	00.5801	20.8976	21.3051
3.00	01.7097	0.60	011416	33.9019	00.4934	22.8629	23.6399
3.00	01.7097	0.70	011420	37.9646	00.3928	25.1362	26.0283
3.00	01.7097	0.80	011425	42.2632	00.2647	27.6587	28.4253
3.00	01.7097	0.90	011430	46.7972	00.0000	30.0514	30.5255
3.00	01.6322	0.00	011450	14.5128	00.8806	16.3041	11.1720
3.00	01.6322	0.10	011433	17.1469	00.8151	16.3310	12.9905
3.00	01.6322	0.20	011422	20.0211	00.7464	16.8457	14.9093
3.00	01.6322	0.30	011416	23.1345	00.6734	17.7760	16.9270
3.00	01.6322	0.40	011414	26.4863	00.5942	19.0790	19.0381
3.00	01.6322	0.50	011414	30.0756	00.5061	20.7247	21.2321
3.00	01.6322	0.60	011416	33.9019	00.4036	22.6839	23.4906
3.00	01.6322	0.70	011420	37.9646	00.2730	24.9056	25.7733
3.00	01.6322	0.80	011425	42.2632	00.0000	27.0702	27.8061
3.00	01.5554	0.00	011450	14.5128	00.8270	15.7639	11.4787
3.00	01.5554	0.10	011433	17.1469	00.7593	15.9695	13.1965
3.00	01.5554	0.20	011422	20.0211	00.6864	16.5895	15.0311
3.00	01.5554	0.30	011416	23.1345	00.6069	17.5830	16.9730
3.00	01.5554	0.40	011414	26.4863	00.5178	18.9203	19.0104
3.00	01.5554	0.50	011414	30.0756	00.4139	20.5742	21.1252
3.00	01.5554	0.60	011416	33.9019	00.2810	22.5010	23.2806
3.00	01.5554	0.70	011420	37.9646	00.0000	24.4361	25.2344
3.00	01.4798	0.00	011450	14.5128	00.7660	15.3201	11.7773
3.00	01.4798	0.10	011433	17.1469	00.6951	15.6717	13.3961
3.00	01.4798	0.20	011422	20.0211	00.6164	16.3807	15.1432
3.00	01.4798	0.30	011416	23.1345	00.5274	17.4263	17.0028
3.00	01.4798	0.40	011414	26.4863	00.4229	18.7862	18.9556
3.00	01.4798	0.50	011414	30.0756	00.2884	20.4251	20.9674
3.00	01.4798	0.60	011416	33.9019	00.0000	22.1296	22.8279
3.00	01.4067	0.00	011450	14.5128	00.6958	14.9670	12.0740
3.00	01.4067	0.10	011433	17.1469	00.6202	15.4360	13.5931
3.00	01.4067	0.20	011422	20.0211	00.5329	16.2169	15.2473
3.00	01.4067	0.30	011416	23.1345	00.4291	17.2999	17.0145
3.00	01.4067	0.40	011414	26.4863	00.2944	18.6603	18.8619
3.00	01.4067	0.50	011414	30.0756	00.0000	20.1343	20.6107
3.00	013375	0.00	011450	14.5128	00.6144	14.7039	12.3754
3.00	013375	0.10	011433	17.1469	00.5315	15.2630	13.7918
3.00	013375	0.20	011422	20.0211	00.4305	16.0956	15.3447
3.00	013375	0.30	011416	23.1345	00.2976	17.1930	17.0019
3.00	013375	0.40	011414	26.4863	00.0000	18.4392	18.6164
3.00	012745	0.00	011450	14.5128	00.5194	14.5328	12.6857
3.00	012745	0.10	011433	17.1469	00.4245	15.1538	13.9949
3.00	012745	0.20	011422	20.0211	00.2963	16.0122	15.4338
3.00	012745	0.30	011416	23.1345	00.0000	17.0388	16.8877
3.00	012203	0.00	011450	14.5128	00.4083	14.4535	13.0029
3.00	012203	0.10	011433	17.1469	00.2887	15.1067	14.2003
3.00	012203	0.20	011422	20.0211	00.0000	15.9296	15.4680
3.00	011770	0.00	011450	14.5128	00.2740	14.4552	13.3144
3.00	011770	0.10	011433	17.1469	00.0000	15.0993	14.3792
3.00	011450	0.00	011450	14.5128	00.0000	14.5128	13.6000

CONFIDENTIAL

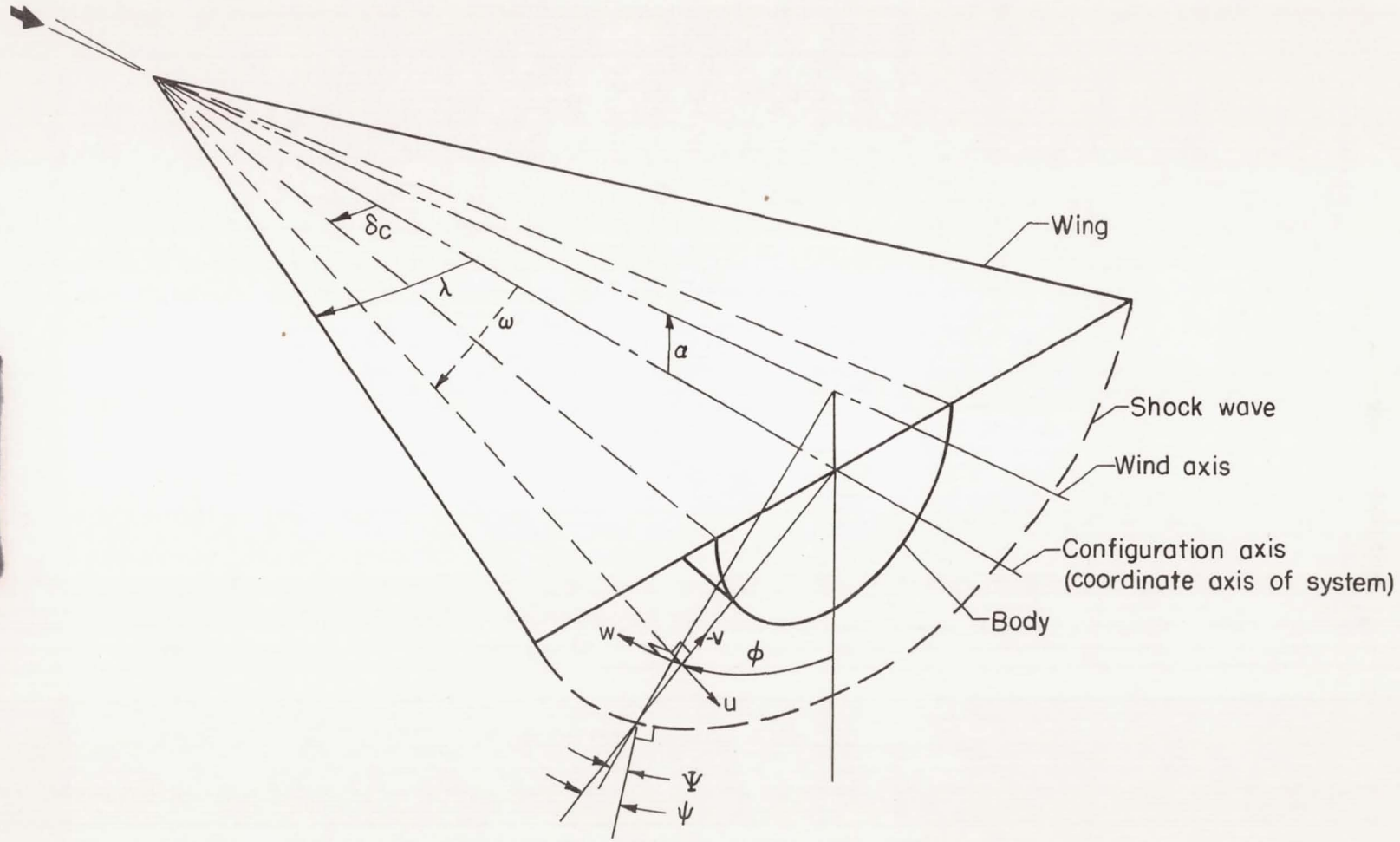

Figure 1.- Schematic diagram of polar coordinate system.

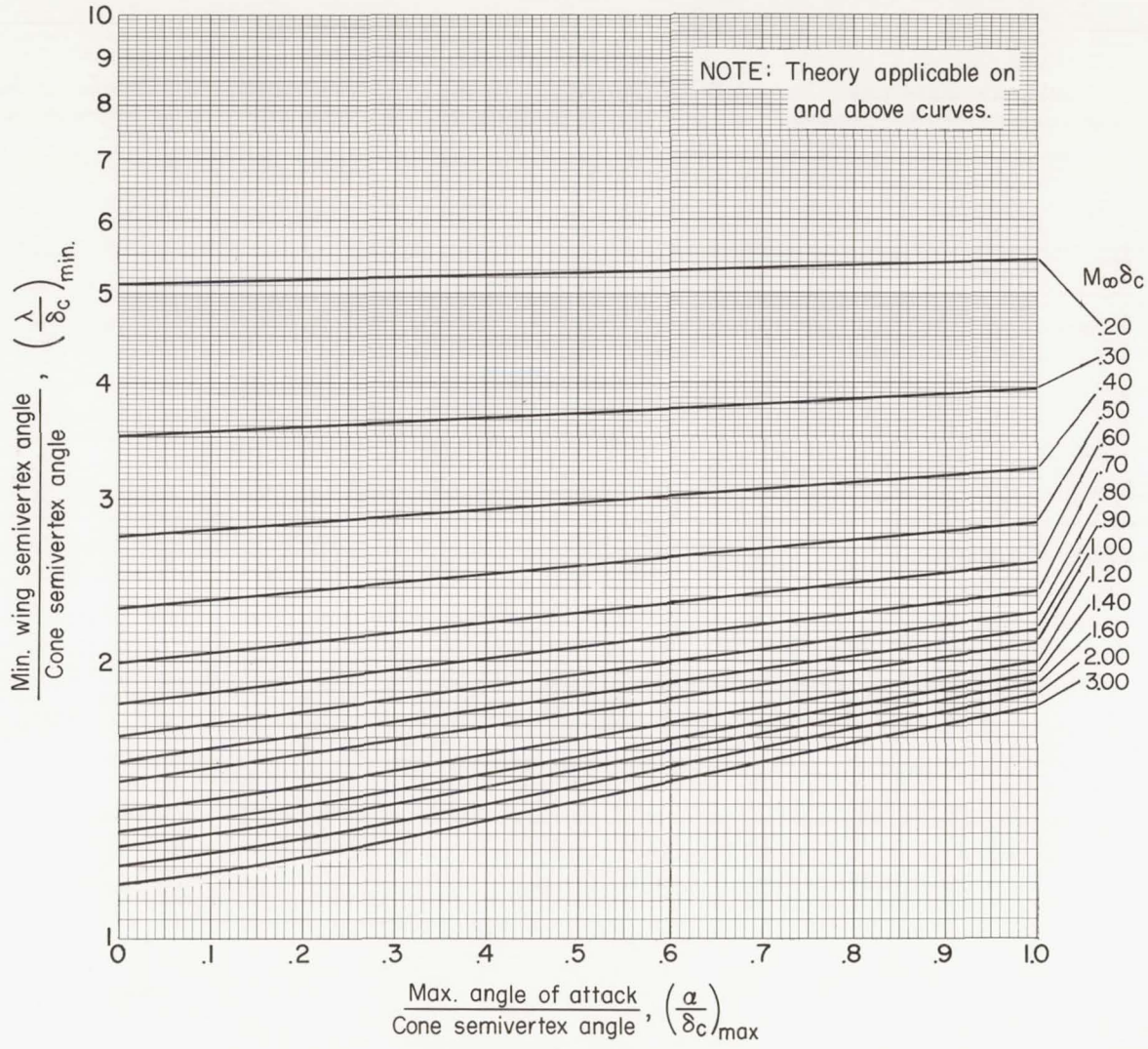

Figure 2.- Variation of wing semivertex angle with maximum angle of attack for applicability of theory; $(\Psi)_{\pi/2} = 0$.

CONFIDENTIAL

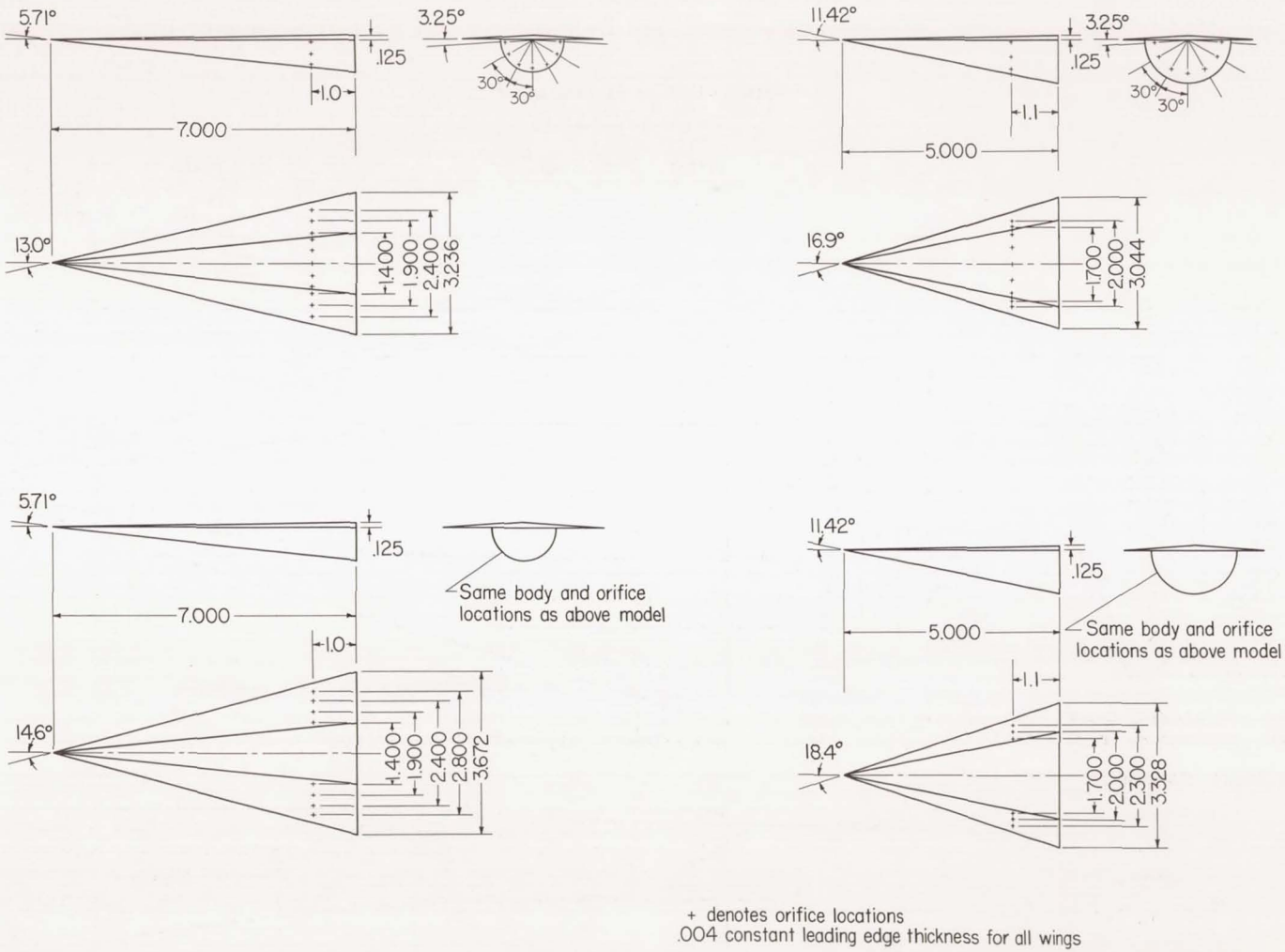

\+ denotes orifice locations
.004 constant leading edge thickness for all wings

(a) Conical models.

Figure 3.- Dimensions of pressure-distribution test models showing location of pressure orifices.

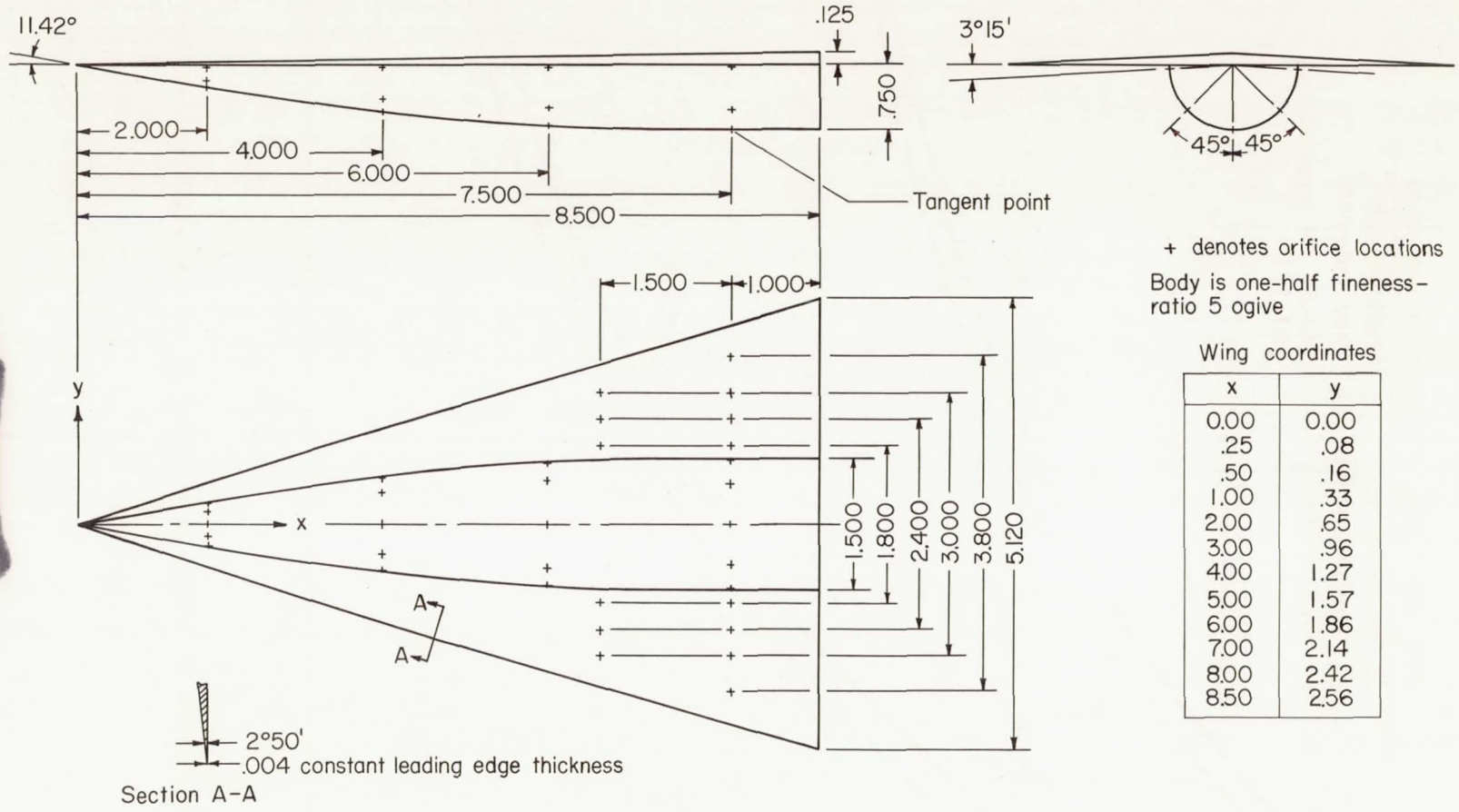

Wing coordinates

x	y
0.00	0.00
.25	.08
.50	.16
1.00	.33
2.00	.65
3.00	.96
4.00	1.27
5.00	1.57
6.00	1.86
7.00	2.14
8.00	2.42
8.50	2.56

(b) Ogive model.

Figure 3.- Concluded.

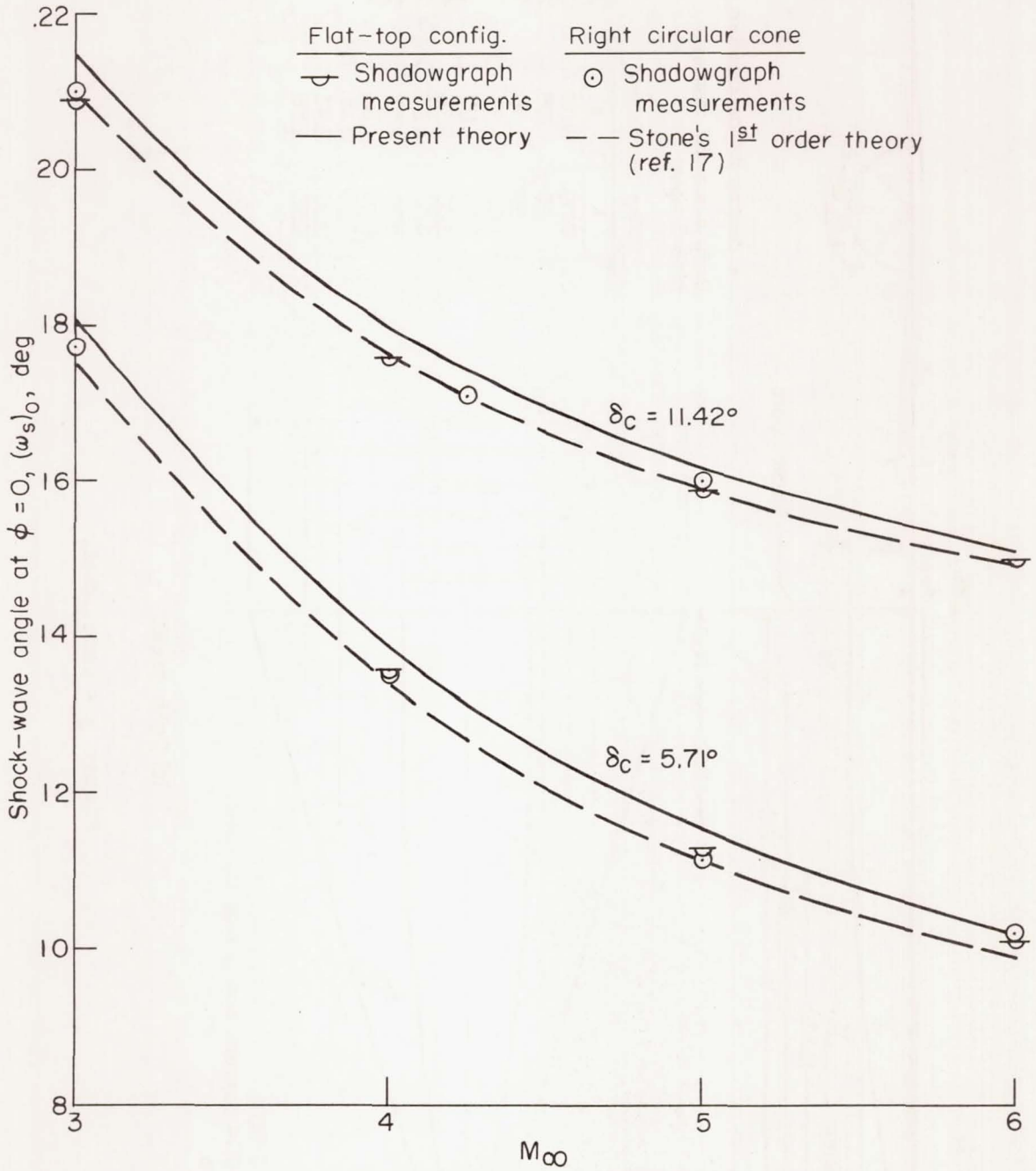

Figure 4.- Variation of shock-wave angle at $\varphi = 0$ with Mach number for $\alpha = 3^\circ$.

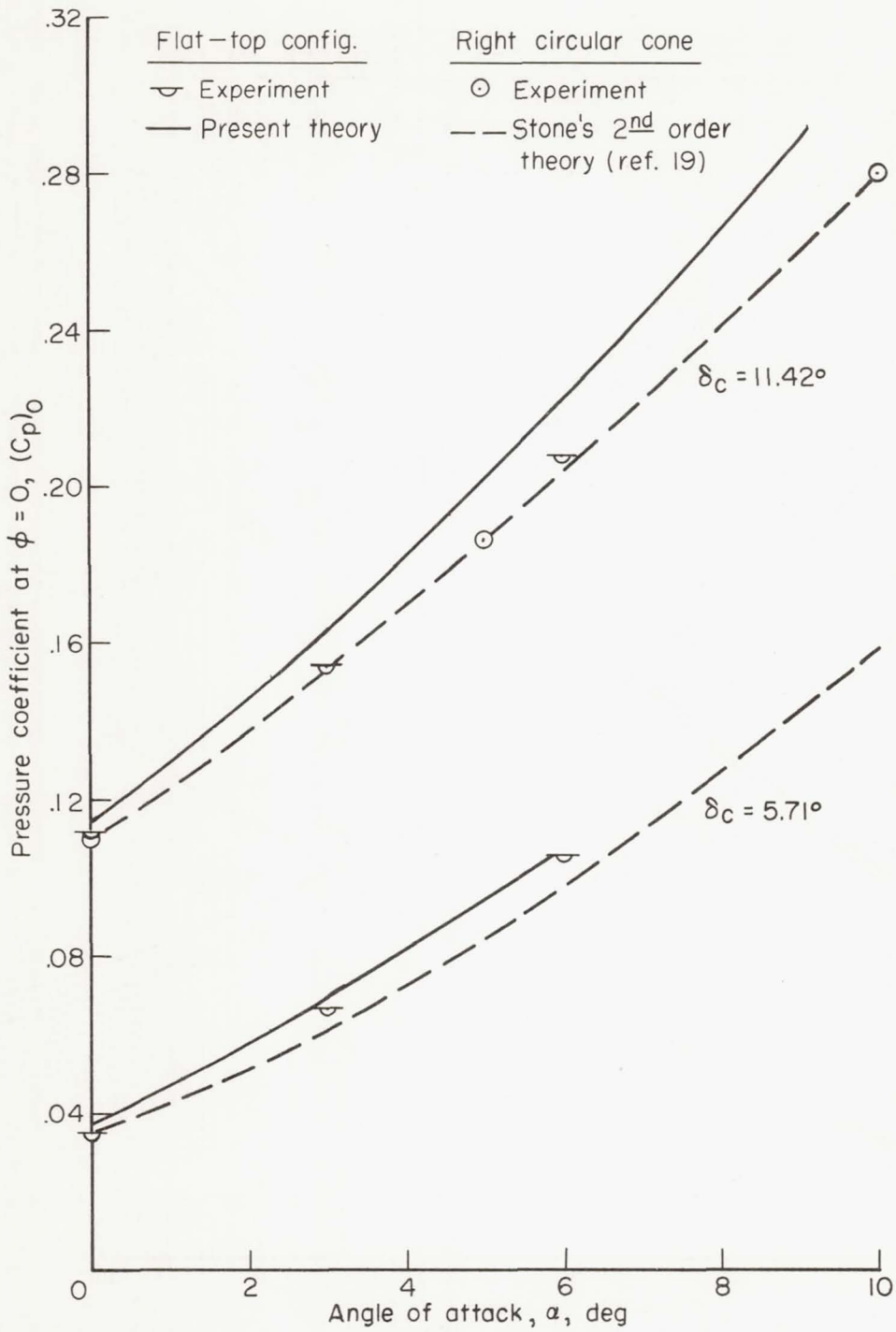

(a) $M_\infty = 3.0$

Figure 5.- Variation of pressure coefficient at $\varphi = 0$ with angle of attack for Mach numbers 3.0 and 5.0.

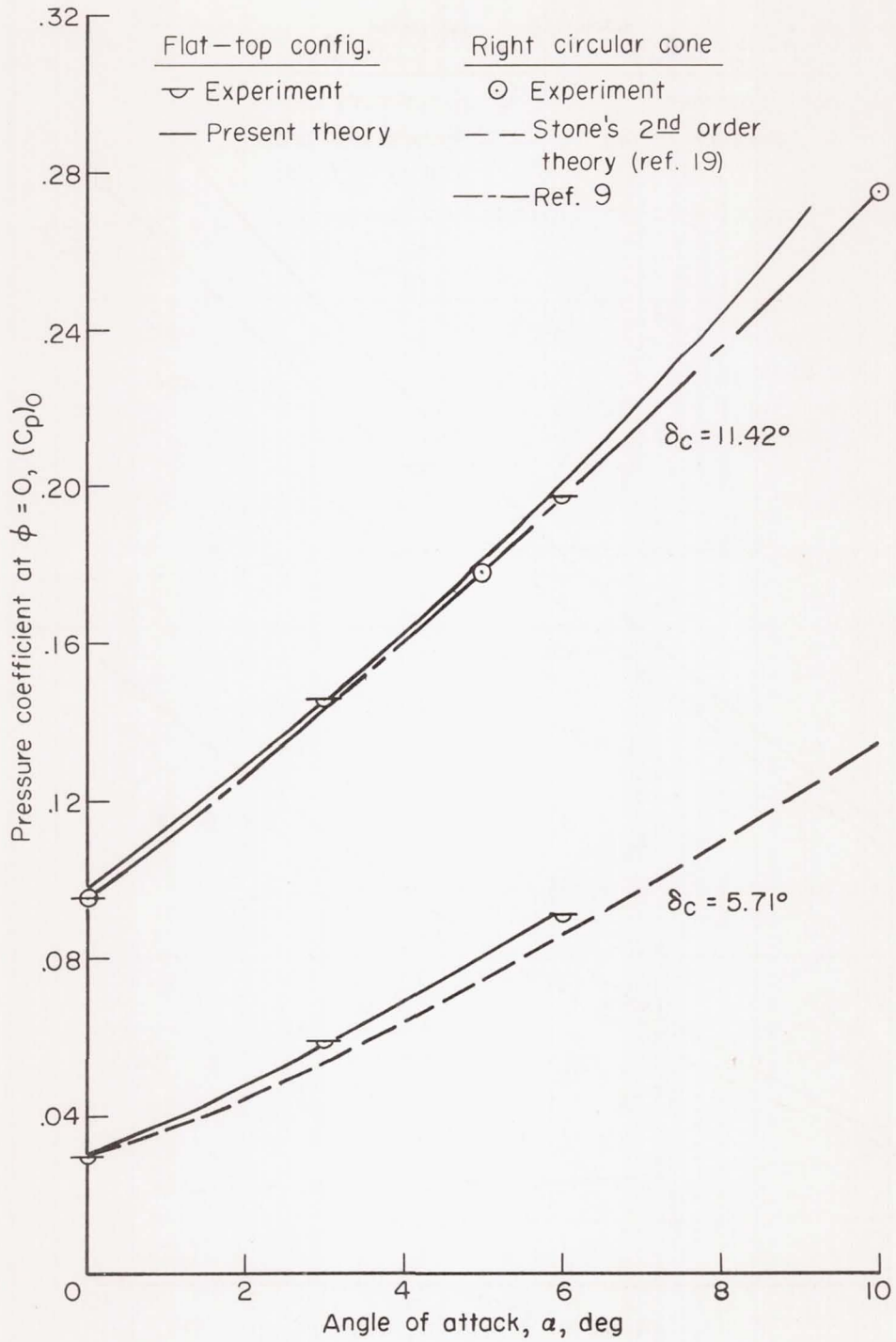

(b) M_∞ = 5.0

Figure 5.- Concluded.

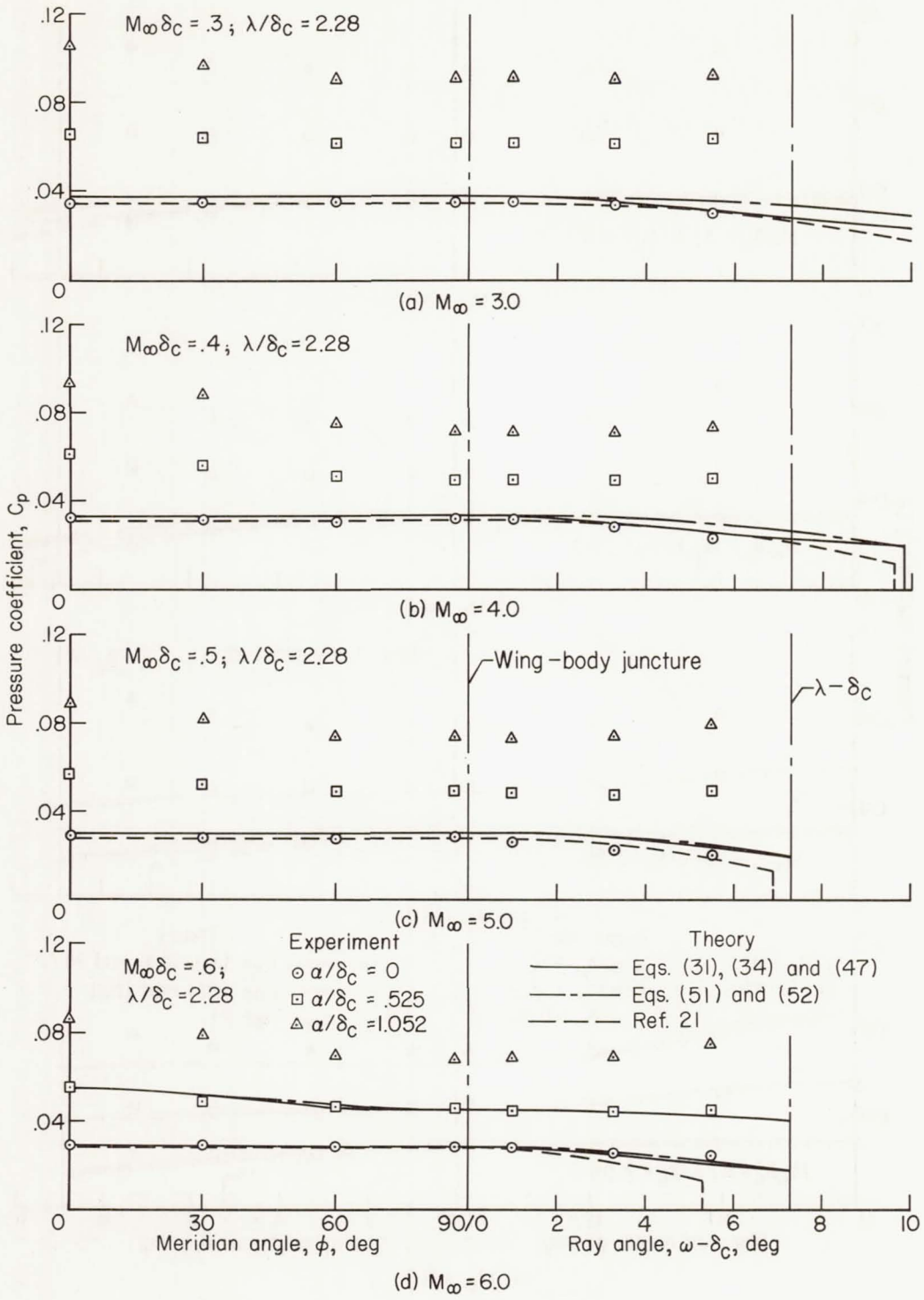

Figure 6.- Surface pressure coefficients for configuration with $\delta_c = 5.71^\circ$ and $\lambda = 13^\circ$ at angles of attack of 0°, 3°, and 6°.

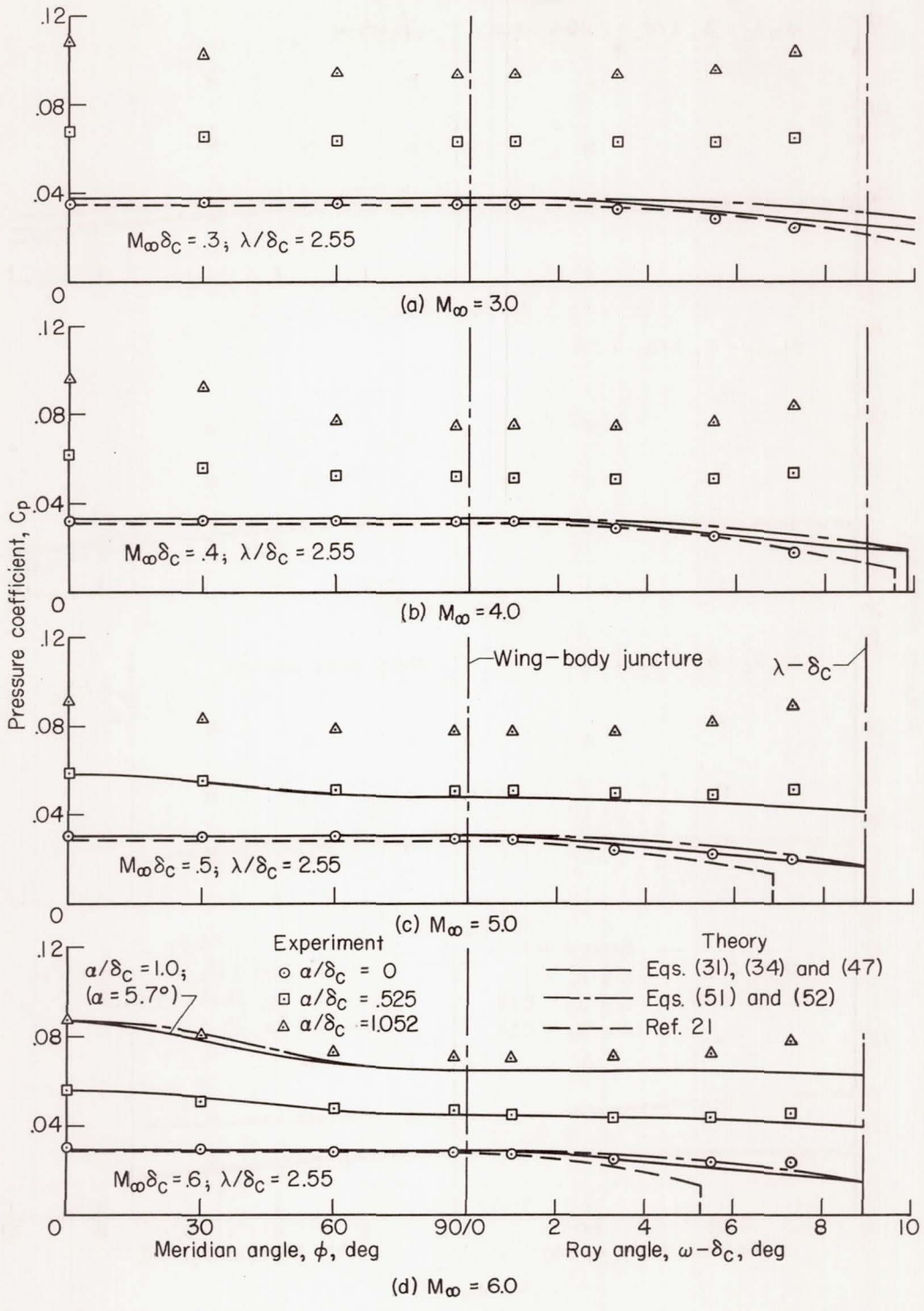

Figure 7.- Surface pressure coefficients for configuration with $\delta_c = 5.71°$ and $\lambda = 14.6°$ at angles of attack of $0°$, $3°$, and $6°$.

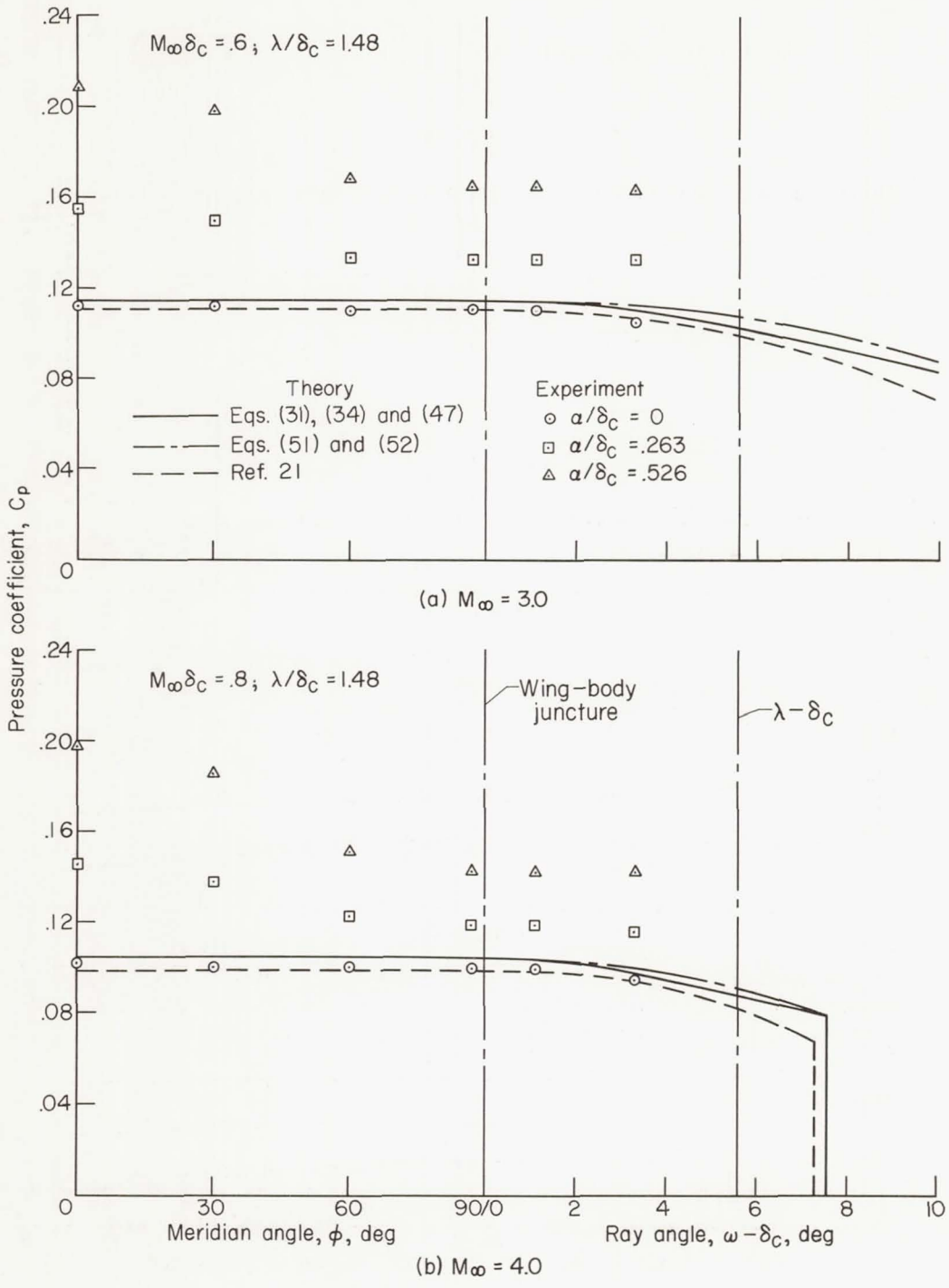

Figure 8.- Surface pressure coefficients for configuration with $\delta_c = 11.42^\circ$ and $\lambda = 16.9^\circ$ at angles of attack of 0°, 3°, and 6°.

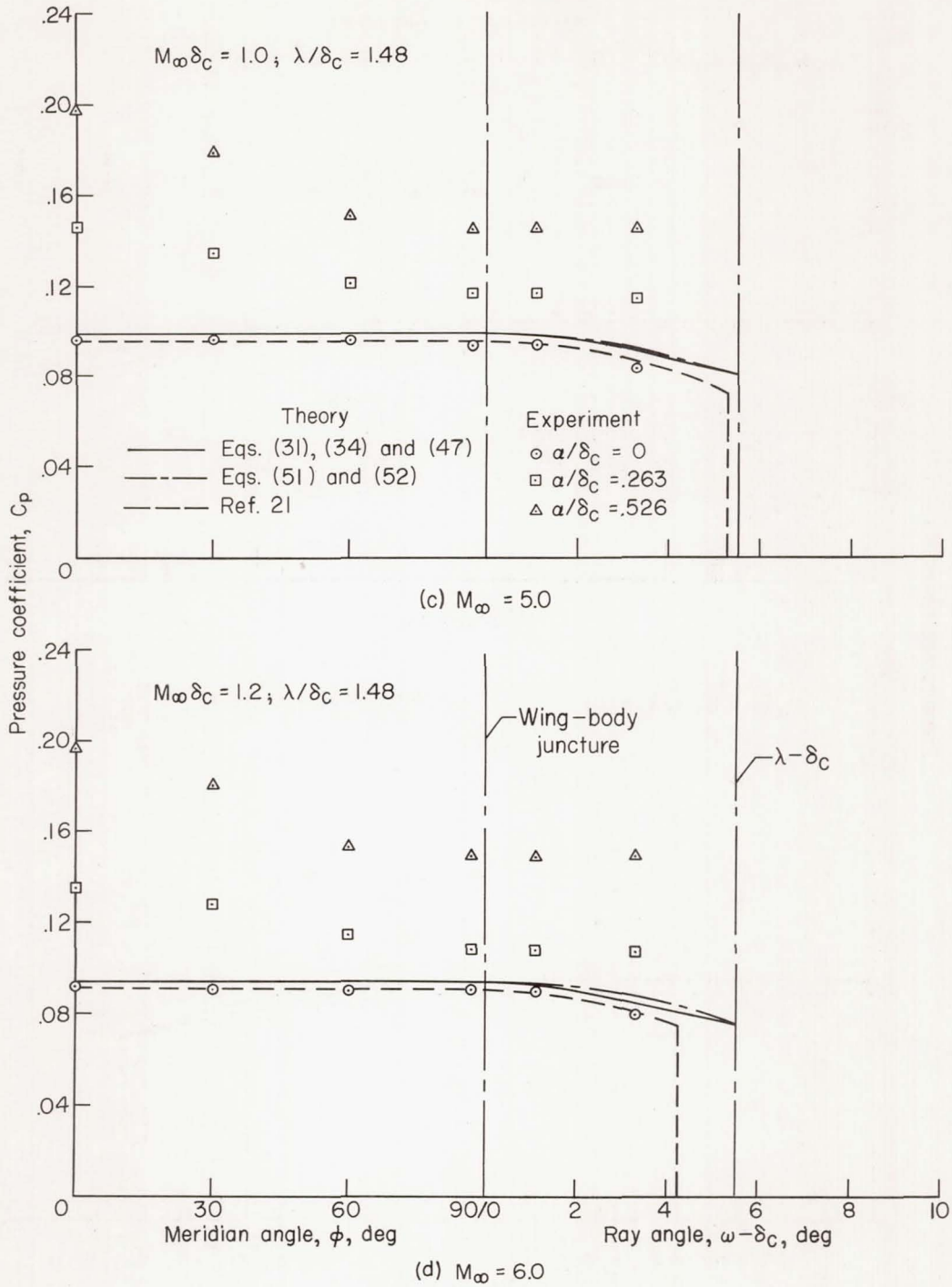

Figure 8.- Concluded.

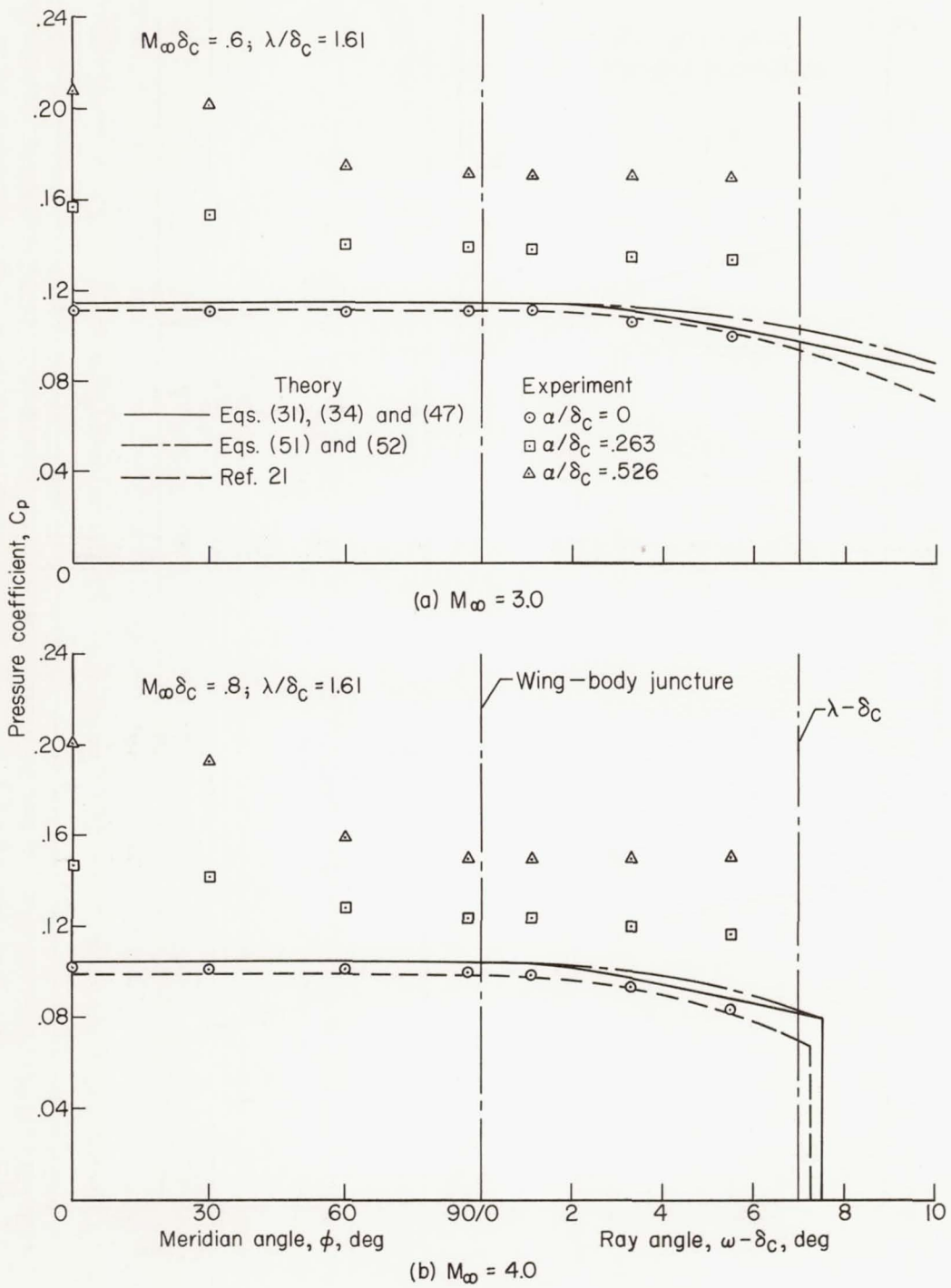

Figure 9.- Surface pressure coefficients for configuration with $\delta_c = 11.42^\circ$ and $\lambda = 18.4^\circ$ at angles of attack of 0°, 3°, and 6°.

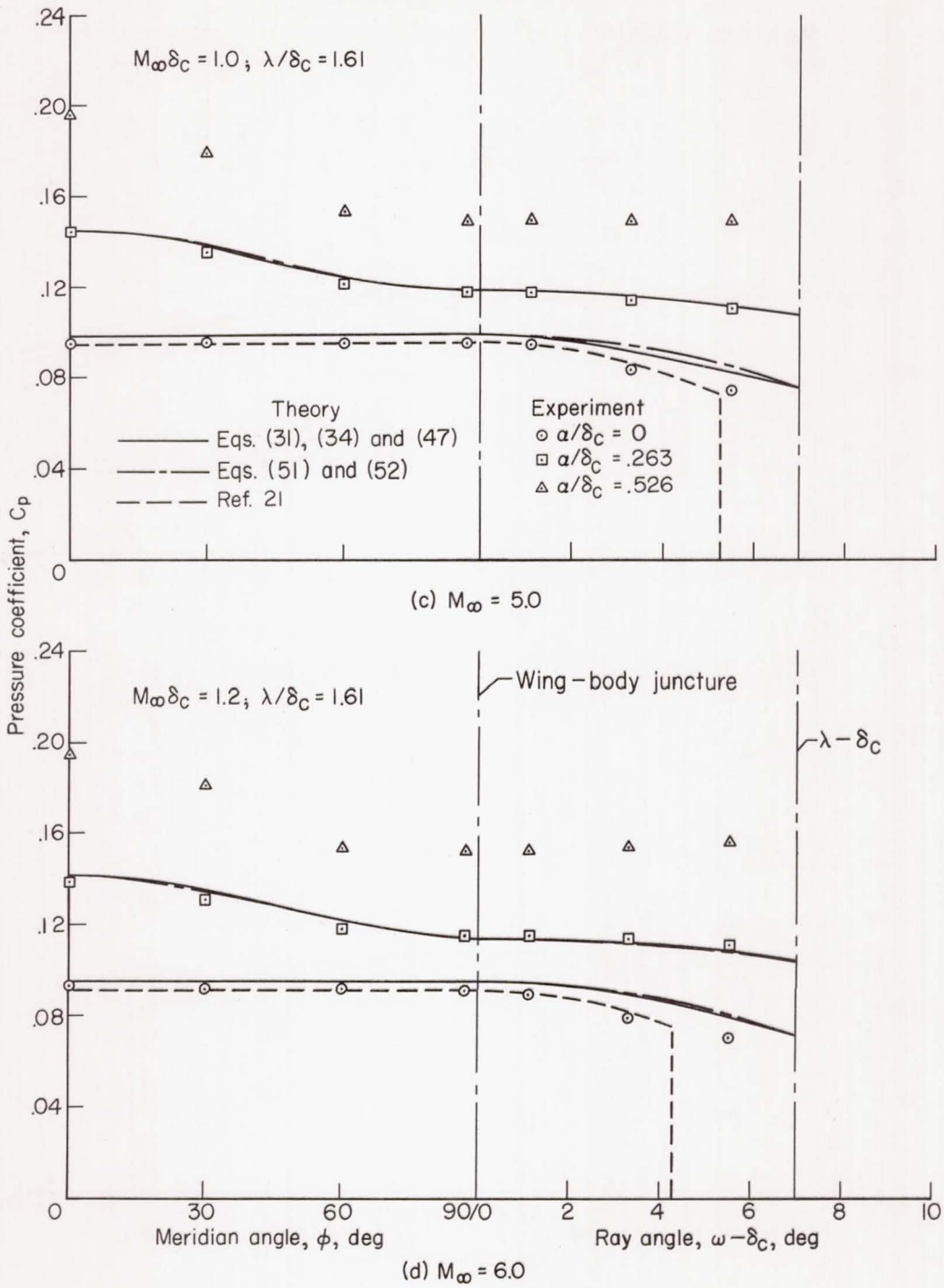

Figure 9.- Concluded.

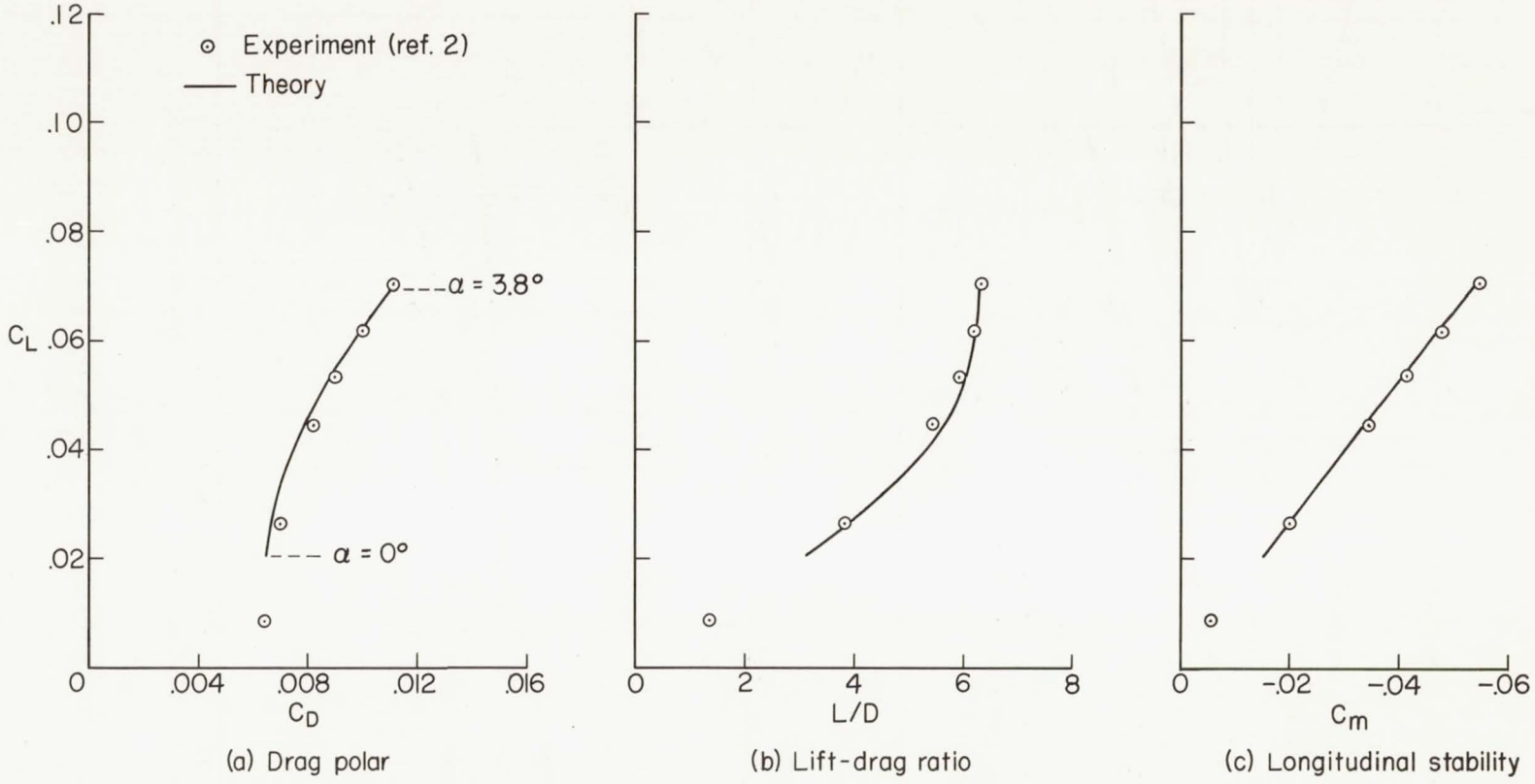

Figure 10.- Aerodynamic characteristics of a conical flat-top wing-body configuration at $M_\infty = 5.0$; $\delta_c = 5.71°$; $\lambda = 15°$.

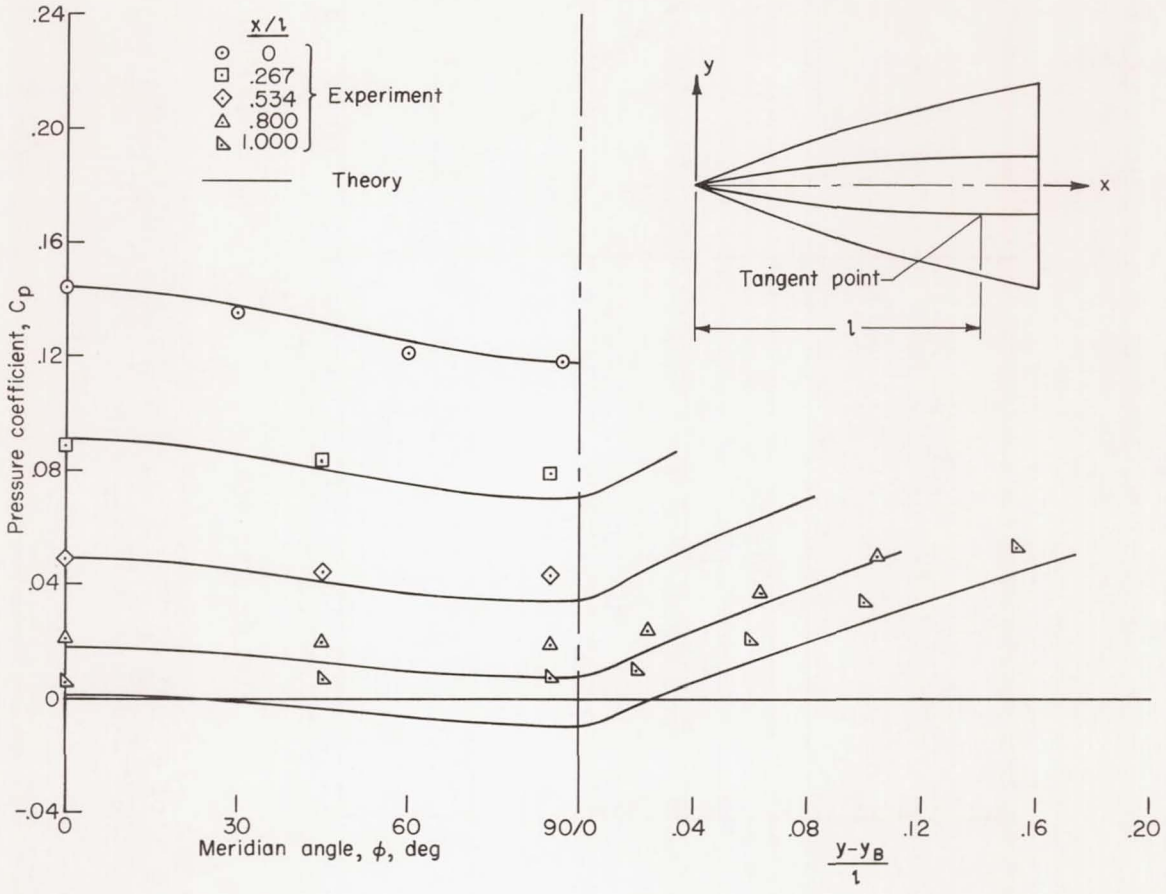

Figure 11.- Variation of surface pressure coefficient on ogive configuration at $M_\infty = 5.0$ and $\alpha = 3^\circ$.